LOW COST Z-SOURCE CONVERTER/INVERTER SYSTEM FOR WIND POWER GENERATION

By

Uthane Supatti

A DISSERTATION

Submitted to
Michigan State University
in partial fulfillment of the requirements
for the degree of

DOCTOR OF PHILOSOPHY

Electrical Engineering

2011

ABSTRACT

LOW COST Z-SOURCE CONVERTER/INVERTER SYSTEM FOR WIND POWER GENERATION

By

Uthane Supatti

With world electricity activity growing steadily, the demand for renewable energy sources is also expected to increase drastically. Wind, a free, clean, and inexhaustible source of energy, is increasingly competitive with other energy sources.

Variable speed wind turbines are known to provide more effective power capture than fixed speed wind turbines. However, the grid is set at a fixed frequency at most loads. The voltage source inverter (VSI) with a DC chopper circuit has traditionally been used for this voltage level and frequency conversion. The traditional VSI, however, has the limitation of only providing output voltages that are lower than input voltages. For this reason, the DC chopper circuit is used to add a boost feature. Even though this topology is functional, the extra active devices and controls add additional system costs and complexities. Alternatively, the Z-source inverter presented recently not only overcomes the voltage limitation of the traditional inverter, but also uses fewer components [1]. Moreover, it is more efficient and reduces cost. As a result, it is well suited for wind turbine systems.

This dissertation presents the application of the Z-source inverter for wind power systems. The operational principle and control method of the proposed system are herein explained in detail. Simulation and experimental results are provided in order to verify the validity of the developed wind turbine generation system.

Dedicated to:

My parents, Pramual and Tu Supatti

My beloved sisters, Nichapa and Akkarapannee Supatti

ACKNOWLEDGEMENTS

TABLE OF CONTENTS

LIST OF TABLES

LIST OF FIGURES

LIST OF ABBREVIATIONS

A/D   Analog to Digital

AC   Alternating Current

AWEA   American Wind Energy Association

DC   Direct Current

DFIG   Doubly-fed Induction Generator

DOE   U.S. Department of Energy

DSC   Delayed Signal Cancellation

DSP   Digital Signal Processing

EMF   Electromotive Force

EMI   Electro Magnetic Interference

G   Generator

GB   Gearbox

GTO   Gate Turn-off Thyristor

HC   Harmonic Compensator

HCS   Hill-Claim Searching

IEEE   Institute of Electrical and Electronics Engineering

IG   Induction Generator

IGBT	Insulated-Gate Bipolar Transistor
MPPT	Maximum Power Point Tracking
PE	Power Electronics
PI	Proportional-integral
PLL	Phase-locked-loop
PMSG	Permanent Magnet Synchronous Generator
PR	Proportional Resonant
PSF	Power Signal Feedback
PV	Photovoltaic
PWM	Pulse Wide Modulation
RMS	Root Mean Square
SCR	Silicon Controller Rectifier
THD	Total Harmonic Distortion
TSR	Tip Speed Ratio
VAR	Volt Ampere Reactive
VSI	Voltage Source Inverter
WECS	Wind Energy Conversion System

Chapter 1. Introduction

1.1 Wind Energy Development

The global electrical power demand is steadily increasing. The absolute dependence on conventional energy resources such as oil, coal or natural gas to meet the global demand is problematic for many reasons: its environmental impacts such as pollution and global warming caused by greenhouse emissions, the rising and unstable prices for fossil fuels, and for some nations energy security is considered as an indispensable part of the national security.

Therefore, renewable energy sources have become more and more important resources for generating the worldwide electrical power. Among renewable energy, wind energy is the fastest growing. The wind energy is free, clean, and inexhaustible source of energy. However, employing the wind energy to generate electrical power is challenging as the wind speed is unpredictable. The change of wind speed will result in the variation of the power, voltage and frequency of wind turbine generators. However, most of the loads require the fixed frequency and voltage.

The advancement of power electronics in terms of efficiency and functionality along with their declining cost has increased the contribution of renewable energy systems in the electricity generation and solved significant problems in integrating those technologies with existing power systems. Therefore, using power electronics technology is the promising strategy to efficiently convert and deliver extracted wind power to usable electrical power.

1.2 Wind Power Capacity Growth

Wind power generation is the fastest growing renewable energy system. As shown in the Annual Wind Industry Report (year ending 2008) of AWEA [2] and in the 2008 Wind Technologies Market Report of DOE [3], the development of a wind power system has increased continuously. Table 1 shows the international ranking of wind capacity [2]. In 2008, the new wind power generation capacity has been globally installed over 28,000 MW and the accumulative global wind power capacity is over 120,000 MW through the end of 2008.

Table 1 International ranking of wind power capacity

Annual Capacity (2008, MW)		Cumulative Capacity (End of 2008, MW)	
US	8,558	US	25,369
China	6,246	Germany	23,933
India	1,810	Spain	16,453
Spain	1,739	China	12,121
Germany	1,665	India	9,655
France	1,200	Italy	3,731
Italy	1,010	France	3,671
U.K.	869	U.K.	3,263
Portugal	679	Denmark	3,159
Australia	615	Portugal	2,829
Rest of world	3,999	Rest of world	18,106
Total	28,390	Total	122,290

In the U.S, the accumulative installed capacity of wind power is about 25,369 MW. This actual installation capacity (only in 2008) was more than double what the report considered necessary to meet the 2030 goal. This goal is designed that the power from renewable energy

could provide 20% of the US electricity by 2030 [3]. Figure 1-1 shows percentage of U.S. electricity, and Figure 1-2 shows the renewable electricity percentage of U.S. electricity in 2008 [2]. It was detailed that there was 3% of electricity production obtained from non-hydro renewable generation, which wind power contributed to over 42% of all non-hydro renewable generation. This wind power increased up from 33% in 2007. As a conclusion, it is confirmed that the wind power is continuing to growth. Moreover, it has played a key role as a promising renewable energy source to electricity generation. Far beyond that, the need of wind power is increasing in future renewable and sustainable energy.
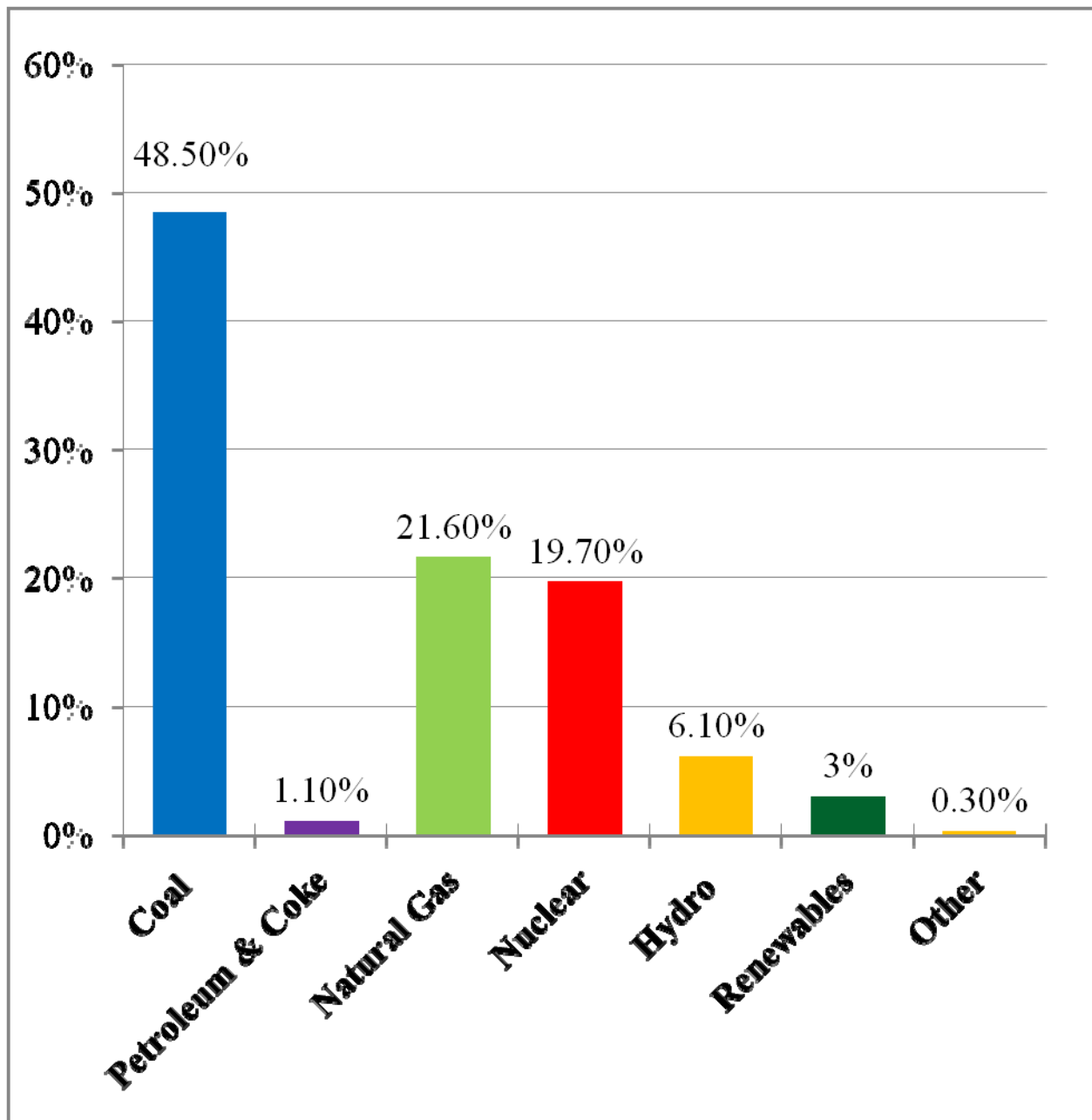
Figure 1-1 Percentage of U.S. Electricity

For interpretation of the references to color in this and all other figures, the reader is referred to

the electronic version of this dissertation
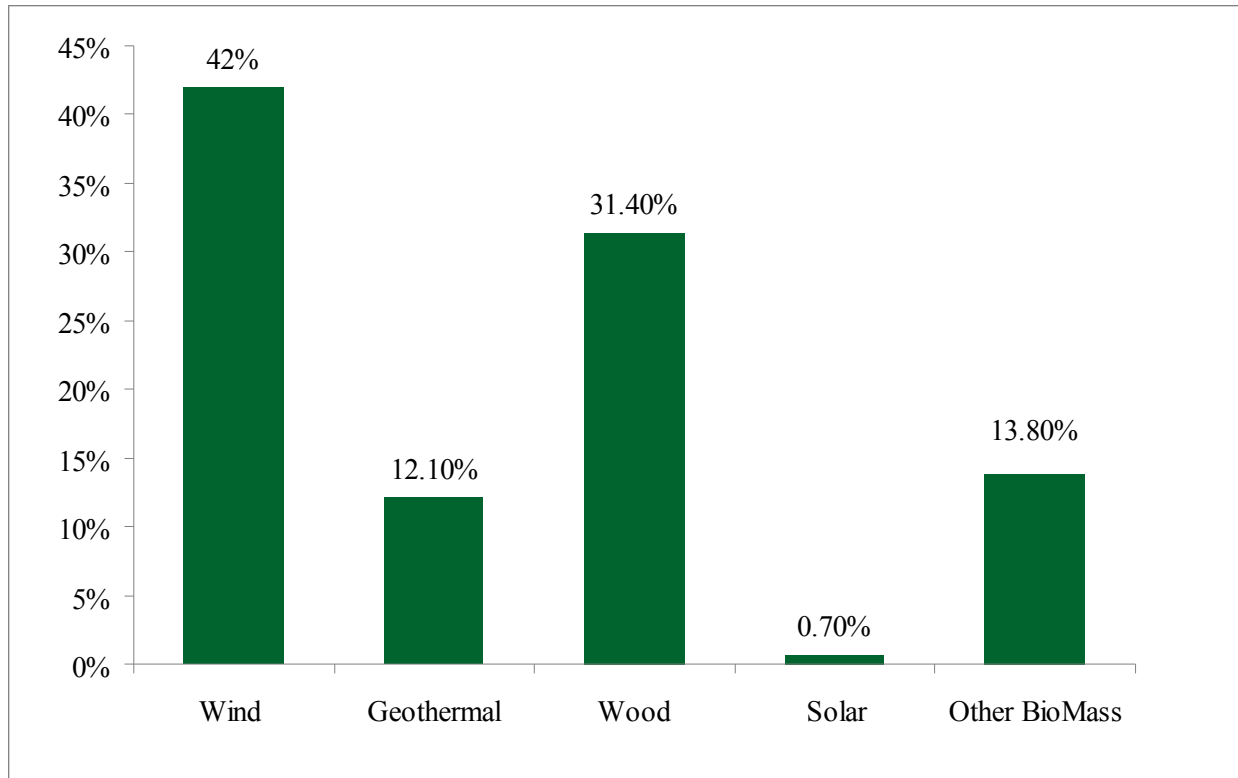
Figure 1-2 Renewable electricity as percentage of U.S. electricity

Nevertheless, in order to get appropriate and usable power from wind energy, a wind turbine and generator are used to convert the wind energy to wind power and eventually to electricity. After that power electronics are utilized to transfer variable frequency and variable voltage to useable constant frequency and voltage for utility grid systems.

1.3 Wind Energy Conversion Devices

1.3.1 Dutch Windmills

Figure 1-3 shows a Dutch windmill [4], [5]. This type of windmill has been used for a very long time as grain-grinding windmills. In the earlier design, they were also very useful for pumping water. Dutch windmills operated on the thrust exerted by wind. The wind exerted a force in the direction of rotation. Nowadays, the Dutch windmill is not widely used since it requires high-skill operators, but provides less efficiency.

Figure 1-3 Dutch Windmill

1.3.2 High–speed propeller wind turbines

The high-speed propeller type wind turbines are one of the horizontal-axis wind turbines which are widely used today for electrical power generation. They do not operate on thrust force, but on aerodynamic forces. These aerodynamic forces will develop when wind flows around a blade of aerofoil design. Turbine blades are shaped a lot like airplane wings, as shown in Figure 1-4. As the wind flows around the blade, the air is split and passed above and below it. The blade upper's surface is shaped so the wind over the top speeds up and stretches out [6]. This decreases the air pressure above the blade. The air flowing below the blade moves in a straighter line, so its speed and air pressure remain the same. Because of the pressure difference between lower and upper blades, the high air pressure always moves towards the low air pressure. The blade, which is in the middle, is lifted by the force from the pressure difference, which is known as lift force and is shown in Figure 1-4 [7]. This lift force generates the torque for the wind turbines. Figure 1-5 shows the arrangement and angle of a high-speed propeller wind turbine [8]. The horizontal-axis wind turbines are efficient and very suitable for electrical power generation.
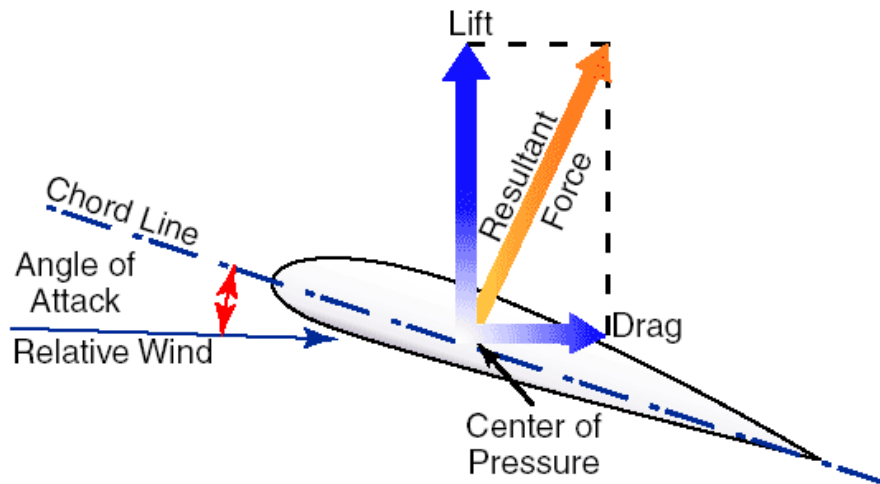
Figure 1-4 The aerodynamic force in an aerofoil moving in the relative wind direction
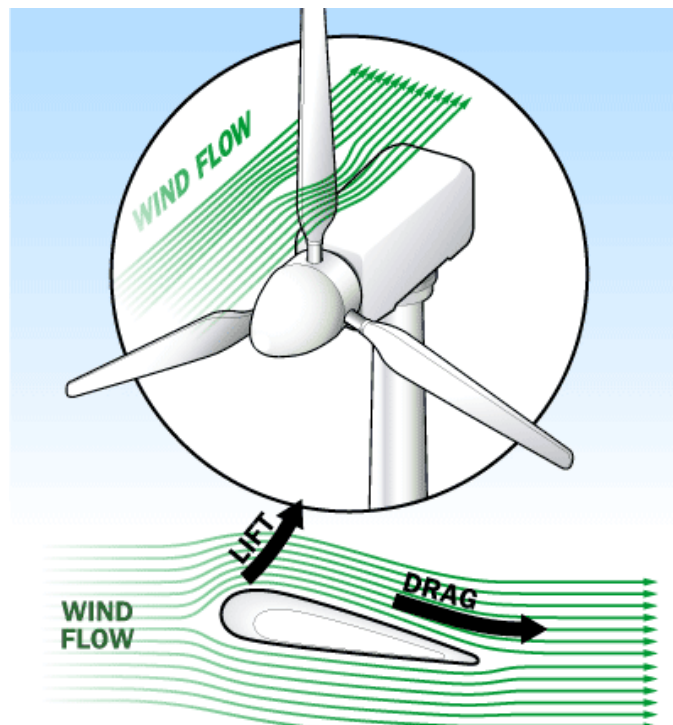
Figure 1-5 High-speed propeller wind turbine

1.3.3 The Savonius Rotor

The Savonius rotor is a vertical-axis device that works entirely because of the thrust force of wind. It has a shape like a drum cut into two halves vertically, as shown in Figure 1-6.

Direction of rotation
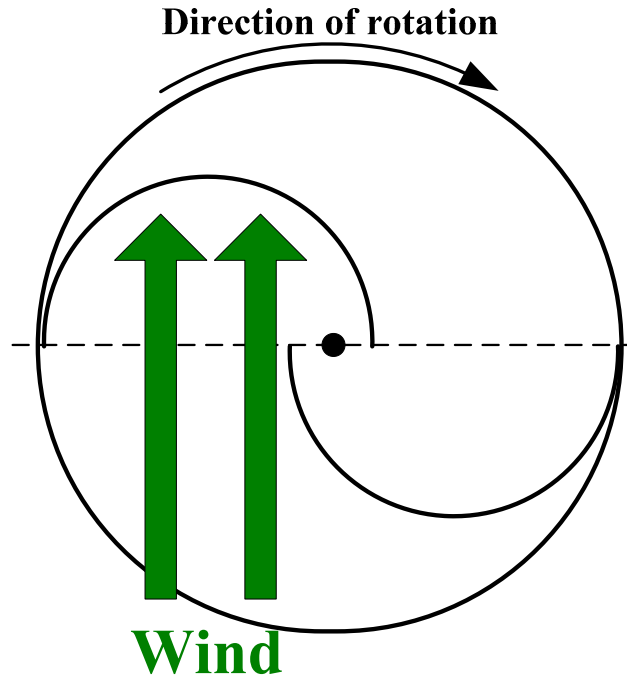
Wind

Figure 1-6 Top view of the Savonius Rotor

As the wind blows onto one side of the rotor, the force exerts on two surfaces in different directions. This happens because of the different and overlapping surfaces, convex and concave. This scenario can be simply explained by saying that when the wind blows onto the concave surface, force is exerted on it and turns around to push the convex curve concurrently. These two different directions of force create the torque for the rotor. The Savonius rotor is simple and economical. However, it has comparatively low efficiency, so it is only utilized for pumping water.

1.3.4 The Darrieus Rotor

Lift force

Lift force

Wind

Airspeed due to rotation

Resultant airflow(red arrow) forms positive angle of attack to wing
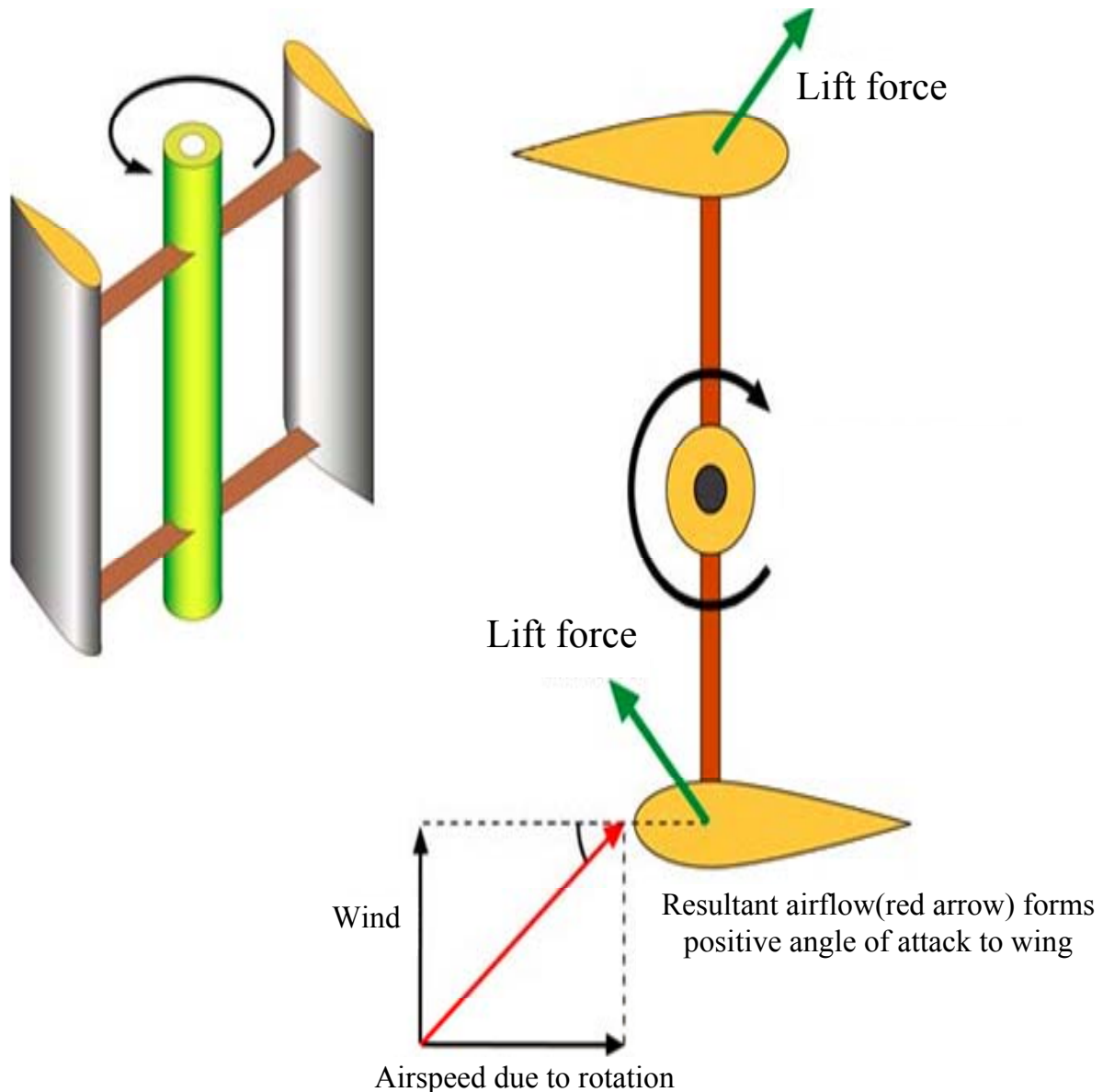
Figure 1-7 The Darrieus Rotor

This rotor has no starting torque (zero torque at stand still). The torque will be developed when it has already been rotated. Therefore, it needs an external starter. An electrical machine will first be used as a motor to provide the starting torque and after that it will work as a

generator once the Darrieus starts generating power [4]. The Darrieus rotor operates on lift force, like the horizontal-axis propeller-type wind turbine shown in Figure 1-7 [9]. So it is high efficiency and high speed. This advantage makes the rotor suitable for electrical power generation. The cost is low because the generator can be at ground level. However, because of the limited structure of this system, it cannot take advantage of high speed winds, which are available at high elevations.

1.3.5 Power Coefficient

Power coefficient (C_p) is the conversion efficiency of wind energy into the mechanical energy of the shaft. The power coefficient is expressed as

$$C_p = \frac{Power\ Output\ from\ the\ Wind\ Machine}{Power\ contained\ in\ Wind} \qquad (1\text{-}1)$$

The efficiency is different from the power coefficient. The efficiency includes the losses in mechanical transmission, electrical generation, etc., whereas the power coefficient is just the power conversion from wind energy to mechanical energy. The normal curves of different types of wind turbines versus the Tip Speed Ratio (*TSR*) are shown in Figure 1-8 [10]. In this picture, the high speed propeller type wind turbine provides a higher power coefficient compared to the others. Therefore, this type of wind turbines is widely used for wind energy conversion systems.
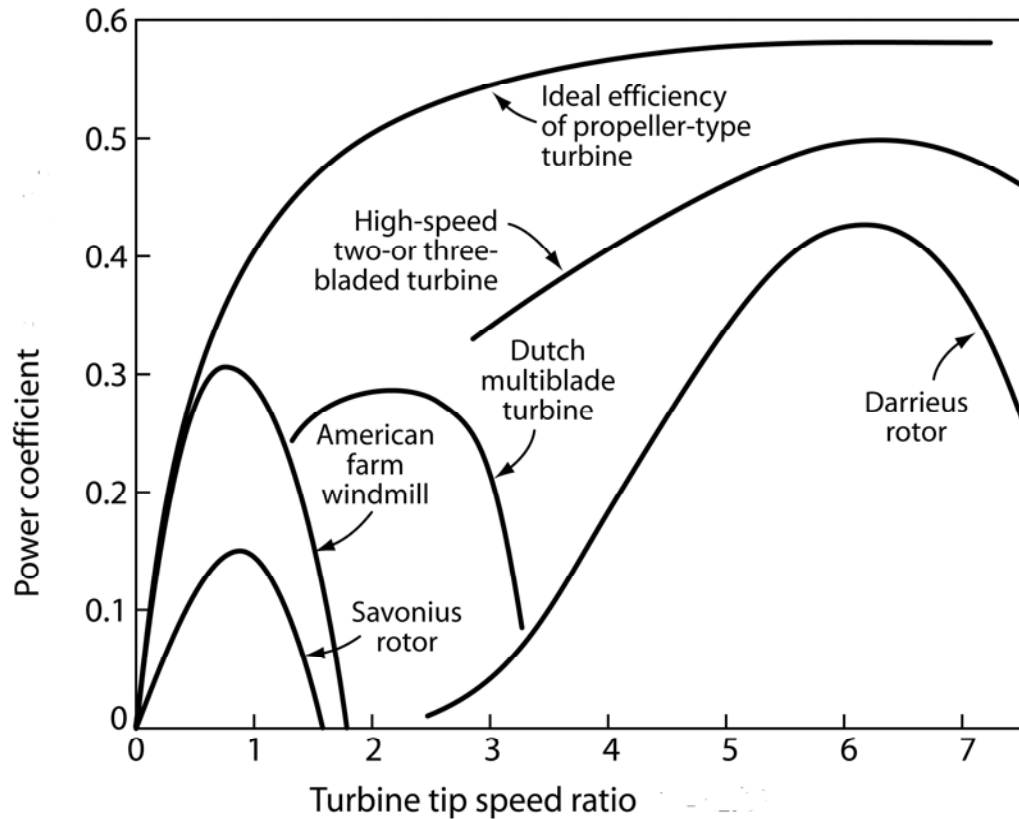
Figure 1-8 Curves of C_p versus *TSR* for different types of wind turbines

1.4 Constant and Variable Speed Wind Turbine

There are typically two operating modes of wind turbine generation systems, constant speed and variable speed operating mode. Most modern wind turbine generation systems are engineered for variable operating mode. The variable speed wind turbine has more efficient power capture than the constant speed wind turbine. It offers better power capture since its rotational speed can be varied to achieve optimum power capture at any wind speed. Therefore,

variable speed wind turbines have the advantages of increased energy capture. Moreover, it reduces mechanical stress and aerodynamic noise at low wind speed.

In contrast with variable speed wind turbines, constant speed wind turbines can only operate at the fixed speed regardless of wind speed. However, there is a maximum power capture at any given wind speed, so rotational speed needs to be changed in order to achieve maximum power capture. Therefore, as the rotational speed is fixed, it could not tract the maximum power. Even though there is greater wind speed, it is not possible for the maximum power captures. Therefore, the constant speed wind turbine system provides less power capture.

1.5 Wind Turbine Characteristics

The amount of power transformed from the wind velocity, v, is described in (1-1) [11].

$$P = \frac{1}{2} \rho A C_p v^3 \qquad (1\text{-}1)$$

P : aerodynamic wind power

C_p : power coefficient of wind turbine

ρ : air density

A : blade swept area, rotor area$[m^2]$

v : wind speed [m/s]

As shown in Figure 1-9, C_p is the power coefficient of a wind turbine which is the function of the tip-speed ratio, λ. The tip-speed ratio is defined as the ratio of the tip speed of the turbine blades to the wind speed which is expressed in (1-2)

$$\lambda = \frac{V_{tip}}{v} = \frac{R\omega_m}{v}$$
(1-2)

where λ = Tip-speed ratio, R = Rotor radius (m), ω_m = Rotational speed (rad/s).

The maximum value of C_p is only achieved at one particular tip speed ratio. As mentioned above, there are two types of wind turbines categorized by its operation. These are constant and variable speed wind turbine. For the constant or fixed - speed wind turbines, the rotor speed is constant, whereas the wind speed is not. So, there is only a particular wind speed at which a wind turbine can generate the maximum power coefficient. At the other wind speeds, the power coefficient is reduced.
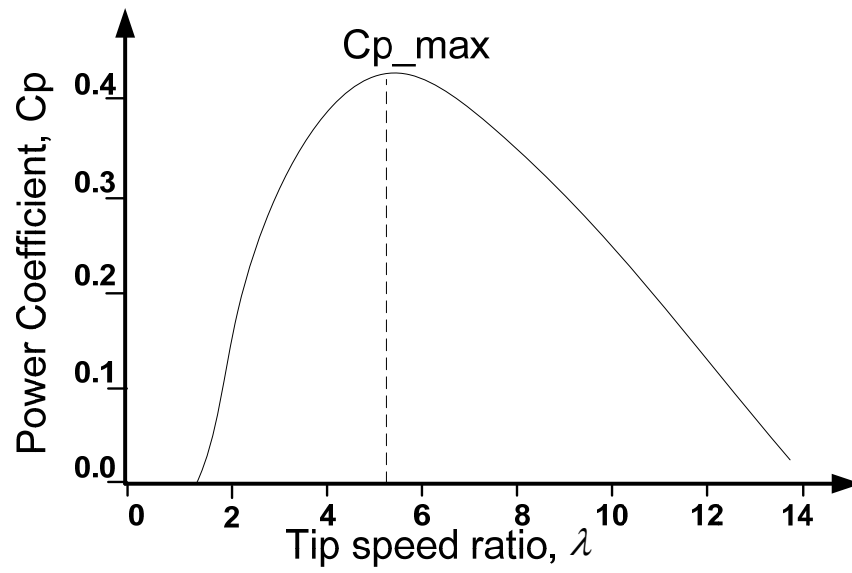
Figure 1-9 Curve showing variation of the power coefficient of performance with the tip speed ratio

In the case of the variable speed wind turbine, the rotational speed is changed in response to wind speed changes, so that C_p is held at its maximum value. Therefore, the variable speed wind turbine is capable of more efficient power capture than the fixed-speed wind turbine. Note that when the wind speed increases, the output power of the generator increases as a function of the rotational speed. Figure 1-10 represents the relationship between the turbine output power and rotational speed regarding to wind speed changes on the variable wind turbine systems. The rotational speed needs to be dynamically adjusted respecting to the wind speed to obtain the maximum power captured.
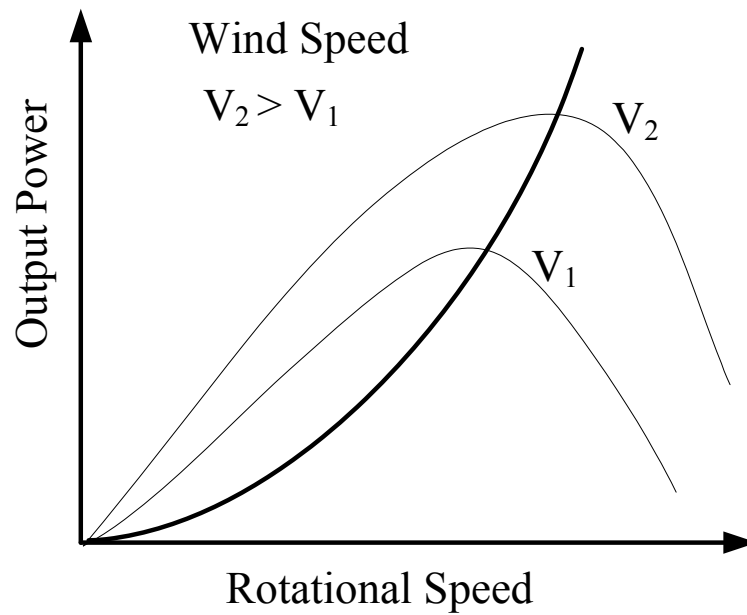
Figure 1-10 Relationship between the turbine output power and rotational speed

1.6 Wind System Configurations

For the past two decades, wind energy has been widely used as a utility generation technology. It plays a significant role in electricity generation. The main component of a popular wind power system is depicted in Figure 1-11 [13]. The system includes turbine blades, a gear box, a generator, potential power electronics and a transformer [12] .
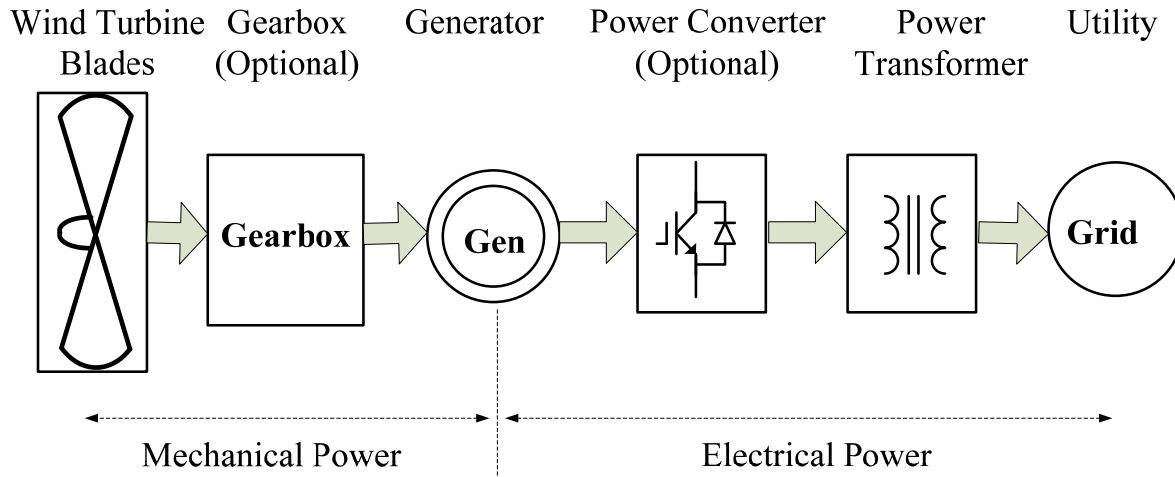
Figure 1-11 Main components of the wind generation system

A gearbox, an optional part of a wind power system, is used to increase the relatively low rotor speed of the turbine up to speeds close to the synchronous speed of the generator. It can lower the weight of the generator and avoid a slow speed generator design with a large number of poles, [14]. Nonetheless, it is heavy and not very reliable. Additionally, the power loss in the gearbox accounts for the high proportion of the total system loss, thus reducing overall efficiency.

Wind turbine system configurations can generally be divided into three different main categories as follows.

1. Systems without power electronics

2. Systems with partially rated power electronics

3. Systems with full-scale power electronics

17

1.6.1 Wind power system without power electronics

In the system without power electronics, the generator is directly connected to the grid without any power electronics, as shown in Figure 1-12. An induction machine is used as a generator of the wind turbine system where it operates at a constant speed (variation of 1-2%) [13, 15]. Reactive power is required in order to operate the induction generator. This reactive power can be obtained from the reactive compensator, which can reduce the reactive power demand to the grid. The power is aerodynamically controlled by rotating the blades using either pitch, stall, or active stall control.
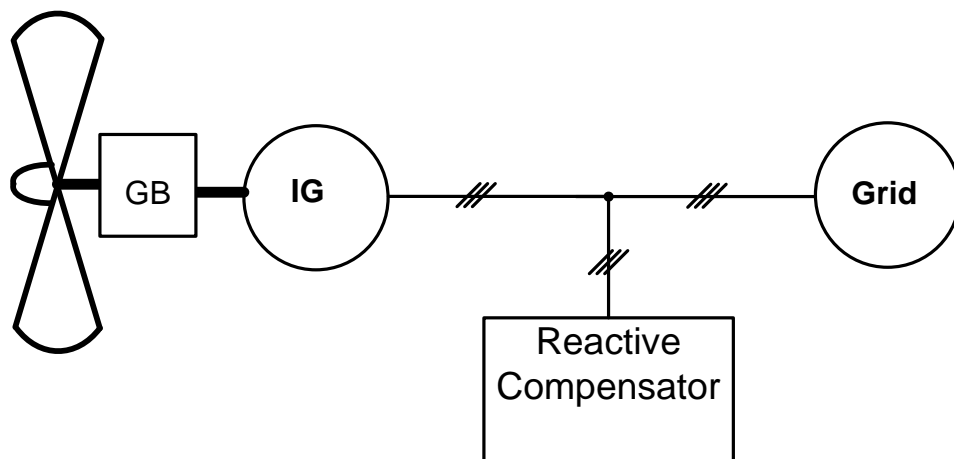
Figure 1-12 Cage induction generator based fixed speed wind turbine without power electronics

Additionally, the soft starter (not shown in Figure 1-12) can be used in order to reduce inrush current during start up.

1.6.2 Wind power system with partially-rated power electronics

A system with partially-rated power electronics requires a wound-rotor induction machine where both the stator and rotor windings are accessible. Power from the rotating rotor is taken through slip rings. Shown in Figure 1-13, an extra resistor is added in the rotor and can be controlled by power electronics, allowing the speed to vary by 2-5%. A soft starter and a reactive compensator are still needed for this configuration.
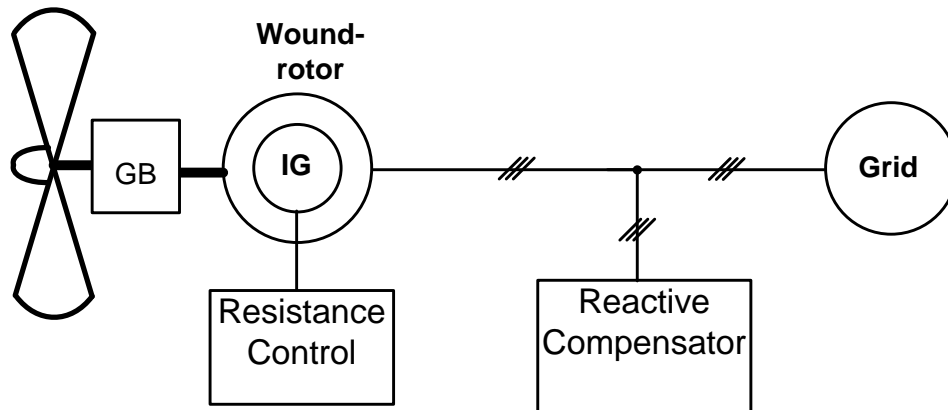
Figure 1-13 Wind turbine topology with partially rated power electronics

Another system with partially-rated power electronics is a system with a wound rotor induction machine, known as a doubly-fed induction generator (DFIG) shown in Figure 1-14 [16]. The stator winding of the generator is directly connected to the utility grid, whereas the rotor winding is connected to the converter through slip rings. This configuration allows the wind turbine to have some amount of variability in speed operation. The electrical power will be delivered to the utility grid through both stator and rotor winding if the generator is running at a super-synchronous speed. However, the reactive power will be drawn from the grid and

delivered into only the rotor if the generator is running at a sub-synchronous speed. The advantage of this configuration is that it provides reactive power compensation and increases energy capture from the wind. Moreover, the required converter transfers a maximum of 25-30% of the wind turbine rated power. This indicates that only a small size converter is needed.
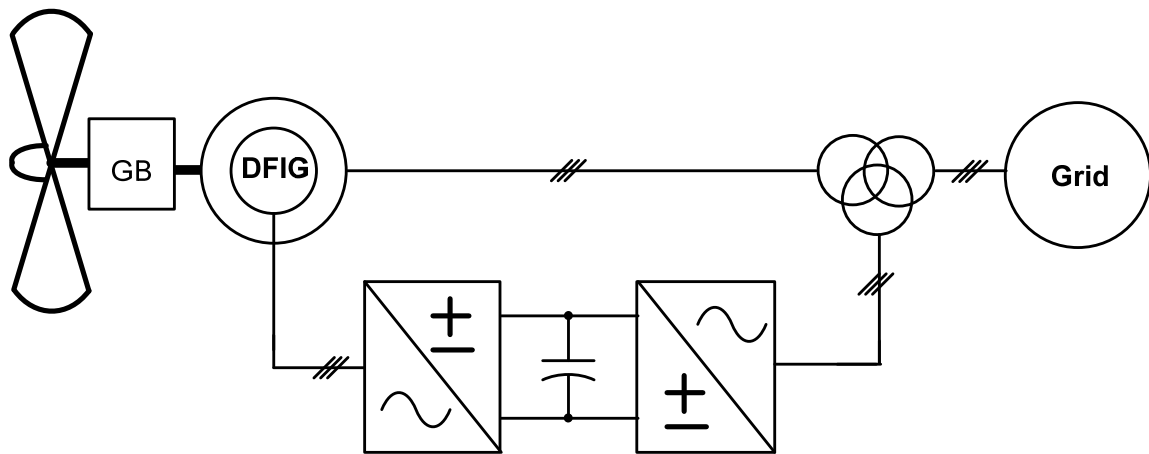
Figure 1-14 Doubly-fed induction generator

1.6.3 Wind power system with full-scale power electronics

Wind power system with the full scale power electronics has the configuration which utilizes the power electronic systems to interface the wind turbine with the grid. Unlike either the wind power system without power electronics or with partial power electronics, the wind power system with full-scale power electronics allowed all power generated by wind power system to be transferred to the grid through the power electronic systems. The configuration of the system shows in Figure 1-15.

This structure allows the wind turbine to operate in a variable speed mode, capturing more energy. Moreover, the system behaves like a power plant. It provides better technical performance. In respect to control performance, it provides faster reactive and active power control. Additionally, the system can always deliver both reactive and available active power to the grid.

Many types of generators, for example an Induction synchronous Generator (IG) and Permanent Magnet Synchronous Generator (PMSG), can be used in this configuration in order to convert wind power to electrical power with variable voltage and variable frequency. Then, the power electronics based rectifier and inverter are used to convert the full-rated output power of the generator, with variable voltage and frequency, into the constant voltage and frequency system, which is suitable for the utility grid interconnection.
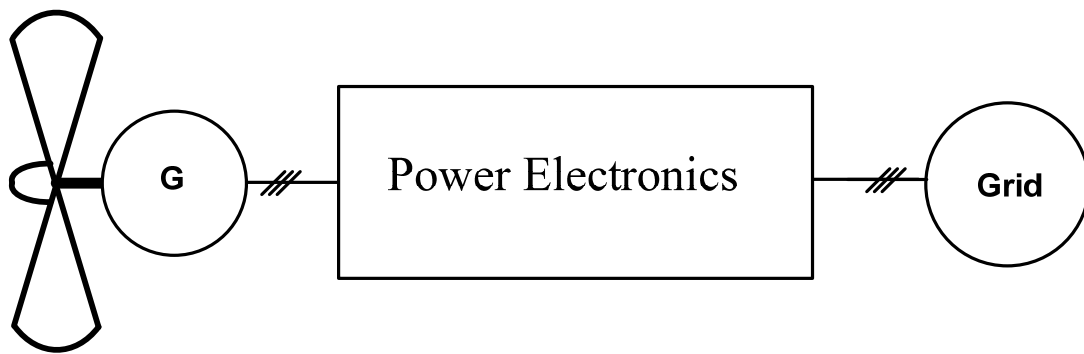
Figure 1-15 Wind turbine system with full-scale power electronics

The disadvantages of this configuration are that the system is more complex and has more sensitive power electronic parts. Moreover, this configuration introduces additional losses from the rectifier and inverter.

1.7 Technology Barriers of full-scale power electronics for Wind Power Generation System

As mentioned above, the wind turbine system with full-scale power electronics can provide more energy capture. However, power converter systems, for example rectifier, converter and inverter are required in order to appropriately convert the generator output to the utility grid.
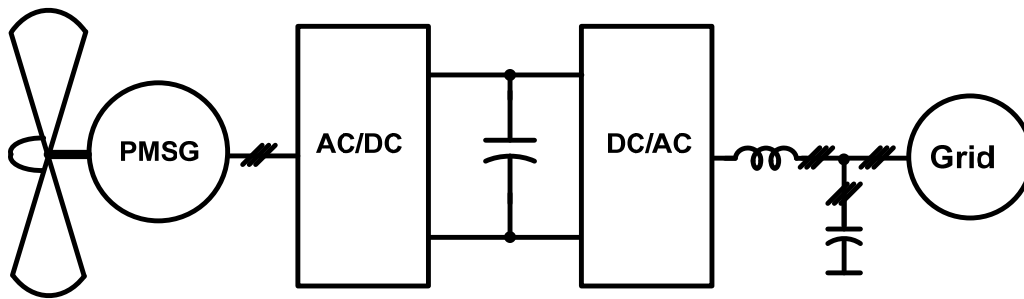
Figure 1-16 PMSG based typical wind energy conversion system

A typical wind energy conversion system based on PMSG is shown in the Figure 1-16. This system utilizes a full AC–DC and DC-AC converter to convert variable speed variable frequency generator output to the constant frequency and constant voltage utility grid.   The energy extracted from the wind is shifted through the DC-link capacitor by the AC-DC converter or rectifier [39]. Then it is further shifted to the utility grid by the DC-AC converter or inverter.
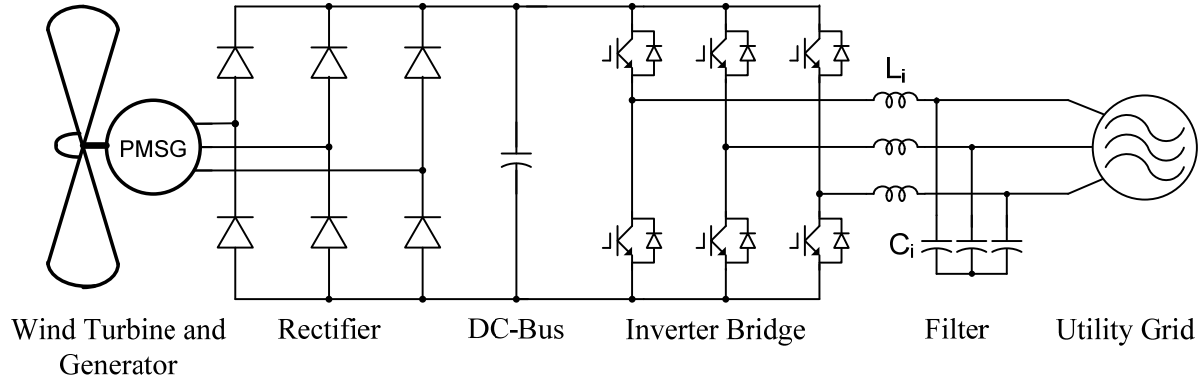
Figure 1-17 Typical inverter Block Diagram

An example of this structure shows in Figure 1-17. This configuration is typically used for wind power generation system, since it is simple and cost effective. In this system, the DC-link capacitor offers decoupling between the generator-side and grid side converter. However, using such configuration can efficiently transfer power from the terminal of the generator to the utility grid only when the generator produces a DC-bus voltage high enough for the inverter to generate the output voltage to the utility grid. It is said that in order to achieve appropriate power flow control in the system, the DC-bus voltage must be higher than the peak phase voltage of the utility grid [47]. When the wind speed is low, the generator output voltage is also low. So, the DC-bus voltage is not high enough to produce the output voltage to the grid. In this scenario, the typical inverter cannot transfer power to the grid effectively. This limitation makes the typical inverter not perfectly fit for this application.

Using uncontrolled diode rectifier is possible with the wind turbine systems that are interfaced with a pole-changing wind turbine generation to realize variable speed wind turbine operation [47-48]. However, in this particular configuration, the rectifier voltage is regulated by changing pole of the generator. To do so, the system requires a winding arrangement and pole-changing controller and these requirements are the main concern of this configuration.
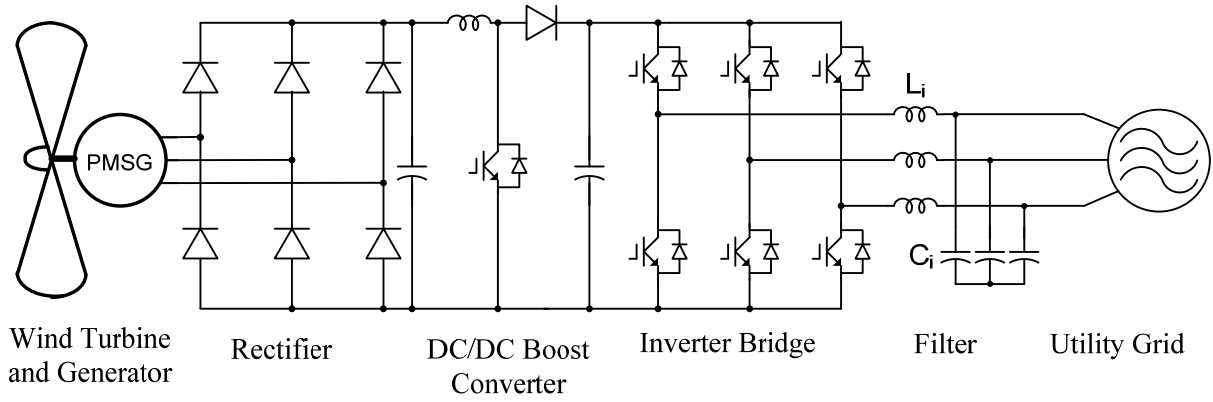
Figure 1-18 Typical inverter with adding DC-DC boost converter

Therefore, adding boost feature is necessary for this configuration. Several types of converters like a conventional DC-DC boost converter [49] or buck-boost converter [50] is required for this structure. The wind power generation system with boost converter shows in Figure 1-18. Even though, this two-stage converter can overcome the aforementioned problems, it is not a good candidate for small to medium wind power generation systems. This is because the two-stage converter is complex and not cost effective.

1.8 Research Objectives and Scope

This dissertation details the research work for developing a variable speed wind power generation system using the Z-source converter/inverter. Attention is focused mainly on developing the inverter and interfacing the modular permanent magnet generator into the power network to capture optimal power.

This dissertation proposes the Z- source converter/inverter for wind generator systems and its control on the maximum power capture and grid interconnection. The control structure is on a power delivery to the utility grid and MPPT control. The operating principle of the proposed system is explained in details. In addition, different converter topologies have been

24

comparatively reviewed. The control for grid interconnection is also introduced. Finally the conclusion and future work is also detailed.

Chapter 2. Converter Topology Review

As mentioned, the wind power system configuration is categorized into three primary groups which are a) system without power electronics, b) system with partial power electronics and c.) system with full power electronics. Converter topologies for wind power generation will be reviewed in this chapter. The system with full-scale power electronics is focused and compared with their advantages and disadvantages.

2.1 Soft Starter

Figure 2-1, the soft starter (a power converter) and its configuration with wind power system is employed to reduce the transient current which may occur during connecting and disconnecting the generator to the utility grid [17-19]. The induction machine works as a generator, when the generator speeds exceed the synchronous speed and then the soft starter activates. By controlling the firing angle of thyristors, the generator is smoothly connected to the grid.
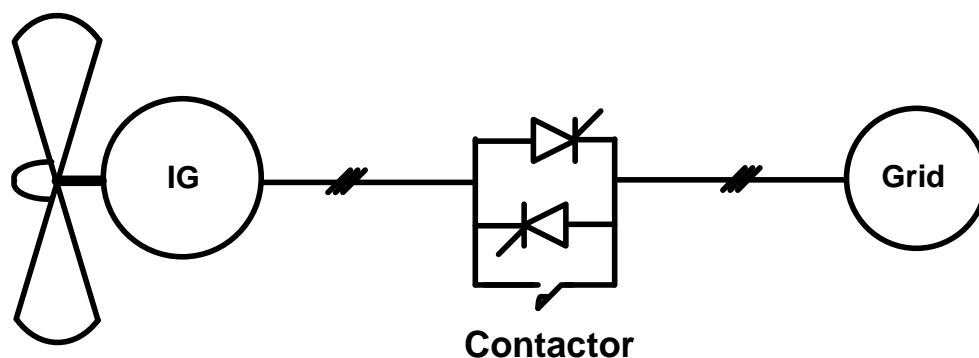
Figure 2-1 The wind power system configuration with soft starter

There are two anti-parallel connected thyristors for each phase with a bypass of contactor as shown in

Figure 2-1. To reduce losses during normal operation, contactors that bypass the soft-starter are used when the generator is completely connected to the grid. The soft-starter is inexpensive and is a standard converter in many wind turbines.

2.2   Full scale-power electronic with diode rectifier

2.2.1 Thyristor supply-side inverter
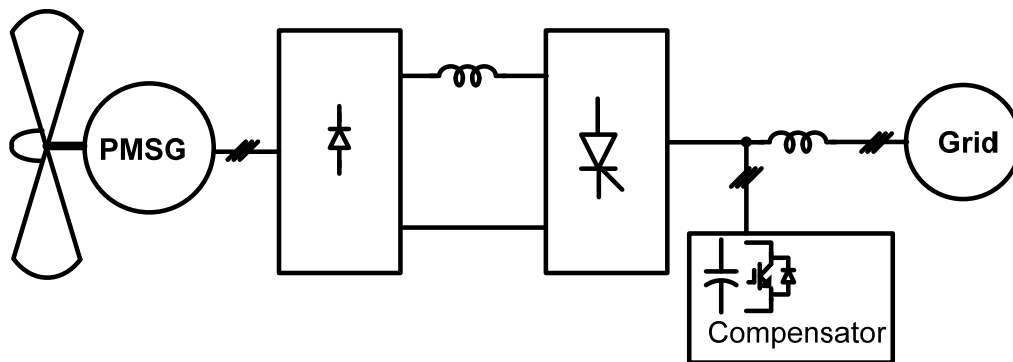
Figure 2-2 PMSG based with diode rectifier and thyristor supply-side inverter

The AC-DC-AC power electronic interface consists mainly of a diode rectifier and a thyristor inverter [20]. The thyristor ignition angle can be adjusted continuously to control turbine speed, so that the optimal energy capture is achieved. The reactive power and harmonic characteristics

of the thyristor converter system have to be compensated to meet the standards for grid connection.

Advantages of this structure include lower device cost and higher available power rating than hard-switched inverters. Nevertheless, a major drawback of this topology is the need for an active compensator for the reactive power demand and harmonic distortion created.

2.2.2 Intermediate boost converter
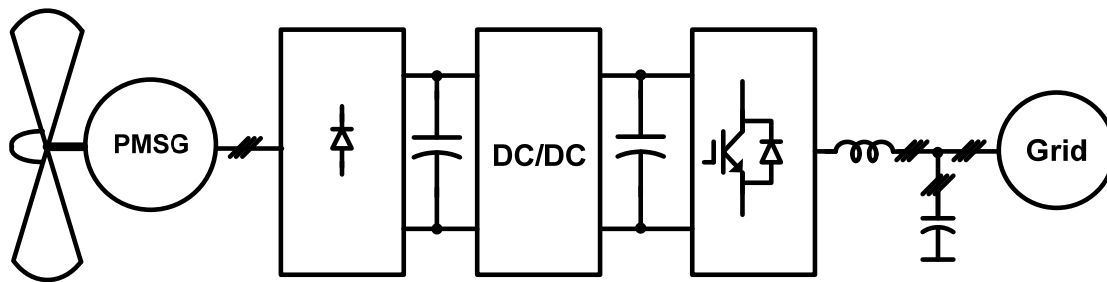
Figure 2-3 PMSG based with diode rectifier and intermediate DC-DC converter

A typical power electronic topology with the use of a permanent magnet synchronous generator is shown in Figure 2-3 [21]. The output from the wind turbine, three-phase variable voltage and variable frequency, is rectified by using a diode bridge. With the change of wind speed and generator speed, the generator output voltage and frequency will change, hence changing the DC voltage at the bridge rectifier's terminal. To maintain a constant DC-link voltage of the inverter, the extra step-up chopper is used to regulate the rectifier voltage.

The extra DC-DC converter provides obvious advantages. For example, the DC-link voltage does not need to be controlled by the inverter. This makes the control more flexible. The DC-link

voltage is controlled through the DC-DC converter, providing appropriate voltage to the inverter bridge. The power converter to the grid enables a fast control of active and reactive power. Nevertheless, it is a more complex system and requires more power electronic parts [12].

2.3 Full scale-power electronic with Back-to-back PWM converters

2.3.1 PMSG based WECS with back-to-back PWM converter

The back-to-back converter is widely used in wind power systems. The configuration of the system is shown in Figure 2-4 [22]. It simply consists of a PWM rectifier and a PWM inverter connected with a common DC-link. The properties of these combinations are as follows.

- The grid-side converter may be operated to give sinusoidal line currents.

- The DC-link voltage must be higher than the peak main voltage.

- The DC-link is also controlled through the grid-side converter.

- The DC-link voltage is regulated by controlling the current flow to the grid.
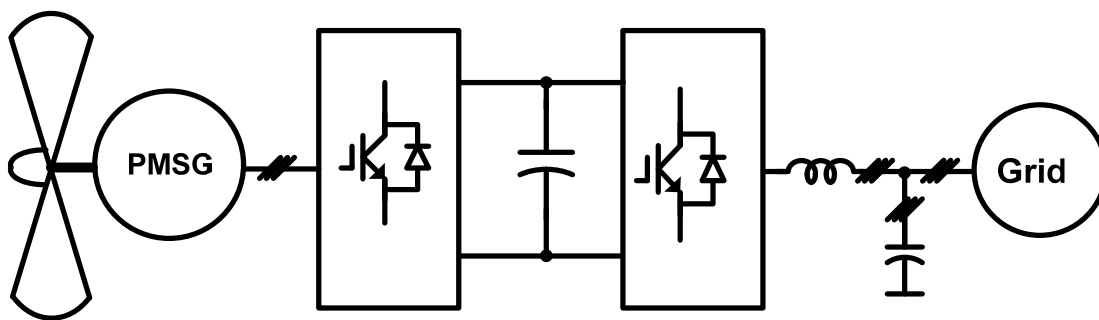
Figure 2-4 PMSG based with back- to- back PWM converters

The MPPT control is carried out on the generator side rectifier. The generator side rectifier is controlled through the PI controller where the q-axis current is set to zero to obtain maximum electrical torque with minimum current. The rotor speed is controlled through the generator side converter. The optimum rotor speed is determined by the MPPT for each wind speed in order to get maximum rotor power.

The PWM modulation reduces the current harmonic component in the input and output of the system. For this reason, it reduces the torque pulsation on the generator and improves the output power quality. This topology was introduced to the wind power system by [22].

Advantages:

- The PWM modulation reduces the current harmonic component in the input and output of the system.

- It reduces the torque pulsation on the generator and improves the output power quality.

Disadvantages:

- The DC-link capacitor is known as a drawback since it is heavy and bulky. It increases the cost and reduces the lifetime of the overall system.

- Switching losses is also a problem since with every commutation both the grid and generator side converter is affected with hard switching and a natural commutation. The system consists of two PWM-converters, so that the switching losses might be doubled.

2.3.1.1 IG based WECS with back-to-back PWM converters

This system includes a squirrel cage induction generator and a double-side PWM converter, as shown in Figure 2-5 [23] [24]. This topology overcomes the problem generated by using squirrel cage induction generators with shunt passive or active VAR (volt ampere reactive) powering the utility grid through diode rectifiers and a line-commutated thyristor inverter. However, problems include poor line power factor and harmonic distortion in both the line and the machine.
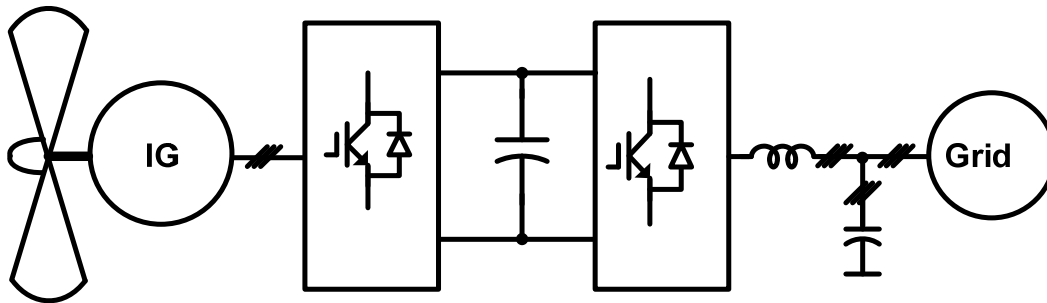
Figure 2-5 Induction generator with back- to- back converter

The variable frequency and variable voltage power from the induction generator is rectified by a PWM IGBT rectifier. The rectifier also supplies the excitation that is required by the generator. The inverter topology is identical to that of the rectifier and it supplies the generated power at 60 Hz.

Advantages[23]：

- Unity power factor control is possible without harmonic current injection. This can satisfy IEEE 519 standard.

- The squirrel cage induction machine is extremely rugged, reliable, economical, and universally popular.

- There is no harmonic copper loss because machine current is sinusoidal.

- Continuous power generation from zero to highest turbine speed is possible.

- Power can flow in two directions permitting the generator to run as a motor for start-up. Similarly, the turbine can be stopped by using the regenerative breaking mode.

- The inverter can be operated as a VAR/harmonic compensator when spare capacity is available.

Disadvantages (for high power system, about 1.5MW) [24]:

- The power converter (1 p.u.) is expensive.

- Inverter output filters and EMI filter are rated for 1 p.u. output power, making filter design difficult and costly.

- For the entire operating range, the converter efficiency plays a significant role in overall system efficiency.

2.3.2 Doubly-fed induction generator
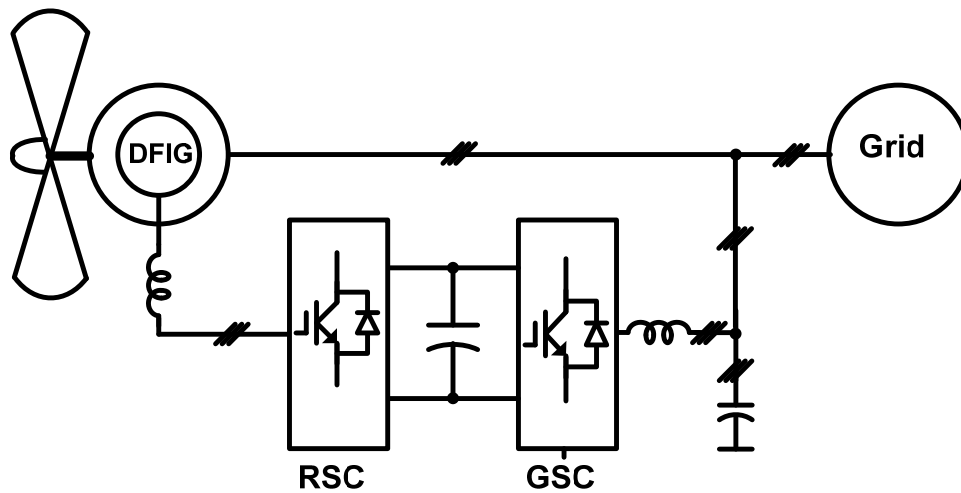
Figure 2-6 Doubly-fed induction generator

One of the well-known wind turbine generation using a variable-speed constant-frequency scheme to produce electricity is a doubly-fed induction generator (DFIG). The configuration is shown in Figure 2-6 [16]. The stator of the DFIG is directly connected to the three-phase utility grid, whereas the rotor winding is connected to the grid through the back-to-back voltage source converters. This rotor winding terminals are connected to the power converter through slip rings.

The DFIG supplies power at a constant voltage and constant frequency while the rotor speed varies. This makes the DFIG suitable for variable speed wind power generation.

The grid side converter is usually controlled to maintain the DC-link voltage at a constant regardless of the magnitude and direction of the rotor power. The grid side converter is also responsible for reactive power control through alternating of the q-axis current (to operate at unity power factor). The rotor side converter controls the electrical frequency in the rotor windings, and the real and reactive power flows. The variable rotating speed of the wind turbine is controlled by the rotor variable supply.

For a high power wind turbine, the gear box is necessary to adapt the low-rotating speed of the DFIG (high-power wind turbine) to medium-rotating speed of DFIG.

The full range operation of speed, from zero to rated speed, is not possible for this turbine. This limited speed range is caused by the converter, which is normally smaller than the rated power of the generator. Generally, the converter only has to handle a partial of 30 % of the total power. This means that if the speed is in the range of 30 % above and below synchronous speed, the converter has the rating of 30% of the rated turbine power. This means that converter power rating is half of the rotor-speed span of the wind turbine rating. This small converter leads to lower losses.

If the generator is running super-synchronously, electrical power is delivered through both the rotor and the stator. However, if the generator is running sub-synchronously, electrical power is only delivered into the rotor from the electrical grid[13].

Advantages of using DFIG:

- The converter only needs to handle 30% of the turbine rated power. This outstanding feature makes the required converter smaller, reducing losses and improving system efficiency.

- Filters are rated for 0.3 p.u. of total system power, so this can significantly reduce the cost of inverter filters and EMI filters [24].

- Suitable for high power applications.

- Control may be applied at a lower cost due to reduced converter power rating.

- Using the back-to-back converter in the rotor circuit with the DFIG makes the possibility of decoupled control of generator's reactive and reactive power.

- Moreover, the power factor control can be implemented at low cost because the DFIG system generally operates like synchronous generator[24].

Disadvantages :
- Increased control complexity due to increased number of switches in converters.

- Be susceptible to grid disturbances because stator winding is directly connected to the grid.

- Needed periodic slip ring maintenance.

- Requires a maintenance intensive gearbox for connection to wind turbine because it is not direct drive.

2.3.3 Multilevel inverter for High Power- Medium-Voltage Converter Topologies

Multilevel converters are very interesting for wind power system because of their outstanding features, increasing voltage of converter and decreasing harmonics.

Because of this, a bulky transformer could be avoided when the converter output is appropriate to the grid network. Therefore, it can decrease the cost per megawatt and increase the efficiency of the wind-energy conversion. The general configuration of multilevel inverter for wind power system is shown in Figure 2-7 [25]. The selected multilevel converter is shown in Figure 2-8.
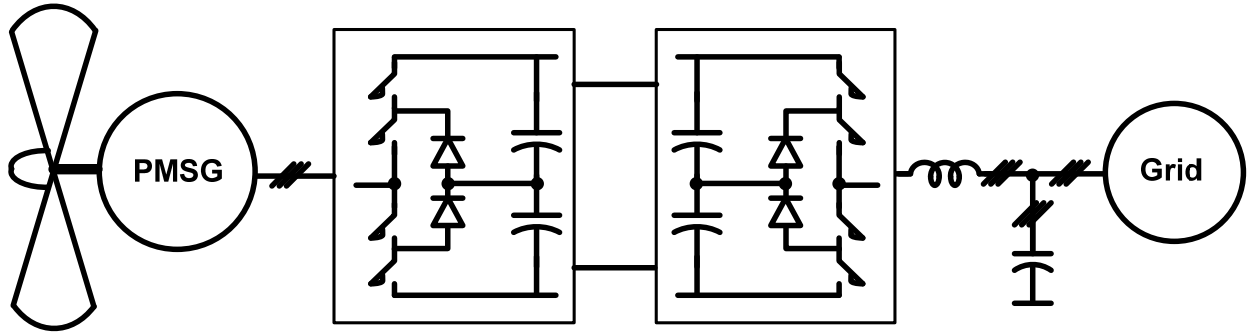
Figure 2-7 Multilevel converter based for wind power generator system.

(a)　　　　　　　　　　　　　(b)
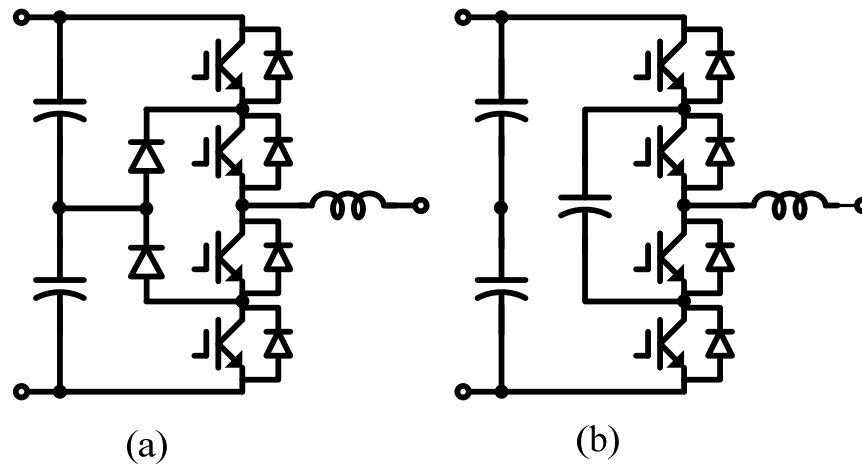
Figure 2-8 Multilevel topologies

a) One inverter leg of a three-level diode clamped multilevel converter

b) One inverter leg of a three-level flying capacitor multilevel converter

Multilevel converters provide many advantages. Originally, the main purpose of the multilevel converter was to achieve a higher voltage capability of the converter. Moreover, it can reduce EMI and content of harmonics in the input and output voltage.

Switching losses are another feature of the multilevel converter. It is stated that for the same harmonic performance the switching frequency can be reduced to 25% of switching frequency of a two-level converter. However, conducting losses may increase because the number of active switches increase[26].

Disadvantages of multilevel converters are pretty much about voltage balancing. The voltage imbalance between upper and lower DC-link capacitor is the most commonly reported disadvantage of the three-level converter with split DC-link. However, these problems can be solved by the use of modulation control of switches or hardware[27].

The conclusion and comparison of topologies is shown in the Table 2.

Table 2 Topology Comparison
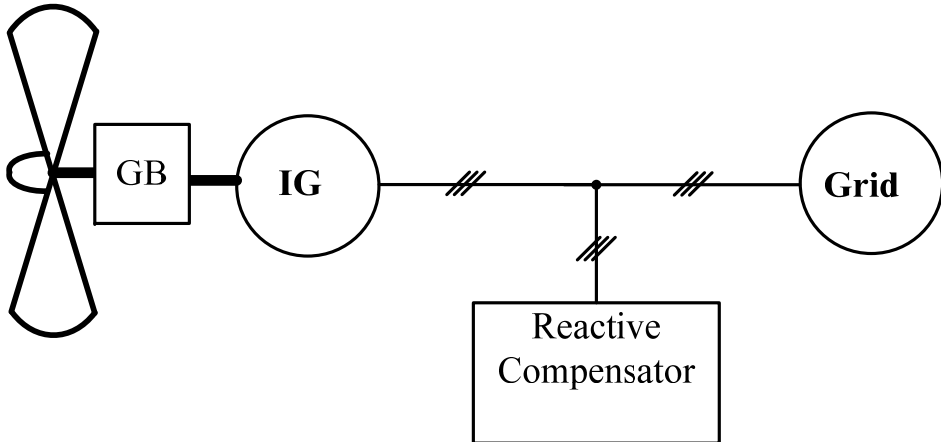
	Topologies	Advantages	Disadvantages
I	Cage induction generator based fixed speed wind turbine without power electronics	• Simple • Rugged, reliable and low maintenance IG	• Needed reactive compensator • Operated at constant speed (1-2%)[13, 15] • Impossible optimal power control • Like a fan operation at no wind or low wind speed • Required soft switching

Table 2 Topology Comparison (Cont'd)
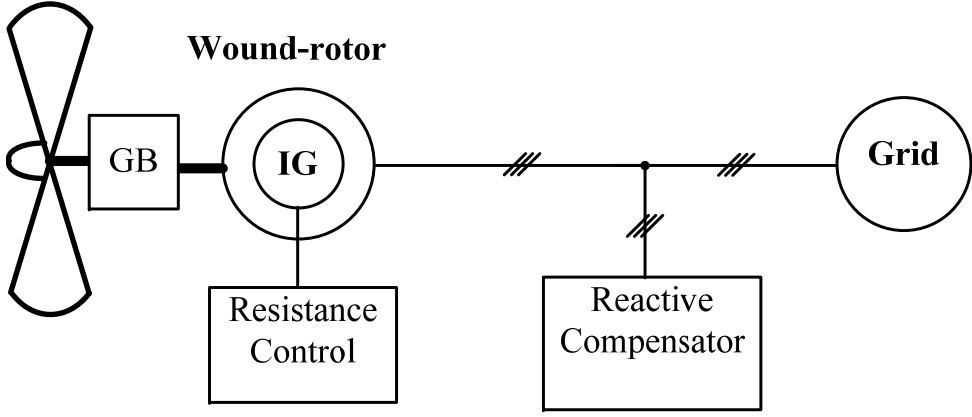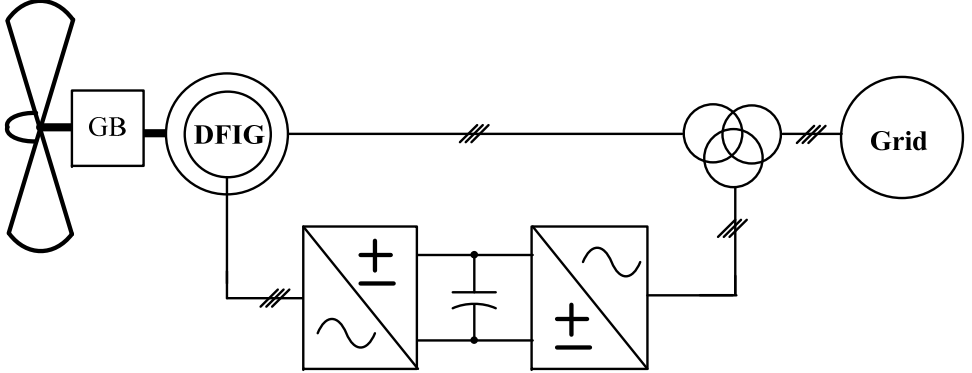
II	**Wound-rotor** GB — IG — Grid Resistance Control · Reactive Compensator Wind turbine topology with partially power electronics	• Simple • Rugged, reliable and low maintenance IG	• Needed reactive compensator • Operated at almost constant speed (2-5%) • Required soft switching • Not possible for optimal power control • Required maintenance of slip rings
III	GB — DFIG — Grid Doubly-fed induction generator	• Be suitable for high power application • Reduced rated power of converter and filter to 0.3 pu • Wider rang of speed (30 %) • Decoupled reactive and active control	• Increased control complexity • Needed periodic slip ring maintenance

Table 2 Topology Comparison (Cont'd)
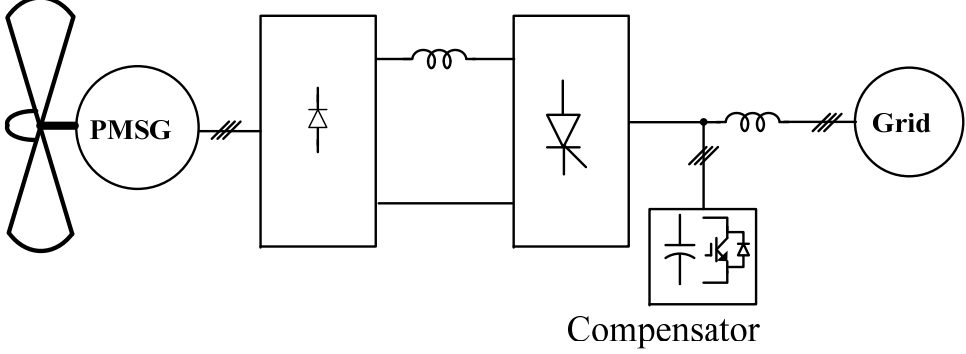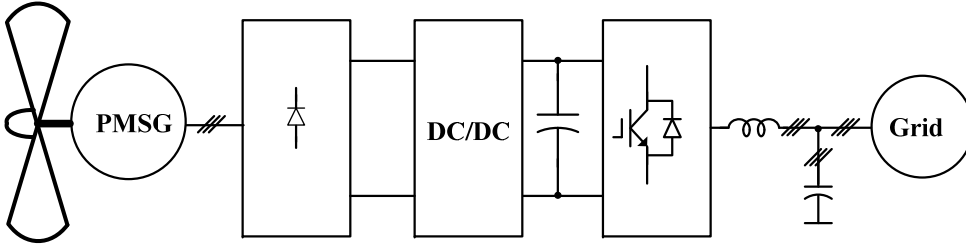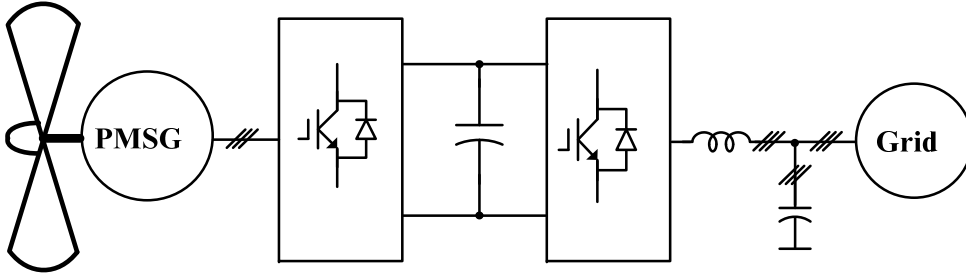
IV	PMSG based WECS with diode rectifier and thyristor supply-side inverter	• Lower device cost • Higher available power rating • Turbine's speed can be controlled through thyrister inverter	• Poor harmonic distortion in machine current • Needed active compensator for reactive power demand and harmonic distortion
VI	PMSG based with diode rectifier and intermediate DC/DC converter	• Output control is more flexible • Fast control for active and reactive power • MPPT is done by DC/DC converter • Wide range speed operation	• Needed extra DC-DC converter • Input PF can not be controlled. • Poor harmonic distortion in machine current[23]
VI		• Wide range of rotor speed • Fast control for active and reactive power • MPPT is controlled through rectifier inverter side • Reduced	• Increased conduction losses and switching losses

Table2 Topology Comparison (Cont'd)
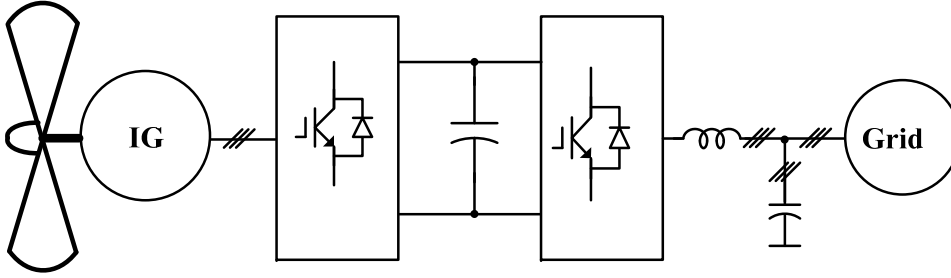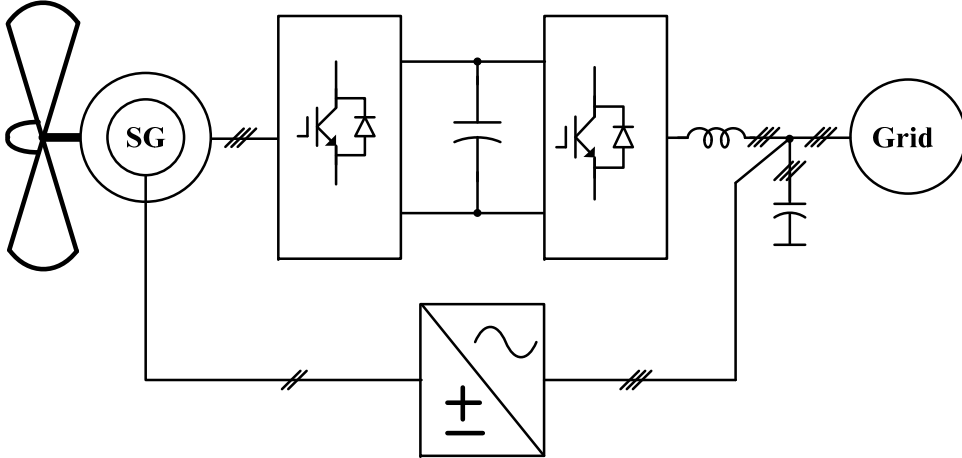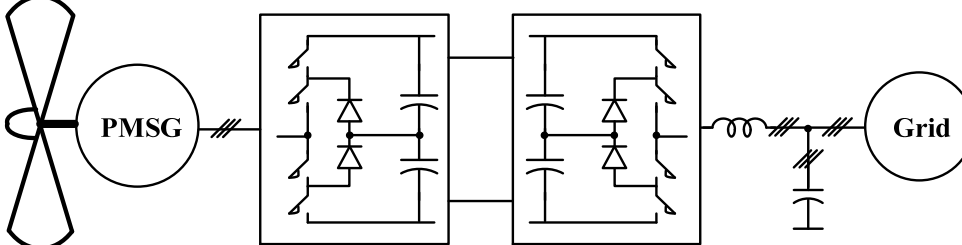
	PMSG based with back- to- back PWM converters	harmonic distortion in line and machine current • Not required reactive power to start PMSG	
VII	 Induction generator with back- to- back converter [23]	• Reduced harmonic distortion in line and machine current. • Fast control for active and reactive power • Increased line and machine power factor [23] • MPPT is controlled through rectifier inverter side • Low capital cost for the construction of IG • IG is rugged and simple design	• Increased conduction losses and switching losses • Required reactive power to start IG

Table 2 Topology Comparison (Cont'd)

VIII	Synchronous generator with back to back converters	• Reduced harmonic distortion in line and machine current. • Fast control for active and reactive power • Increased line and machine power factor [23] • MPPT is controlled through rectifier inverter side • Not required reactive power injection to start SG	• Increased conduction losses and switching losses • Required AC-DC converter for Synchronous generator • Higher maintenance cost comparing to IG
IX	Multilevel converter based for wind power generator system [25]	• Increase more power and more voltage level • Reduce switching losses • Reduce harmonic and EMI • Increased efficiency	• Increase conduction losses • Voltage-balancing problem

Chapter 3. Power Electronics Control and Utility Grid Connection

3.1 Generalized power electronics converter and control

Power captured from wind power is usually transferred to the utility grid. To deliver the wind power captured to the grid, the appropriate control structure is required. Figure 3-1 shows an example of the generalized power electronics converter and its control used in wind power generation systems [46]. In this control structure, the generator can be an induction or permanent magnet synchronous generator. In this example, the induction machine is used as the generator.

The induction generator will take reactive power through the PWM rectifier. However, the reactive power at the grid side which is controlled by the PWM inverter is usually kept to zero. By doing this, it allows the PWM inverter to provide more power to the grid. To control power to the grid, the control algorithm is required for the utility grid interconnection system. The appropriate control structure is very important to provide efficient power delivery to the utility grid. Parameters like current and voltage are also needed for the control algorithm .This chapter will discuss on main control structures for the utility grid connections which mainly are synchronous and stationary frame of reference.

Figure 3-1 Control block diagram for back to back PWM converter fed wind energy system with induction generator

3.2 Control structure for the utility grid interconnections

Two mainly cascade loops, current loop and voltage loop, are applied to the grid-side converter. The internal current loop or fast loop is used to regulate the grid current and an external voltage loop is employed to control the dc-link voltage. The current loop is responsible for the power quality issues and current protection.

3.2.1 Synchronous Reference Frame Control

The synchronous reference frame control, known as dq control, uses a reference frame transformation module, e.g., abc to dq to transform the grid current and voltage waveforms into a reference frame that rotate synchronously with the grid voltage. Because the control variable becomes dc values, the controlling is much easier to be accomplished.

The structure of dq control is shown in Figure 3-2. The active current reference is determined by the outer-loop controller's output. Generally the reactive current is set to zero. However, if the reactive power control is required, a reactive power reference must be applied to the system.

The proportional-integral (PI) controller is mainly used with this control structure since it has a satisfaction behavior when regulating dc variables. The matrix transfer function of the controller in dq coordinates can be written as (3-1) [28].
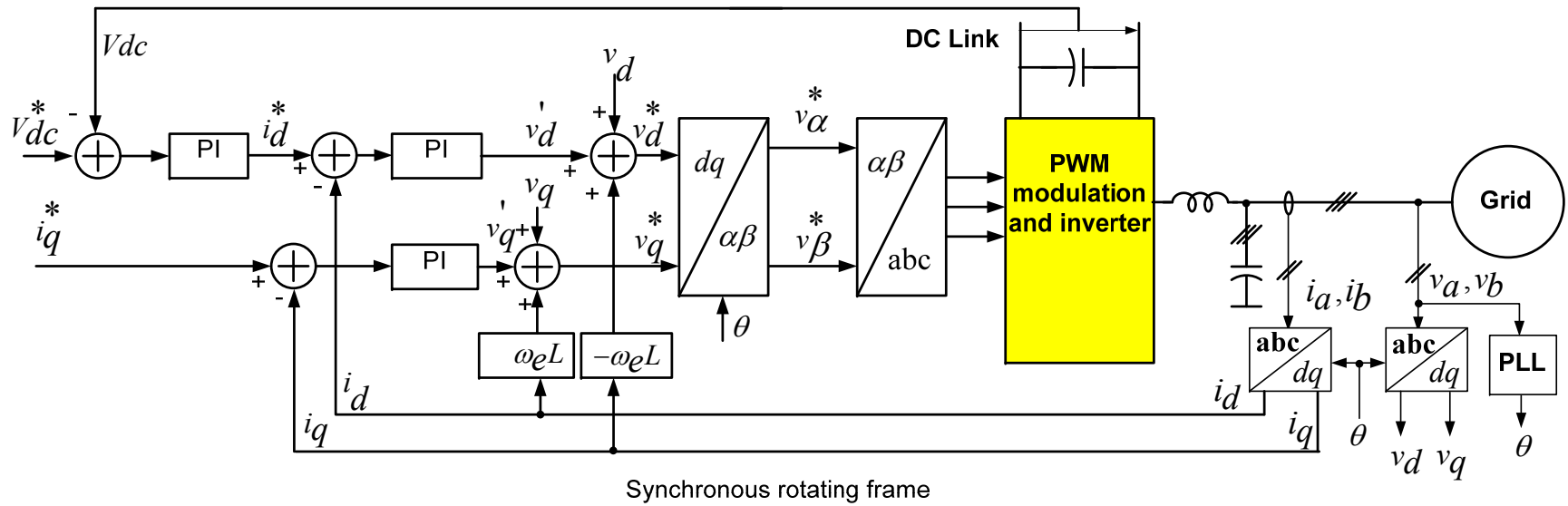
Figure 3-2 General structure for synchronous rotating frame control structure

$$G_{PI}^{(dq)}(s) = \begin{bmatrix} K_p + \dfrac{K_i}{s} & 0 \\ \\ 0 & K_p + \dfrac{K_i}{s} \end{bmatrix} \qquad (3\text{-}1)$$

In this control structure, the phase angle is necessary because the controlled current needs to be in phase with the grid voltage. For this reason, the phase detection is needed and it is derived from the grid voltage. To obtain the phase angle from the grid voltage, the methods which are known as arctangent function[29] and phase-locked loop are utilized.

3.2.2 Stationary Reference Frame Control

Using the stationary reference frame is one of alternative methods for grid connected system. The configuration of this method is shown in Figure 3-3. In this case, the sinusoidal waveforms are controlled. The steady –state error cannot be forced to zero by using PI controller whereas the proportional resonant (PR) controller is applied.

The controller matrix in the stationary reference frame is described as

$$G_{PR}^{(\alpha\beta)}(s) = \begin{bmatrix} K_p + \dfrac{K_i s}{s^2 + \omega^2} & 0 \\ \\ 0 & K_p + \dfrac{K_i s}{s^2 + \omega^2} \end{bmatrix} \qquad (3\text{-}2)$$

where ω is the resonance frequency of the controller, K_p is the proportional gain and K_i is the integral gain of the controller. The controller can provide a very high gain around the reference frequency. This outstanding performance of the *PR* controller makes it possible to eliminate the study-state error between the reference signals and controlled signals. K_i is used to determine the width of the frequency band around the resonance point. The bigger K_i provide the wider band, whereas the smaller K_i introduce the narrow band.
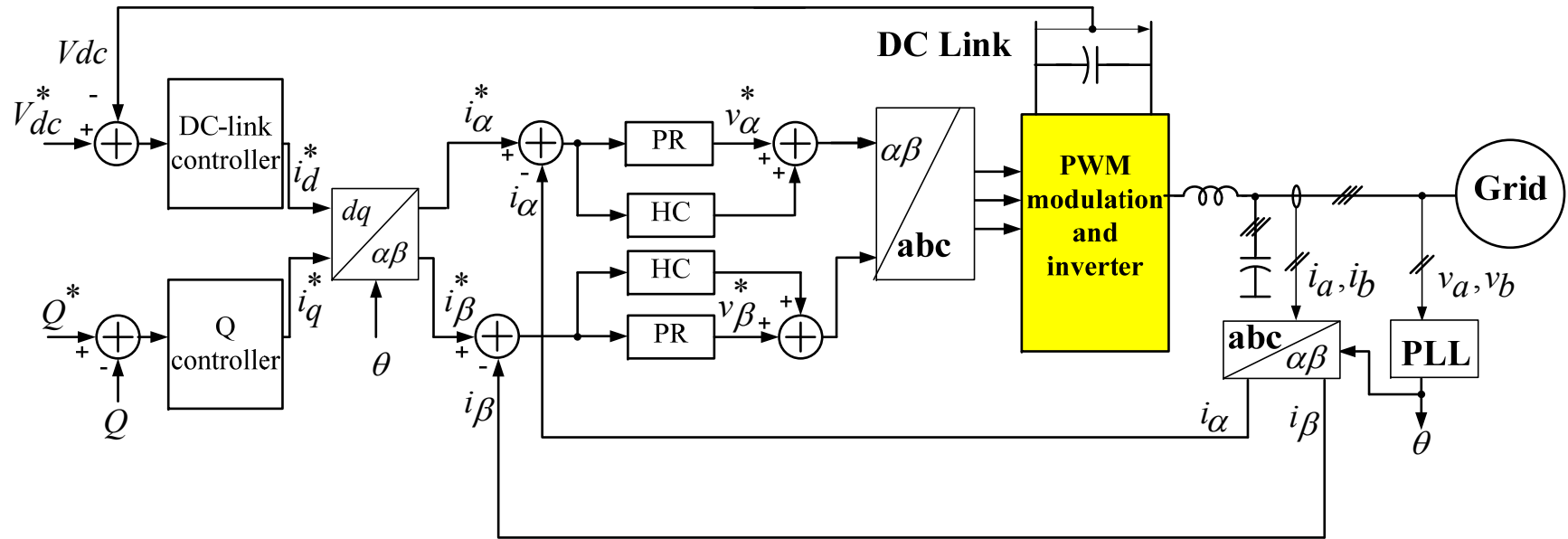
Figure 3-3 Stationary Reference Frame Control

Chapter 4. Grid Synchronization Methods

In order to interface the inverter to the utility grid the important information of the grid like phase voltage and frequency is needed. In this chapter, the grid synchronization methods will be explained in details. There are several types of the grid synchronization algorithm, zero crossing, filtering of grid voltage and phase lock loop technique. Among these methods, the phase lock loop technique offers more accurate synchronization method.

4.1 Zero Crossing

The zero crossing method is the simplest method to be implemented. However, this method gives low performances especially when there are variations on grid voltages such as harmonics.

4.2 Filtering of Grid Voltages

This method is better than the zero crossing but it encounters difficulty to extract the phase angle when grid voltage variation or fault occurs. The voltage angle of the utility grid is accomplished by using arctangent function. The delay of processing signal is also introduced when the filtering is used. This is not acceptable in the aspect of the grid voltage angle. Therefore, the appropriate filter design is essentiality.

The method can be used both dq and $\alpha\beta$ reference frame. However, it is sensitive to voltage unbalance which becomes the main drawback of this method. The summation of filter design is detailed in [30].

4.2.1   *dq* Filter algorithm

In the dq reference frame, since Vd and Vq are dc variables, several filtering techniques can be used to obtain clear signals, for instance notch filter, low-pass filter, and band-stop filter. Among them, the Delayed Signal Cancellation (DSC) is an effective detection method both steady state and transient performance[31]. The *dq* filter algorithm is shown in Figure 4-1.
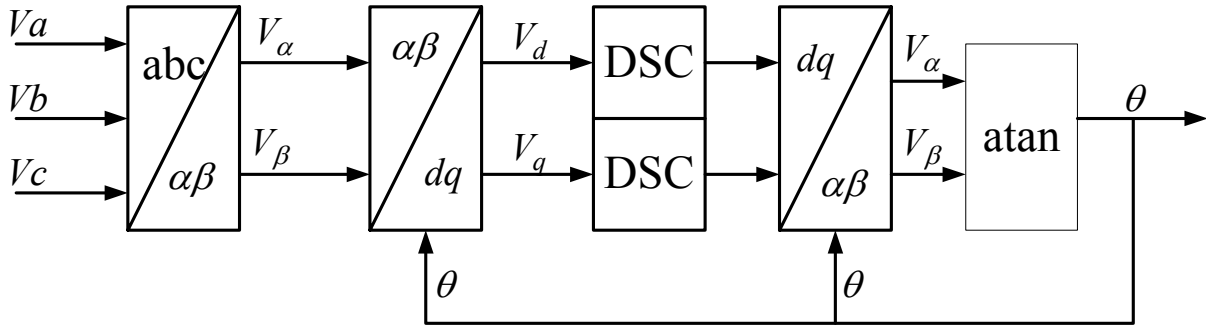
Figure 4-1 Synchronization method using filtering on the *dq* synchronous rotating reference frame

In the $\alpha\beta$ reference frame, the method is expressed as

$$e_{pos}^{\alpha\beta}(t) = 0.5[e^{\alpha\beta}(t) + je^{\alpha\beta}(t - T/4)]$$

$$e_{neg}^{\alpha\beta}(t) = 0.5[e^{\alpha\beta}(t) - je^{\alpha\beta}(t - T/4)]$$

(4-1)

where *T* is the period of fundamental frequency. This method implies delaying of the signal by 1/4 of period at the fundamental frequency. So the inherent time delay is initiated.

4.2.2 $\alpha\beta$ Filter algorithm

The $\alpha\beta$ filter algorithm is depicted in Figure 4-2.
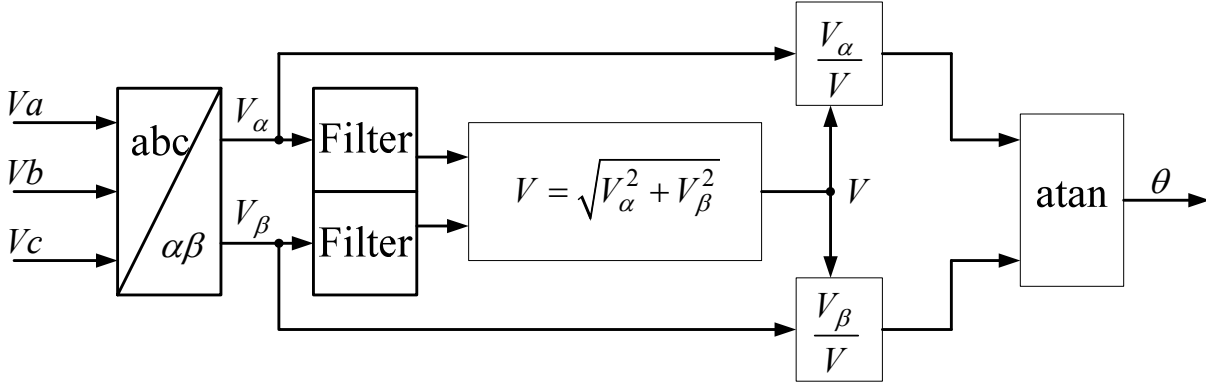
Figure 4-2 Synchronization method using filtering on the *dq* synchronous rotating reference frame

A major drawback of this method is its sensitivity to the grid frequency deviations and voltage unbalance[29].

If the control structure uses the $\alpha\beta$ reference (stationary frame), the grid voltage angle is not necessary because the component reference can be directly used.

4.2.3 Phase Locked Loop Technique

The three-phase *dq-PLL* configuration is shown in Figure 4-3. This grid synchronization method is implemented in the *dq* reference frame. The phase angle is detected by synchronizing the PLL rotating reference frame and the utility voltage vector. The lock is accomplished by setting the reference V_d^* to zero [32]. A PI is used as a controller and the output of this

controller is the grid frequency. The grid voltage angle is achieved after combining the grid frequency. This angle is fed into the $\alpha\beta - dq$ transformation module. This method has a better rejection of grid harmonics, notches, and any other kind of disturbance. The improvement of the overall tracking performance of the PLL is obtained by adding the feed forward frequency command, ω_{ff} [33].
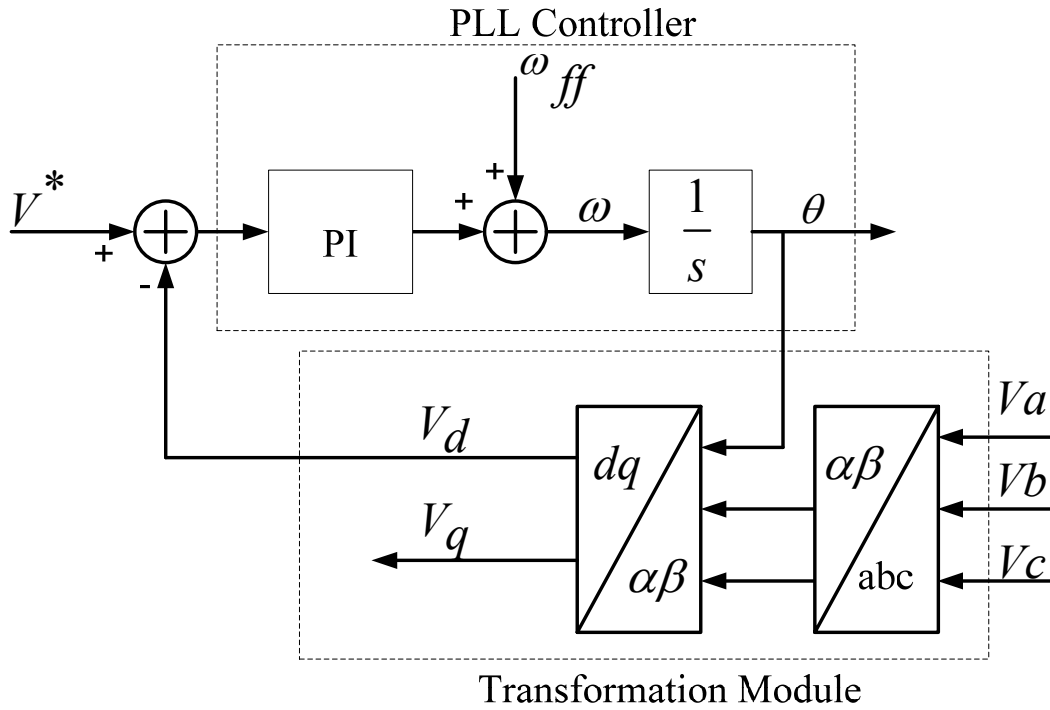
Figure 4-3 Three-phase *dq-PLL* configuration

Table 3 Comparison of some synchronization algorithms [30]

Algorithm	Strong points	Weak points
dq Filter	Simplicity	On frequency shift variation
$\alpha\beta$ Filter	Simplicity	On unbalanced grid
dq-PLL	Works on every grid type, provide ride through capability	Slow dynamics

Chapter 5. Z-source Inverter and Its control

In this chapter, the basic principle and control strategies of the Z-source inverter will be discussed. There are several major control strategies of the Z- source inverter which are simple boost control, maximum boost control and maximum constant boost control methods. Among these control strategies, the maximum boost control strategy provides highest boost factor and lowest voltage stress.

5.1 Z-Source Inverter

Figure 5-1 shows the general structure of the Z-source inverter proposed in [1]. To perform its unique feature, this converter utilizes the impedance network which consists of two capacitors connected in an X fashion with two inductors. These two inductors can be implemented in a split core inductor in order to save space and size.

The operating principle of the Z-source inverter has also been explained thoroughly in [1] .This impedance network provides unique features and advantages over the typical inverters.
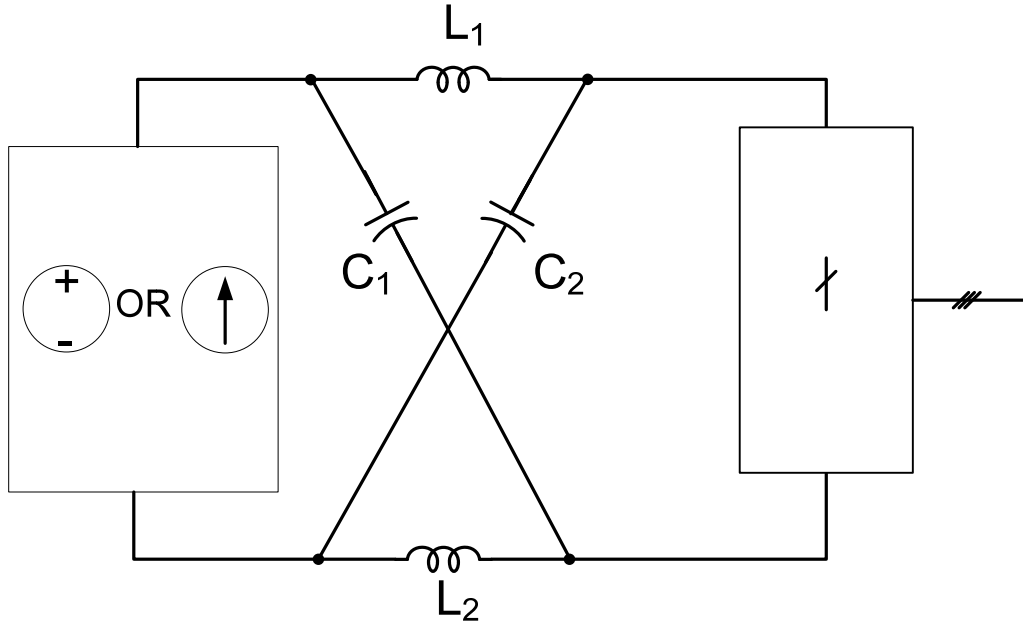
Figure 5-1 General structure of the Z-source converter

The Z-source inverter advantageously utilizes the shoot-through states to boost the dc bus voltage by gating on both the upper and lower switches of a phase leg. Figure 5-2 shows the circuit of the Z-source network during the shoot-through state. Therefore, the capacitor voltage is boosted during this state. This is because the current ramps up through the inductors, whose voltages are $V_L = L \frac{di}{dt}$. Thus inductor voltage increases, due to the increasing current. The capacitors are in parallel with the inductors during this state, therefore the capacitor voltage is also increased, which boosts the dc link voltage during the nonshoot-through states. Therefore, the Z-source inverter can buck (by lowering the modulation index) and boost voltage to a desired output voltage that is greater than the available dc bus voltage. In addition, the reliability of the inverter is greatly improved because the shoot-through can no longer destroy the circuit. Thus it provides a low-cost, reliable, and highly efficient single-stage structure for buck and boost power conversion.
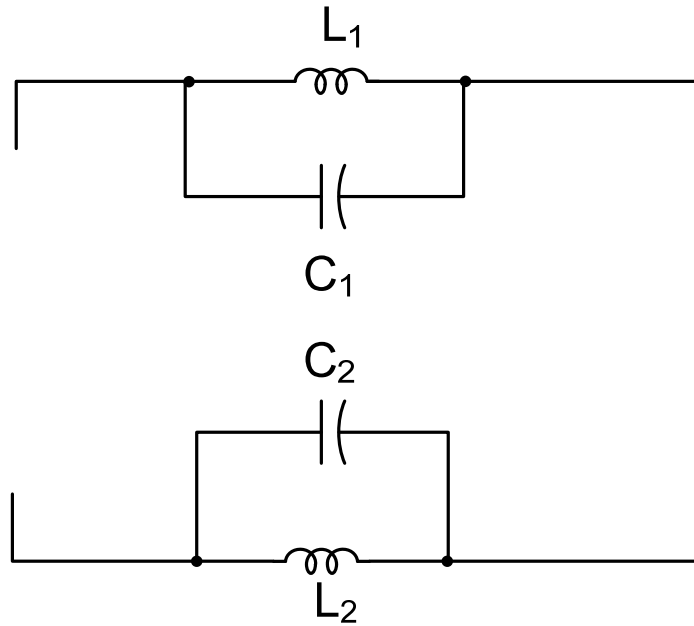
Figure 5-2 Z-source network during the shoot-through state

Figure 5-3 shows an experimental result to verify the principle of the Z- source inverter. During the shoot-through state, the capacitor voltage is boosted during this state because the current ramps up through the inductors. The inductor current increases, so that inductor voltage increases.
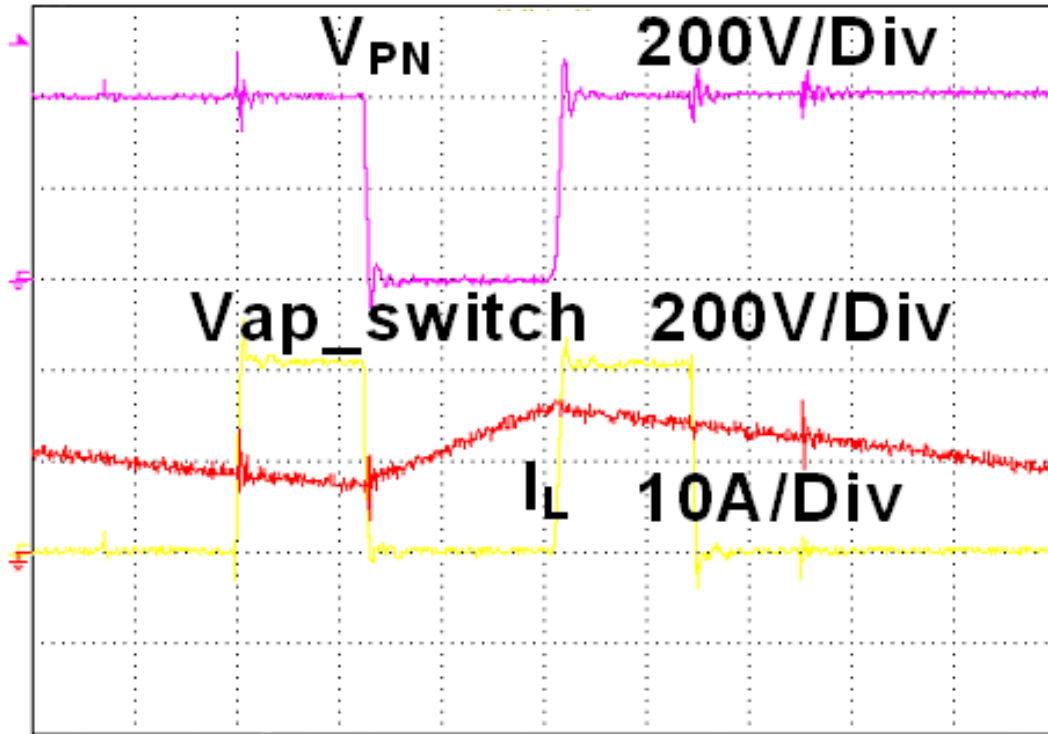
Figure 5-3 Experimental waveforms when shoot-thought state is applied

5.2 Control of Z-Source Inverter

Unlike conventional inverter, shoot-through state can be used in the control of the Z-source inverter to boost up voltage. The control of the shoot-through interval has been detailed as in [34-36]. Based on this reference, there are several methods used to control the Z-source inverter: simple boost, maximum boost, maximum boost with third harmonics injection, and maximum constant boost control. Among them, maximum boost control is chosen for this design because of its lower voltage stress across inverter bridge switches [36]. The Z-source inverter in Figure 5-4 will be used for the discussion on the control strategies.
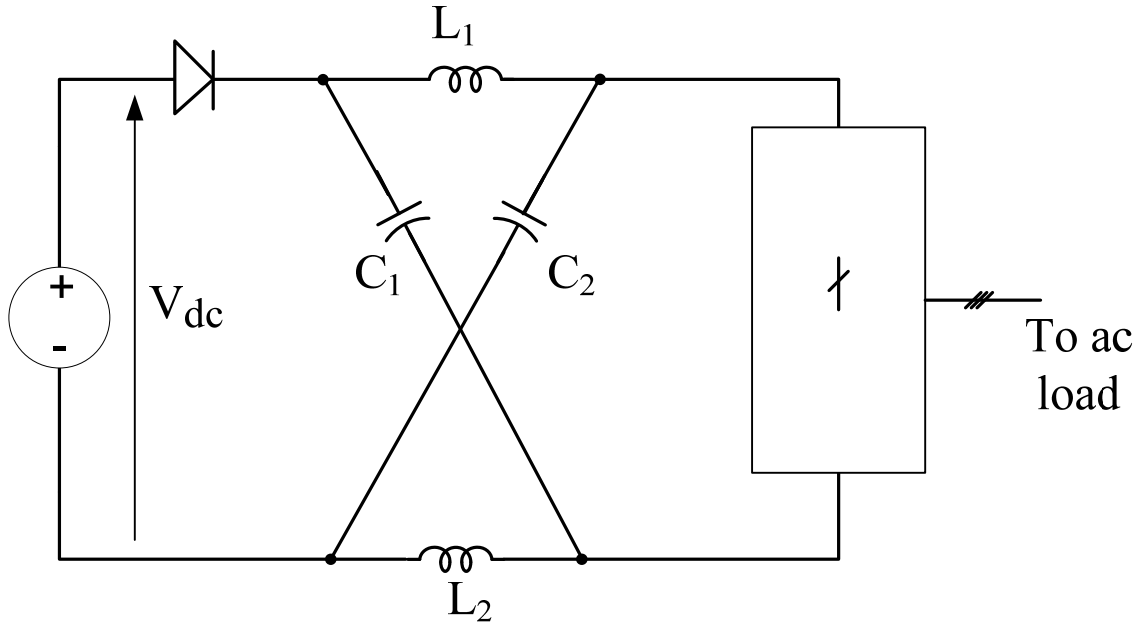
Figure 5-4 Z-source inverter

5.2.1 Simple Boost Control Strategy

5.2.2

Figure 5-5 shows the simple boost control strategy. In this control, two straight line references V_P and V_N are utilized as the control reference to generate shoot- through duty ratio whereas the normal PWM-signal can be generated by the conventional sinusoidal PWM references, V_a, V_b and V_c. D_0 is the shoot through duty ratio which can be expressed as in (5-1) and the boost factor, B can be expressed in (5-2).

$$D_0 = \frac{T_0}{T} \qquad\qquad (5\text{-}1)$$

$$B = \frac{1}{1 - 2D_0}$$ (5-2)

The T_0 is the shoot-through time interval over a switching cycle, T. The modulation index, M,

on this control have to be less than or equal to $1 - D_0$. In this control, as the shoot-through duty

ratio decrease, the modulation index will increase. This shoot-through duty ratio is limited by

modulation index. When the modulation index is equal to one, the shoot-through duty ratio is

zero, hence producing unity boost factor. In this case, the Z-source inverter will operate like a

conventional inverter.

The relationship between the voltage gain and modulation index is expressed   in (5-3) to (5-4)

and the voltage stress across the switch devices is explained in (5-5).

$$G = MB = \frac{\hat{V}_{ac}}{V_{dc}/2} = \frac{M}{2M - 1}$$ (5-3)

$$M = \frac{G}{2G - 1}$$ (5-4)

$$V_S = BV_{dc} = (2G - 1)V_{dc}$$ (5-5)

In order to generate an output voltage which need higher voltage gain, the small modulation

index is required and eventually the voltage stress will increase. The limitation of simple boost

control strategy is the restriction of an obtainable voltage gain because of device voltage rating.
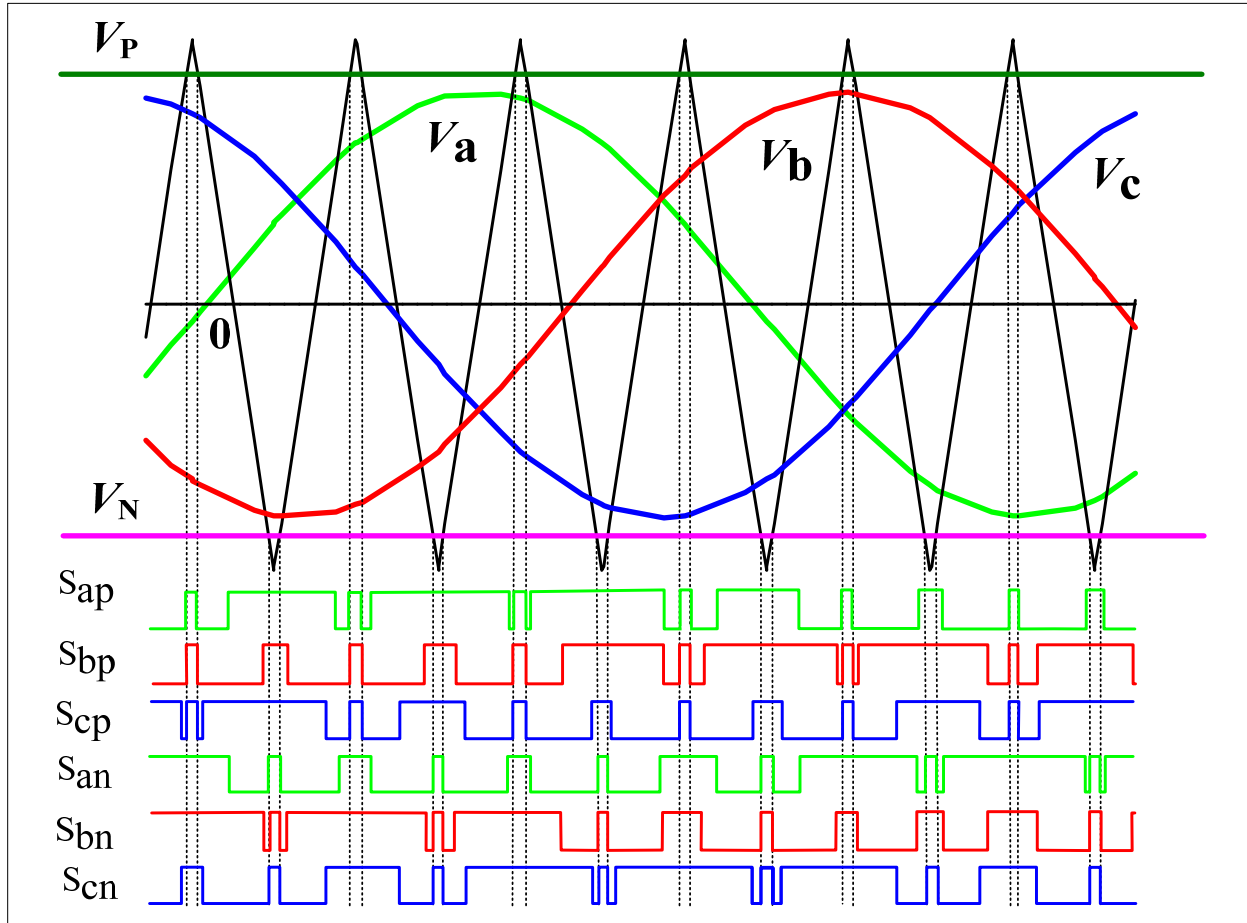
Figure 5-5 Simple boost control strategy

This control strategy provide the constant shoot-through time per switching cycle, hereby producing constant boost factor. As the result, the capacitor voltage and inductor current have no ripples related to output frequency.

5.2.3 Maximum Constant Boost Control Strategy

Figure 5-6 shows the maximum constant boost control strategy. In this control, the shoot

through state is determined by the reference V_P and V_N whereas V_a, V_b and V_c are utilized to generate the normal active-PWM-signal which is similar to a typical inverter. The shoot-through reference signals are periodical with three times of the output frequency. These shoot-through reference signals can be implemented as follows [35]:

I. For $0 < \theta < \dfrac{\pi}{3}$, the first half period, the references can be expressed as (5-6) and (5-7) for upper and lower references, respectively.

$$V_{P1} = \sqrt{3}M + \sin(\theta - \frac{2\pi}{3})M \qquad\qquad (5\text{-}6)$$

$$V_{N1} = \sin(\theta - \frac{2\pi}{3})M \qquad\qquad (5\text{-}7)$$

II. For $\dfrac{\pi}{3} < \theta < \dfrac{2\pi}{3}$, the second-half period, the references can be expressed as (5-8) and (5-9) for upper and lower references, respectively.

$$V_{P2} = \sin(\theta)M \qquad\qquad (5\text{-}8)$$

$$V_{N2} = \sin(\theta)M - \sqrt{3}M \qquad\qquad (5\text{-}9)$$

The upper shoot-through reference is always equal to or higher than the maximum value of the PWM reference signals and the lower shoot-through is always equal to or lower than the minimum value of the PWM reference signals. The shoot-through states only take place during conventional zero states of the conventional PWM references. Therefore, the conventional PWM reference signals which are used to generate active states still regulate output waveforms.
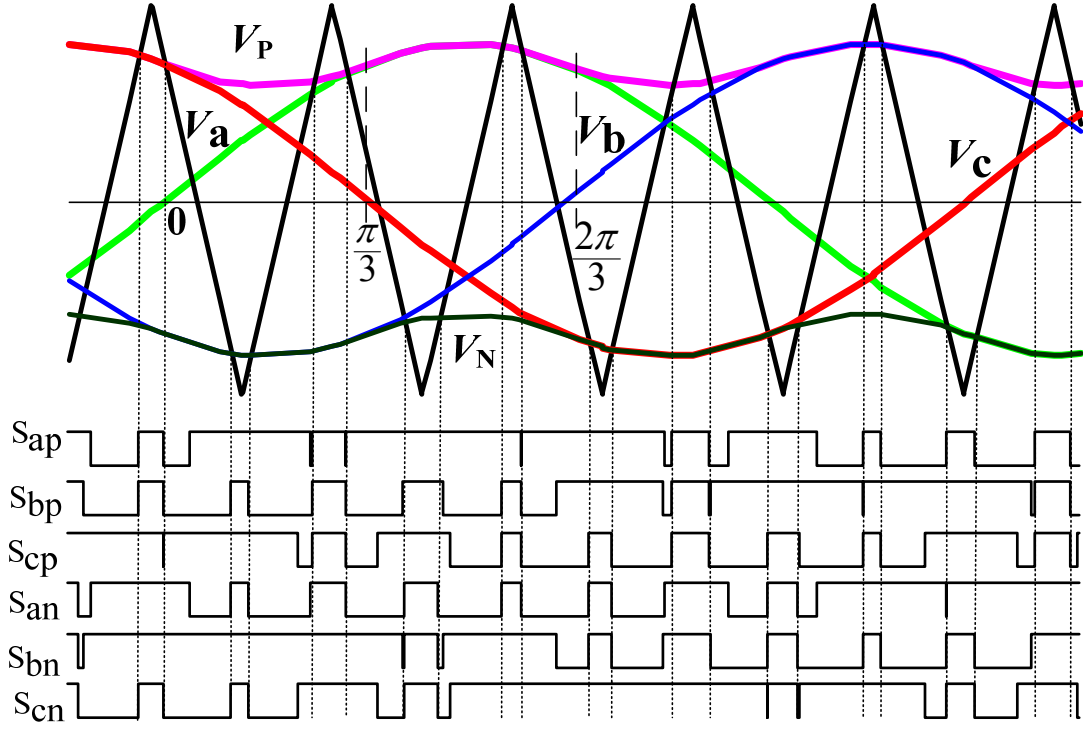
Figure 5-6 Maximum Constant Boost Control

The distance between two reference signals (V_P and V_N) generated shoot-through duty ratio is constant for a given modulation index. This distance is $\sqrt{3}M$ .Therefore the shoot-through duty ratio is constant and can be expressed as in (5-6).

$$D_0 = 1 - \frac{\sqrt{3}M}{2} \tag{5-6}$$

Using constant shoot-through duty ratio can eliminate low-frequency current ripple. This will result in size and cost reducing. In this control, the boost factor and voltage gain are expressed as in (5-7) and (5-8), respectively.

$$B = \frac{1}{\sqrt{3}M - 1} \tag{5-7}$$

$$G = MB = \frac{M}{\sqrt{3}M - 1} \tag{5-8}$$

Voltage stress of the maximum constant boost control strategy is expressed as (5-9).

$$V_S = (\sqrt{3}G - 1)V_d \tag{5-9}$$

This control strategy not only offer maximum constant shoot-through duty ratio, but also reduce device voltage stress.

5.2.4 Maximum Boost Control Strategy
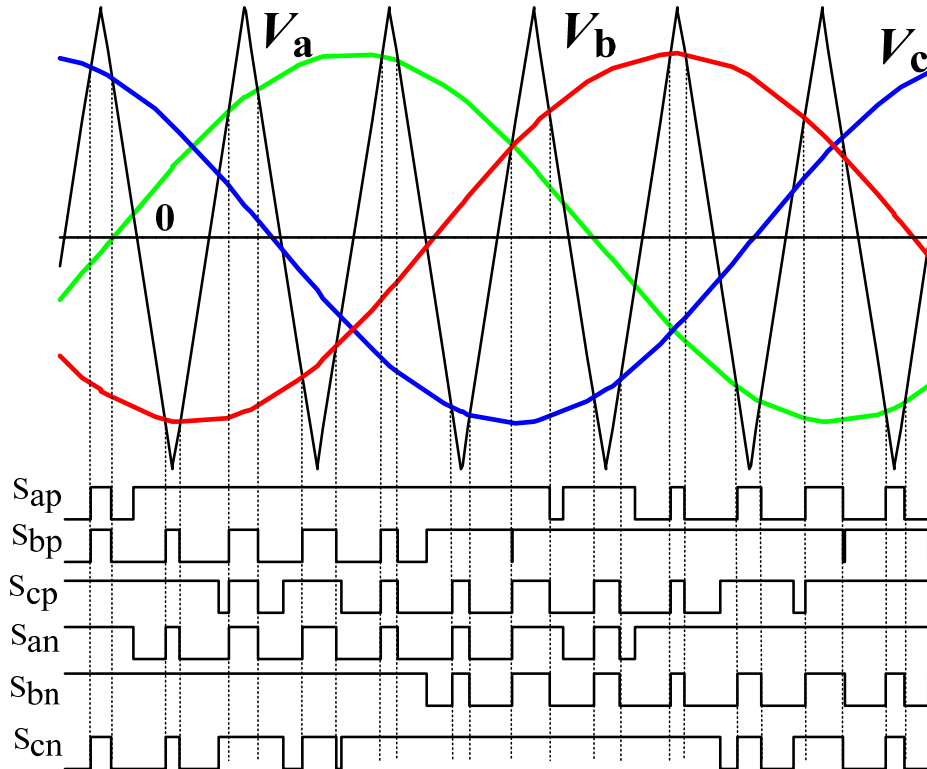
Figure 5-7 Maximum boost control

Figure 5-7 shows the sketch map of maximum boost control principle[36]. In this control method, all six-active states are still unchanged, whereas all zero states are basically turned into shoot-through states. The shoot-through states are determined by comparing the triangle carrier wave with reference signals (V_a, V_b, V_c). With this comparison, the shoot-through states are introduced when either the triangle wave is bigger or smaller than the reference.

The shoot-through duty ratio over one switching cycle in the interval $(\pi/6, \pi/2)$ is expressed as

$$\frac{T_0(\theta)}{T} = \frac{2 - (M \sin\theta - M \sin(\theta - \frac{2\pi}{3}))}{2} \tag{5-10}$$

By integrating the shoot-through over the interval, the average duty ratio is obtained as

$$\frac{\overline{T_0}}{T} = \frac{2\pi - 3\sqrt{3}M}{2\pi} \tag{5-11}$$

The boost factor is determined by the maximum boost control, becoming

$$B = \frac{1}{1 - 2\frac{\overline{T_0}}{T}} = \frac{\pi}{3\sqrt{3}M - \pi} \tag{5-12}$$

Consequently, the output peak phase voltage becomes

$$\hat{v}_{ac} = MB\frac{V_d}{2} = \left(\frac{\pi M}{3\sqrt{3}.M - \pi}\right)\frac{V_d}{2} \tag{5-13}$$

The capacitor voltage can be expressed in (5-13) where V_{C1} and V_{C2} are the voltage across the

capacitor C_1 and C_2, respectively.

$$V_{C1} = V_{C2} = V_C = \frac{1 - \frac{\overline{T_0}}{T}}{1 - 2\frac{\overline{T_0}}{T}} V_d = \frac{B+1}{2} V_d \qquad (5\text{-}14)$$

The voltage gain and voltage stress of the maximum boost control strategy can be expressed as

$$G = \frac{\pi M}{3\sqrt{3}M - \pi} \qquad (5\text{-}15)$$

$$V_S = (\frac{3\sqrt{3}G}{\pi} - 1)V_{dc} \qquad (5\text{-}16)$$

5.3 Control strategy comparison

Figure 5-8 shows the comparison of three-control strategy and the relevant equation shows in the Table 4. As can be seen from the figure, the maximum boost control provides the highest voltage gain, whereas the maximum constant boost control offers a bit higher voltage gain than the simple boost control.
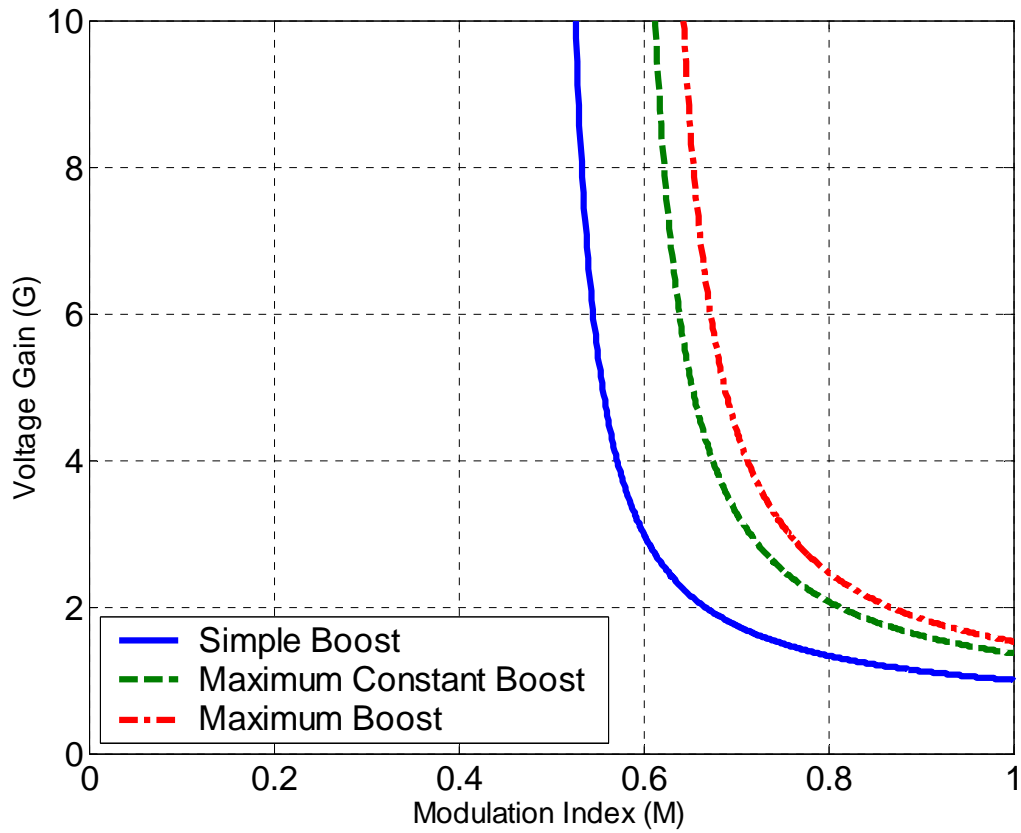
Figure 5-8 Comparison of three-control strategy

Figure 5-8 shows the comparison of voltage stress versus voltage gain. It is clear that the maximum boost control strategy provides lower voltage stress across the inverter bridge switches.

Table 4 Control Strategy Comparison

Control Strategies and its functions	Simple Boost Control	Maximum Constant Boost Control	Maximum Boost Control
Shoot-through Duty Ratio	$\dfrac{T_0}{T}=1-M$	$\dfrac{T_0}{T}=1-\dfrac{\sqrt{3}M}{2}$	$\dfrac{\bar{T}_0}{T}=\dfrac{2\pi-3\sqrt{3}M}{2\pi}$
Boost Factor	$B=\dfrac{1}{(1-2\dfrac{T_0}{T})}$	$B=\dfrac{1}{\sqrt{3}M-1}$	$B=\dfrac{\pi}{3\sqrt{3}M-\pi}$
Voltage Gain	$G=MB$	$G=\dfrac{M}{\sqrt{3}M-1}$	$G=\dfrac{\pi M}{3\sqrt{3}M-\pi}$
Voltage Stress	$V_S=(2G-1)V_{dc}$	$V_S=(\sqrt{3}G-1)V_{dc}$	$V_S=(\dfrac{3\sqrt{3}G}{\pi}-1)V_{dc}$
Voltage Stress/Equivalent DC Voltage	$\dfrac{V_S}{GV_{dc}}=(2-\dfrac{1}{G})$	$\dfrac{V_S}{GV_{dc}}=(\sqrt{3}-\dfrac{1}{G})$	$\dfrac{V_S}{GV_{dc}}=(\dfrac{3\sqrt{3}}{\pi}-\dfrac{1}{G})$
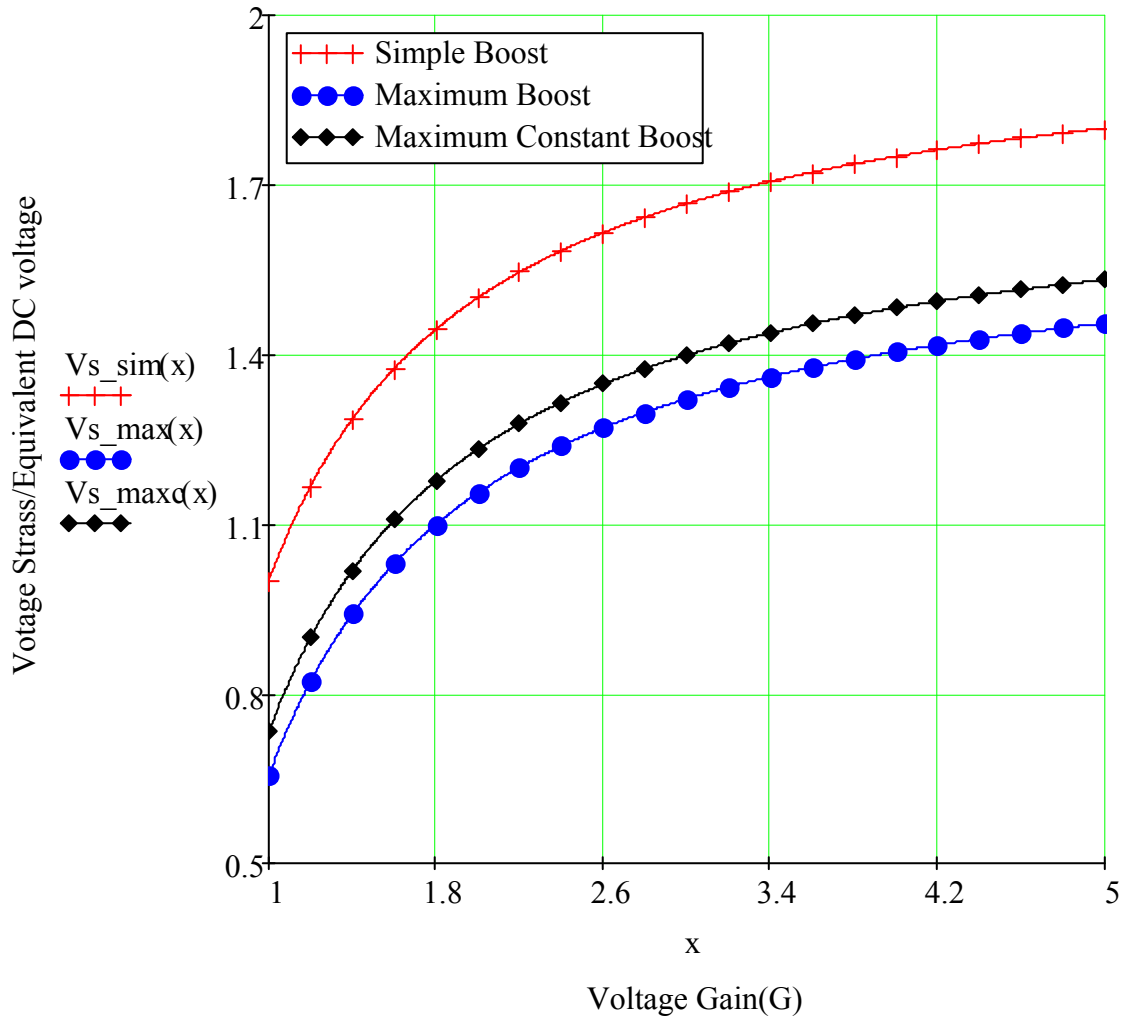
Figure 5-9 The comparison of voltage stress versus voltage gain

The equivalent dc voltage is utilized to study the voltage stress across the switch devices and this equivalent dc voltage is defined as the minimum dc voltage required for the traditional voltage source inverter to produce an output voltage [35] . The equivalent dc voltage is defined as GV_{dc} . This relationship represents the voltage stress that devices at inverter bridge of the Z-source inverter has to handle to achieve the voltage boost. For example, on maximum boost

control strategy, the voltage stress 10% higher than conventional converter to achieve 1.8 voltage gain. In this chapter, the control strategy has been reviewed. The maximum boost control provides highest voltage gain and lowest voltage stress across the switch devices.

Chapter 6.Proposed Z-Source Inverter for WECS-Analysis and Design

6.1 Introduction

Using a Permanent Magnet Synchronous Generator (PMSG) as a power source for wind energy conversion systems has many advantages. The direct-drive PMSG based wind turbine offers high efficiency and low maintenance cost.

In comparison to the back-to-back PWM inverter, an uncontrolled diode rectifier is lower cost, since the back-to-back PWM converter has expensive active power switches whereas the uncontrolled diode rectifier does not.

The diode rectifier is not controllable, so the grid side inverter needs to be used to regulate the MPPT of the system by controlling the generator speed.

The dc-dc boost converter is utilized to maintain the dc-link voltage for the inverter bridge and also to regulate the maximum power point tracking of the turbine without any information of wind speed and generator speed sensor[37].

Since the wind speed is not constant, it makes output voltage of the generator varying. Under the low wind speed and low output voltage, to be sure that the inverter can deliver power to the grid, the boost converter can be used.

In case of the usage of synchronous generator, simple 3-phase diode rectifier with dc-dc chopper is more cost effective solution for ac-dc converter than 3-phase IGBT PWM converter[37].

In this chapter, the Z-source inverter for WECS is discussed. The analysis and design will be focused.

6.2 Conventional Inverter for WECS

Figure 6-1 shows the traditional inverter for wind energy conversion system. The system includes a permanent magnet synchronous generator, diode-rectifier bridge, DC/DC boost converter, inverter bridge, LC filter and utility grid. The system converts ac input voltage to dc voltage by using the diode rectifier bridge. Then the dc voltage is boosted up by using the DC/DC boost converter to appropriate level of voltage to the inverter bridge. At the inverter bridge, the DC voltage is converted to AC voltage by using the inverter which has six switches. Even though this system is functional, it has an active switch that increases losses and cause complexity of control.
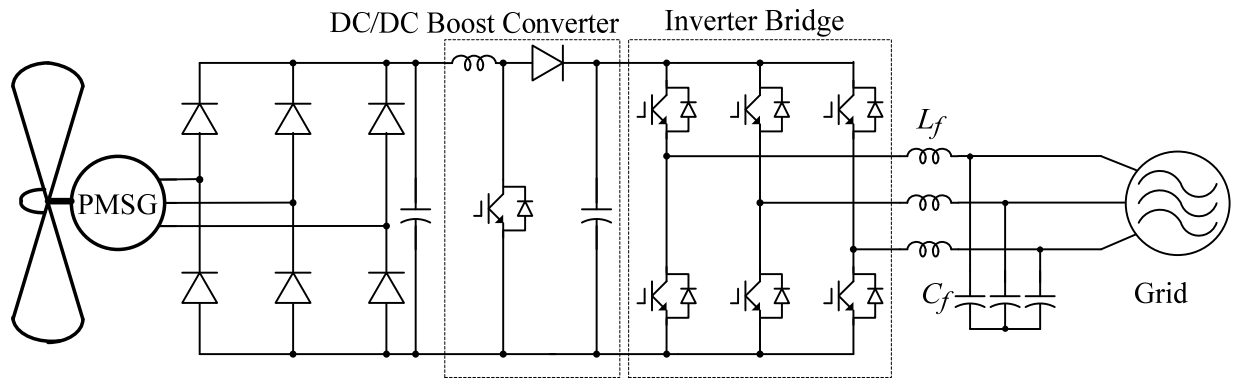
Figure 6-1 Conventional Inverter with DC/DC Boost Converter for the wind power system

6.3 Proposed Z-Source Inverter for WECS

As mentioned above, the conventional inverter with DC/DC boost converter shown in Figure 6-1 has a more active component count and also the DC/DC controller need to be added, leading to system complexity and low efficiency. Alternatively, the proposed Z-source inverter shown in Figure 6-2 [1] overcome problems mentioned. The proposed system includes a variable speed

wind turbine, permanent magnet synchronous generator, diode rectifier with input capacitors (C_a, C_b, and C_c), Z-source network, and an inverter system connected to the utility grid. Input capacitors serve as the dc source feeding the Z-source network [36]. Electrical power can be drawn from the wind power through the wind turbine. The AC power generated from the generator is converted into the DC power through diode bride rectifier circuits and then fed to the Z-source inverter. This system does not need a boost converter, since it has both boost and buck functions. This makes proposed system realistic when the generator voltage is low because of low wind speed. However, when the input voltage is high, the system can also step down the voltage to the design level. These unique characteristics allow the proposed system suitable for variable speed wind power system.
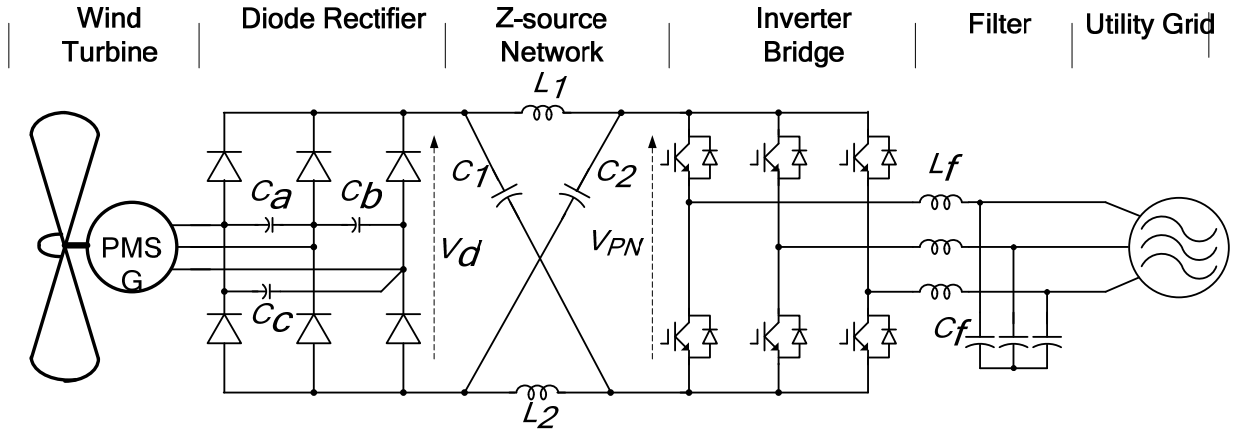
Figure 6-2 Proposed Z-source inverter for wind energy conversion system

It is assumed that the DC voltage fed to the Z-source inverter is defined in (3) where V_{LL} is the line to line voltage of the generator. In the normal operation mode, the inverter bridge voltage, V_{PN}, is equal to the dc input voltage obtained from the diode rectifier bridge, V_d as in (6-1) and

73

(6-2).

$$V_d = \frac{3\sqrt{2}}{\pi} V_{LL} = 1.35 V_{LL} \qquad (6\text{-}1)$$

$$V_{PN} = V_d \qquad (6\text{-}2)$$

The output peak phase voltage, $\hat{v}_{ac}$, generated by the inverter with normal operation mode is expressed in (6-3), where M is the modulation index.

$$\hat{v}_{ac} = M \frac{V_{PN}}{2} = M \frac{V_d}{2} \qquad (6\text{-}3)$$

However, in the boost operation mode where shoot- through states are applied, the voltage across the inverter bridge is expressed as in (6-4).

$$V_{PN} = B V_d \qquad (6\text{-}4)$$

B is the boost factor which is determined by

$$B = \frac{1}{1 - 2\frac{T_0}{T}} \qquad (6\text{-}5)$$

where T_0 is the total shoot-through period over a switching cycle, T. T_0 / T is known as the shoot-through duty ratio, D_0.

This shoot-through duty ratio is directed by the control method of the Z-source inverter which will be discussed in the next section.

Ultimately, the output peak phase voltage generated by the inverter with the boost operation mode is described by

$$\hat{v}_{ac} = M \frac{V_{PN}}{2} = MB \frac{V_d}{2} \qquad (6\text{-}6)$$

Compared with the conventional system in Figure 6-1, in the proposed system, there is no DC/DC converter to boost the voltage in the circuit. Therefore, the size and cost are minimized. Moreover, the dead time is not needed, so this advantage definitely improves the control accuracy and THD value.

Therefore, by using the Z-source inverter, the size, the cost and the number of active switching devices are minimized. Additionally, because the proposed system is single state operation, it provides higher efficiency.

6.4 Equivalent Circuit and Operating Principle for Proposed System
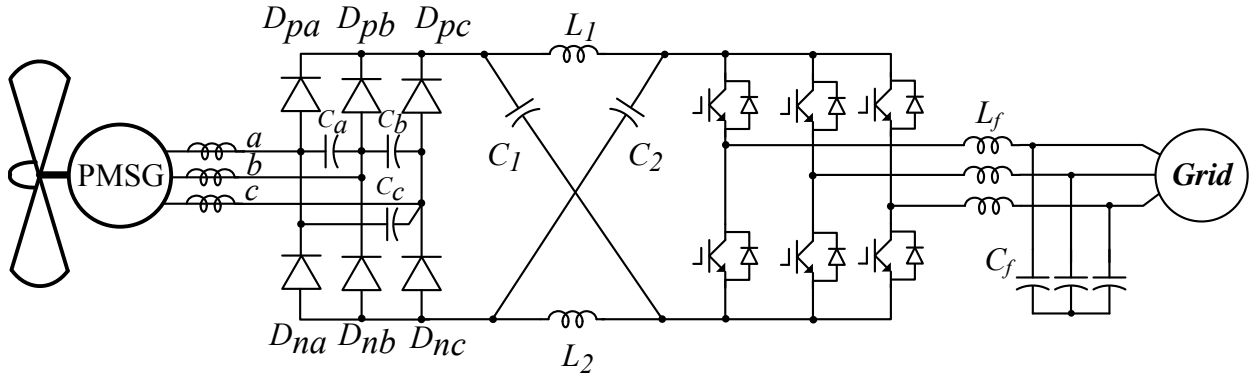
Figure 6-3 Main circuit configuration of proposed Z-source inverter for WECS

The Z-source WECS's main circuit is shown in Figure 6-3. The system composes of a diode rectifier with small input capacitors (C_a, C_b, and C_c), Z-source network (C_1, C_2, L_1, and L_2), and

an inverter bridge. Having this Z-source network and small input capacitors makes the proposed system different from the conditional WECS. Formed by the combination of a diode bride rectifier and small capacitors, a dc source feeds dc current to the Z- source network [38]. The input capacitors are used to suppress voltage surge that may occur due to the line and generator inductance during diode commutation and shoot-through mode of inverter, thus requiring small value of capacitance. At any instant of time, there are only two phases that have the largest potential difference may conduct and carry current from the ac line to the dc side.

The rectifier's six possible conduction intervals per cycle are shown in Figure 6-4 [38]. The two diodes (D_{pa}, D_{pb}, D_{pc} and D_{nb}, D_{nc}, or D_{na}) conduct as a pair with the corresponding capacitor(C_a, C_b, or C_c), respectively. As the result, the diode bridge, viewed from the Z-source network, is modeled as a dc source in series with two diodes shown in Figure 6-5.
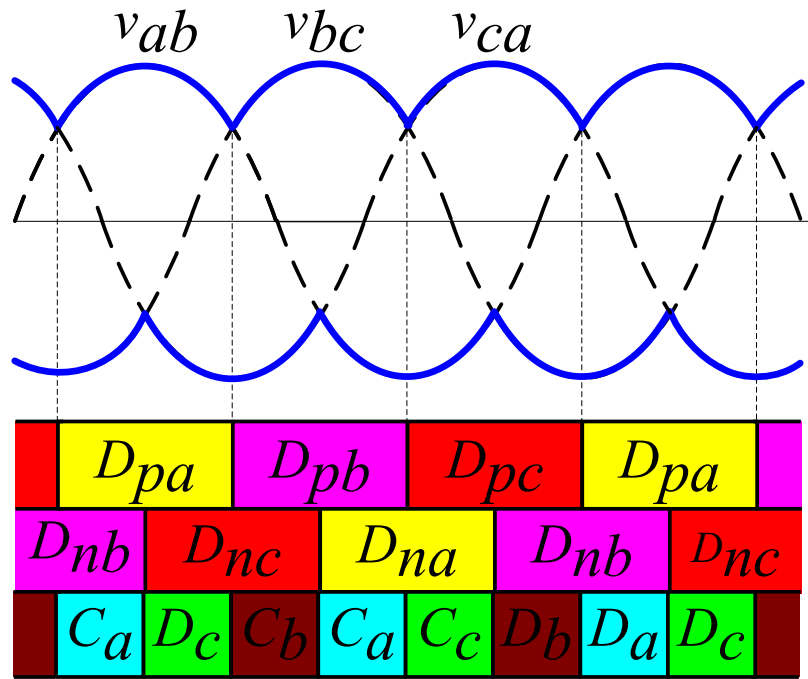
Figure 6-4 Six possible conduction intervals per fundamental cycle
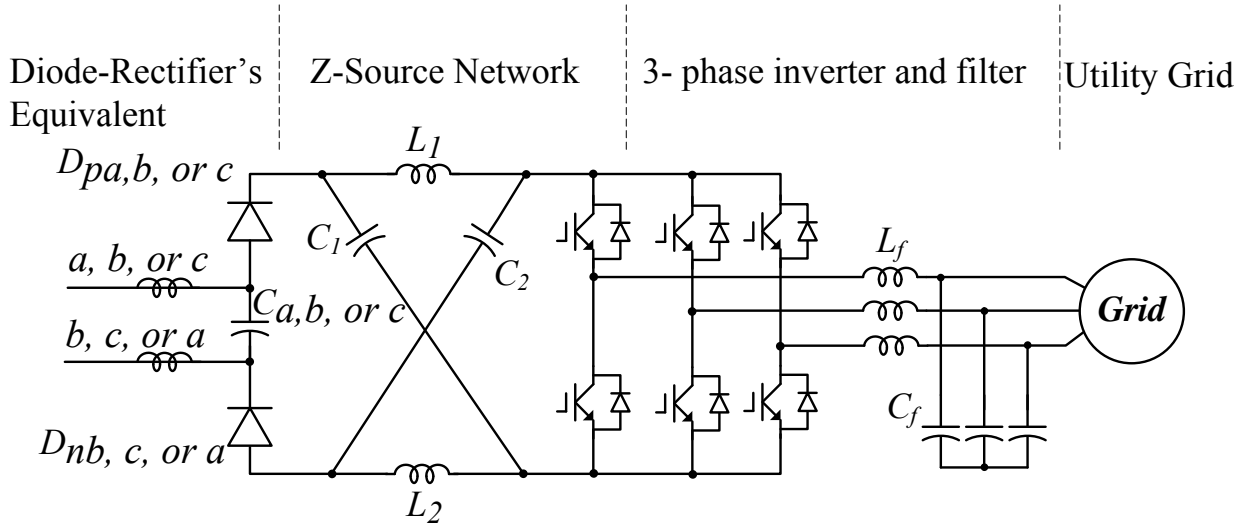
Figure 6-5 Equivalent circuit of the diode bridge viewed from the Z-source network

The order of the suffixes corresponds with their six combinations. For example, D_{pa} and D_{nb} are conducting as a pair with capacitor C_a; D_{pb} and D_{nc} are conducting as a pair with capacitor C_b and so on. When it is viewed from the Z-source, two diodes conduct in a pair and in series acting like one. Ultimately, the proposed Z-source WECS is reduced to the basic Z-source inverter presented in [1] .

An example of operating principle and operating mode is following. Shown in Figure 6-4 , when the potential different between phase a and b is the largest, diodes D_{pa} and D_{nb} conduct as a pair in series with capacitor C_a as the equivalent circuit shown in and Figure 6-5. The other diodes are reversely biased and cut off. Therefore, phase c has no line current (or small resonant/or residual current may exist between the line impedance and capacitors C_b and C_c). Ignoring this small current in phase c, Figure 6-3 and Figure 6-6 can be reduced to Figure 6-8.

78

From this reduced circuit, there are three operation modes which are depending on the interval bridge's switching state.
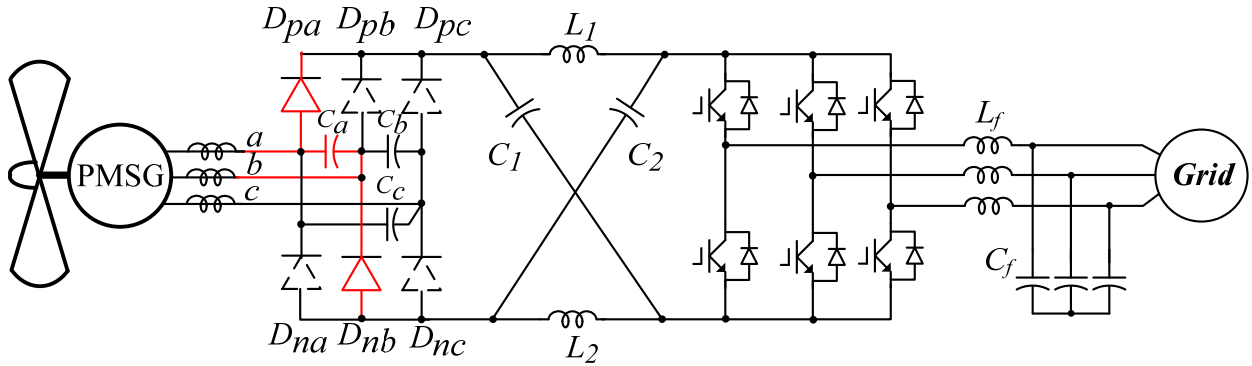
Figure 6-6 The example of equivalent circuit during the interval when the potential difference between phases "a" and "b" is largest.
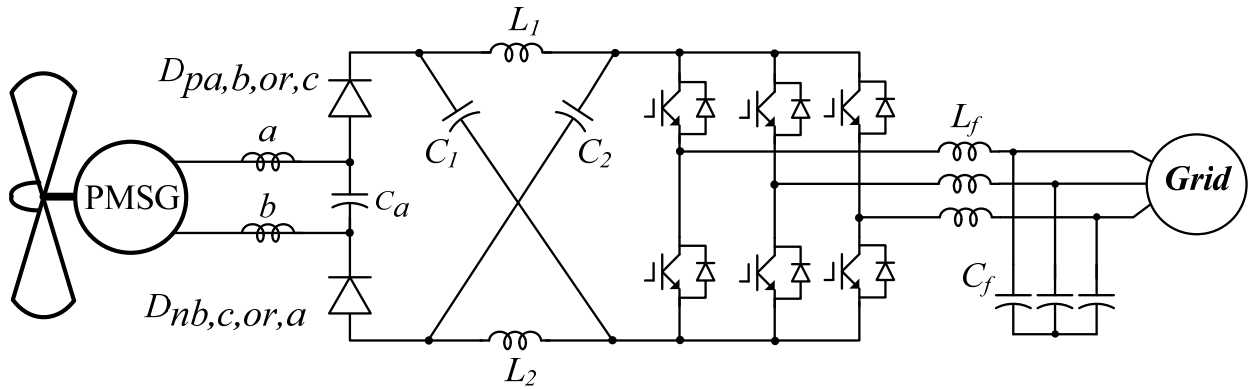
Figure 6-7 Reduced circuit during the interval when the potential difference between phases "a" and "b" is largest.

Mode I: active vectors

The inverter bridge is operating in one of the six conventional active vectors. Viewed from the Z-source network, it is performing as a current source. The diodes (D_{pa} and D_{nb} conduct and

carry currents as shown in Figure 6-8. The Z-source network always forces diodes (D_{pa} and

D_{nb}) to conduct and carry the current difference between the inductor current(I_{Ld}) and inverter

dc current (i_i), ($2I_{Ld}$-i_i). Note that both inductors have an identical current value because of the

circuit symmetry. This unique feature widens the line current conducting intervals, thus reducing

harmonic current.
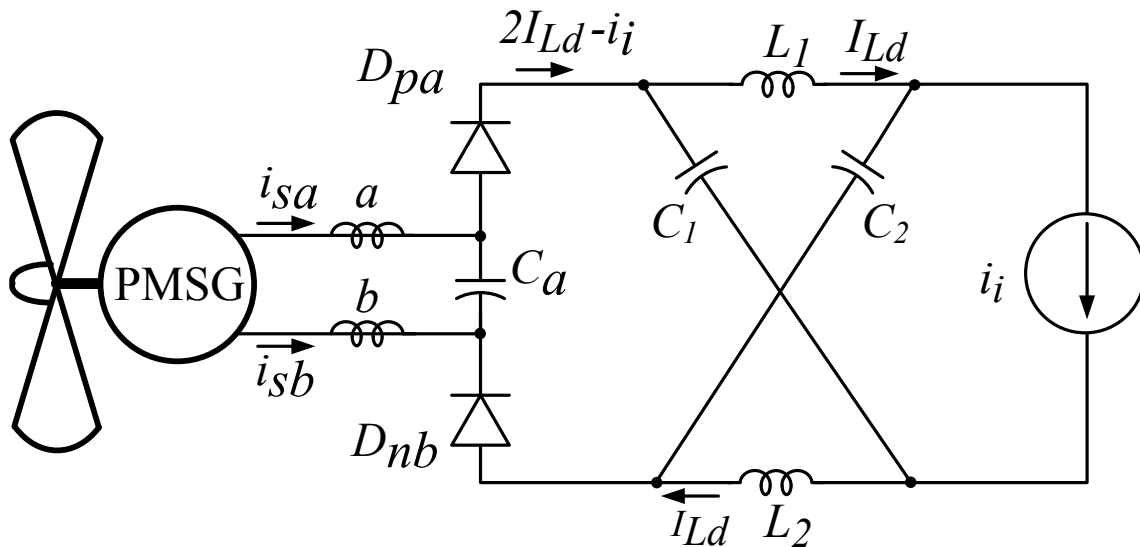
Figure 6-8 Circuit when the inverter bridge is producing one of six traditional active vectors

Mode II: zero vector

The inverter bridge is operating in one of two traditional zero vectors and shorting through

either the upper or lower three devices, thus acting as a open circuit when it is viewed from the

Z-source network. The diodes (D_{pa} and D_{nb}) conduct and carry currents as shown in Figure 6-9.

Under this mode the two diode (D_{pa} and D_{nb}) have to conduct and carry the inductor current,

hence reducing harmonic current.
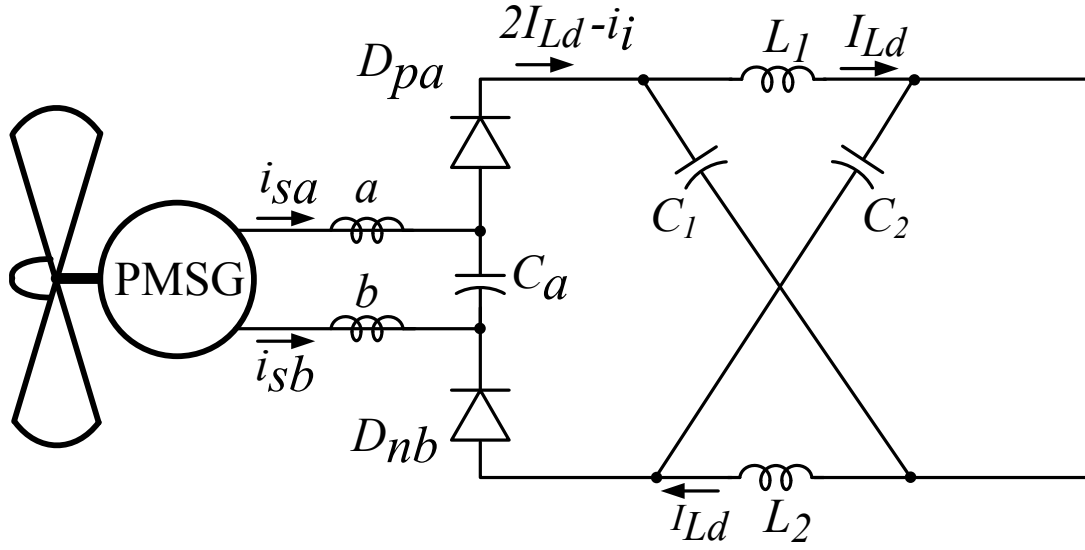
Figure 6-9 Circuit when the inverter bridge is producing one of the two traditional zero vectors

Mode III: shoot-through state

The inverter bridge is operating in one of the seven shoot - through states. In this mode, both diodes are off, separating the dc link from the ac line of the generator. Figure 6-10 shows the circuit under the shoot-though state viewed from the Z-source network. The line current flows to the capacitor(C_a). The capacitor voltage may be boosted depending on the shoot-through period interval. The more shoot-through period interval is applied, the higher capacitor voltage of the Z-source network can be produced. Depending on how much a voltage boost is needed, the shoot-through interval (T_0) or its duty cycle (T_0/T) is determined. The shoot-through interval is only a fraction of the switching cycle. Therefore, it needs a relatively small capacitor(C_a) to suppress the voltage.

The traditional inverter has six active states and two zero states. In six active states, the dc voltage is impressed across the load. However, in two zero states where the load terminals are

shorted through either upper or lower three devices, there is no dc voltage is impressed across the load terminal.

Like the traditional inverter, the Z-source inverter has six active states and two zero states. However, the Z-source inverter has additional shoot-through states where the terminals are shorted to both upper and lower devices. The shorted terminal can be one phase leg, two phase legs or all three phase legs. This shoot-through is not allowed for the traditional inverter. Since the zero state is shorting of either upper or lower devices and shoot-through state is shorting of both upper and lower devices, it produces zero voltage across the load's terminal during these states. For this reason, the shoot-through state still preserves the same PWM properties and voltage waveforms to the load while it boosts dc capacitor voltage.

The different between traditional inverter and the Z-source inverter is that the Z-source inverter has the boost function where as the traditional inverter does not. The capacitor voltage may be boosted depending on the shoot-through period interval determined by required voltage boost.
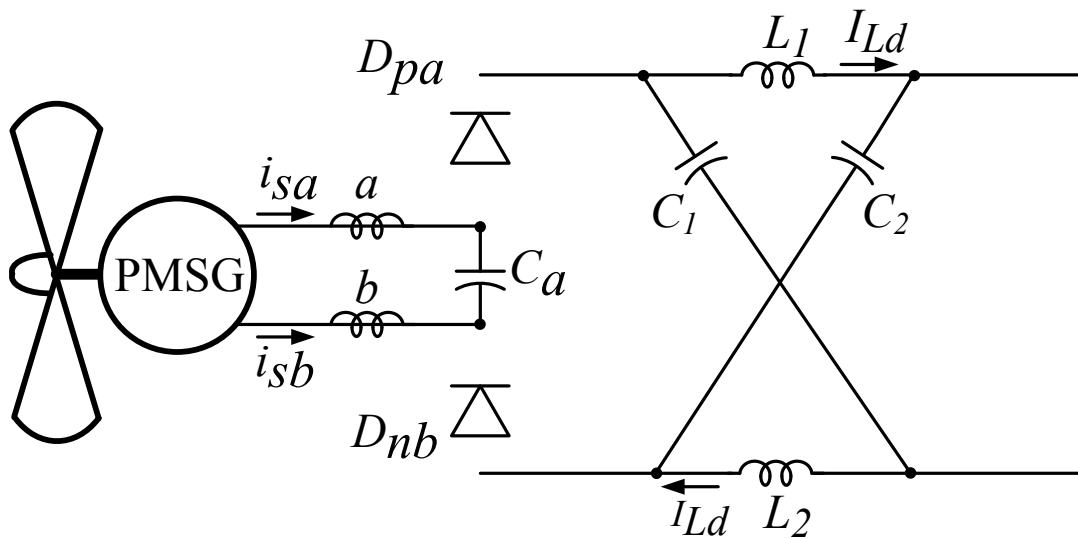
Figure 6-10 Circuit when the inverter bridge is producing one of the shoot-through states

Chapter 7. Topology simulation and experimental verifications

To verify the principle presented in the previous chapter, simulations and experiments have been carried out. The system includes a 10 kW Z-source inverter transferring power from the wind turbine side to the grid side. The circuit for the experimental set up is shown in Figure 7-1.
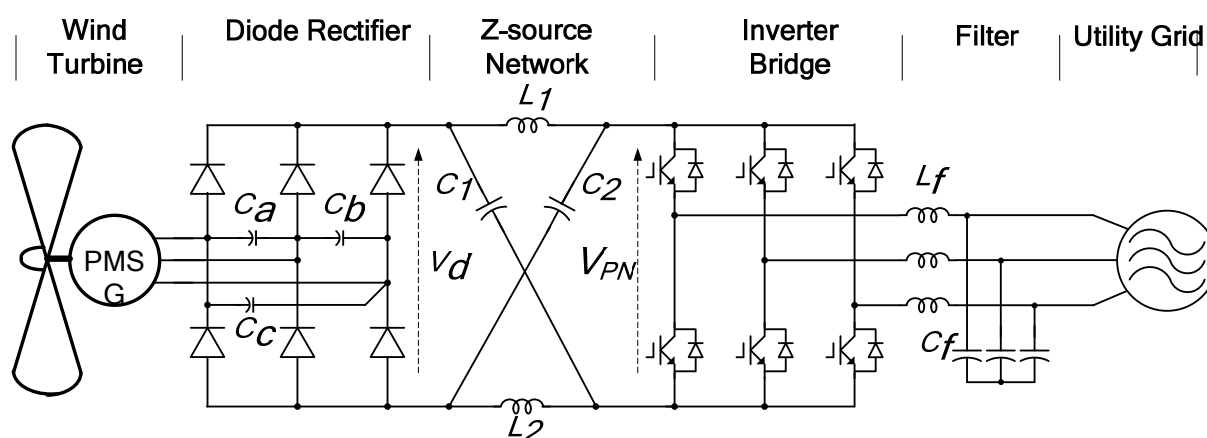
Figure 7-1 The schematic diagram of the experimental set up

The input voltage supplied by the wind turbine generator to the Z-source inverter varies between 150Vrms to 300Vrms. The output voltage of the inverter is held constant at 208Vrms and 60 Hz. The parameters of the system are shown in Table 5 .

Table 5 System parameters

Quantity	Values
Z-source inductors ($L_1 = L_2$)	550 μH
Z-source Capacitors ($C_1 = C_2$)	400 μF
Input Capacitors(C_a, C_b, and C_c)	12 μF
Switching frequency, f_s	10 kHz

7.1 Z- source inductor Implementation and Verification

    This section is to verify inductance of the designed inductor. After the inductor was built, the inductor's test has been conducted based on the test circuit shown in Figure 7-2 and the result shows in Figure 7-3 and Figure 7-4. In the Figure 7-3 and 7-4, V_{GS} is the gate drive signal for the IGBT on the test circuit, V_L is the voltage across the Device Under Test (DUT) and V_{DS} is the voltage across drain and source of the IGBT (used as a switch). The inductor current is represented by i_L.
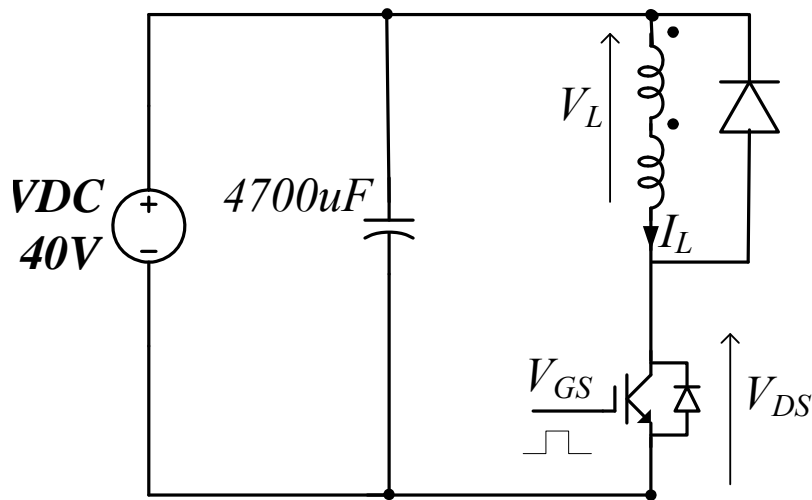
Figure 7-2 Inductor test circuit set up
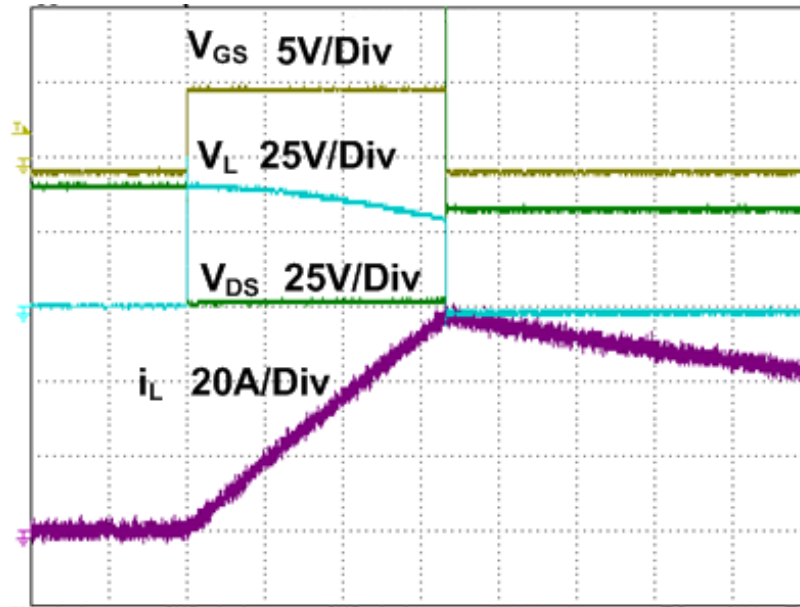
Figure 7-3 Inductor test result: inductance measurement
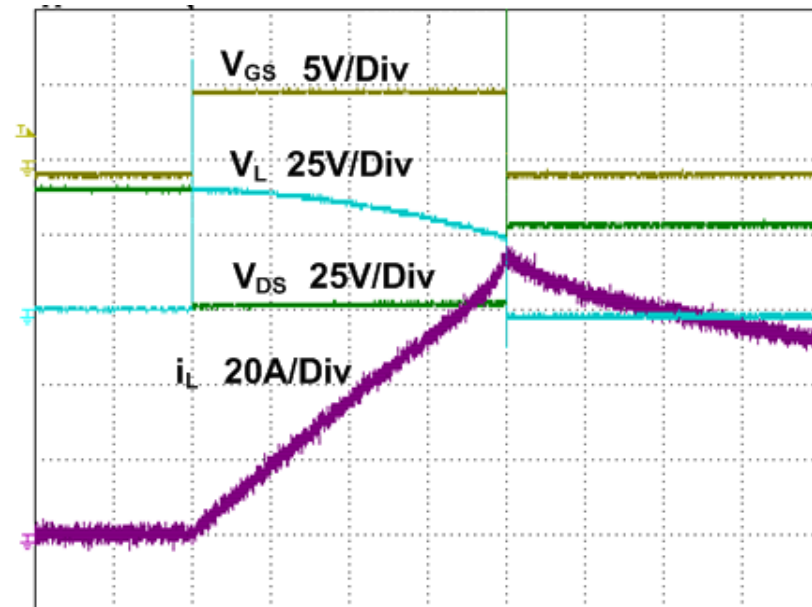
Figure 7-4 Inductor test: maximum current

By using the inductance equation, $V_L = L di/dt$, the inductance is calculated and it is about 550

μH as design. Figure 7-4 shows the maximum current capability that is allowed to flow to the

inductor. This is to ensure that the inductor is not saturated when it is in normal operation mode.

It is shown that the maximum current when the inductor starts to saturate is 70A whereas the nominal-designed operating current is about 25A. Therefore, the designed inductor is appropriate for this application. However, if it is a commercial produce where the size is concern, the maximum current can be reduced.

7.2 Hardware implementation

Based on the operating condition associated with the voltage current and power of the designed Z-source inverter, the main devices like the capacitors and IGBTs have been selected. The 10kW Z-source inverter prototype has been completely built for the test. This prototype is shown in the Figure 7-5. The experiment was conducted under several operating conditions which simulate the profile of a wind turbine generating system. As the wind speed change, the generator voltage, frequency and power will also change. So the test was performed under different wind speed conditions.
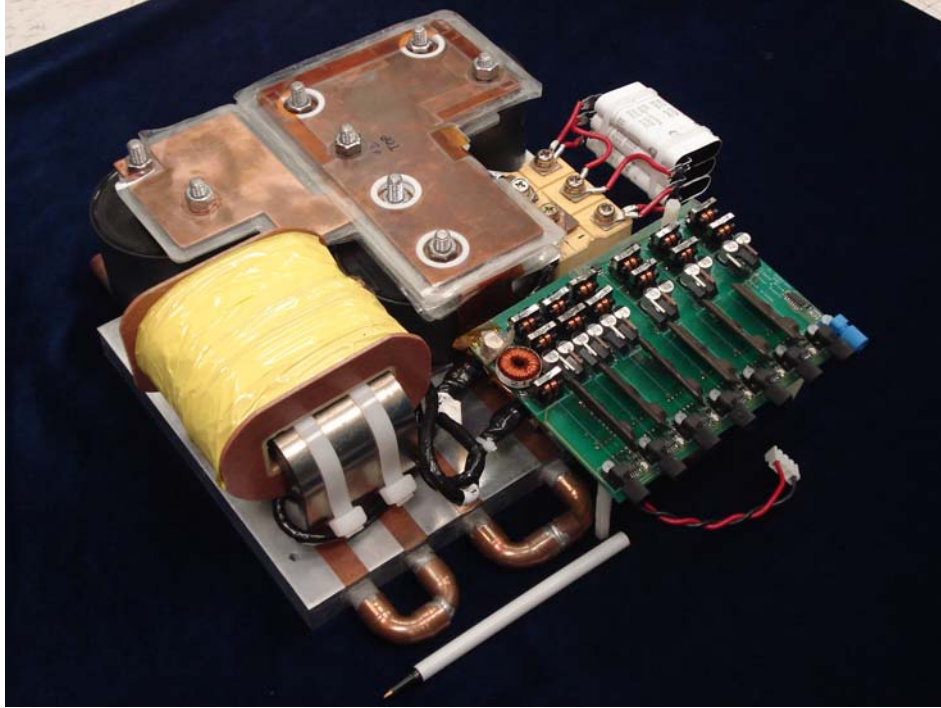
Figure 7-5 A 10kW Z-source inverter for Wind Power System

The simulation and experiment have been carried out in the two operating conditions which are as follows:

1. At low wind speed, the generator produces a voltage of *160Vrms* at *1.5kW*

2. At high wind speed, the generator produces a voltage of *270Vrms* at *3kW*

In the first condition, it is assumed that at low wind speed the generator produces *160Vrms* with *1.5kW*.

With this input voltage, the voltage after the bridge rectifier will be *216Vdc*, whereas the required line to line output voltage is *208Vrms*. With this line to line voltage, the peak phase voltage is roughly *170V*. The boost function will be used when the required voltage and the voltage after the diode rectifier meet the condition of (7-1).

$$\frac{V_d}{2} < \hat{v}_{ac} \tag{7-1}$$

With an input voltage of *160Vrms* and an output voltage of *208Vrms*, the condition in (7-1) is met. Then the boost control mode is needed. So the maximum modulation index can be determined by

$$M = \frac{\pi\left(\dfrac{\hat{v}_{ac}}{V_d/2}\right)}{\left(3\sqrt{3}.\left(\dfrac{\hat{v}_{ac}}{V_d/2}\right) - \pi\right)} = \frac{\pi\left(\dfrac{170}{216/2}\right)}{\left(3\sqrt{3}.\left(\dfrac{170}{216/2}\right) - \pi\right)} = 0.98 \tag{7-2}$$

The boost factor is

$$B = \frac{\pi}{3\sqrt{3}M - \pi} = 1.61 \tag{7-3}$$

The average duty ratio is

$$\frac{\overline{T_0}}{T} = \frac{2\pi - 3\sqrt{3}M}{2\pi} = \frac{2\pi - 3\sqrt{3}(0.98)}{2\pi} = 0.189 \tag{7-4}$$

So, the capacitor voltage will be

$$V_C = \frac{1 - \dfrac{\overline{T_0}}{T}}{1 - 2\dfrac{\overline{T_0}}{T}} V_d = \frac{1 - 0.189}{1 - 2*0.189} 216 = 282V \tag{7-5}$$

7.3 Simulation and Experimental Results

Figure 7-6 and Figure 7-7 show the results of the simulation and experiment with the first testing condition, at low wind speed with the generator voltage of 160Vrms and power of 1.5kW. These results show the generator voltage and current, the output voltage and the output current of the inverter. Figure 7-8 and Figure 7-9 show simulation and experimental results with the same conditions. When the generator voltage is 160Vrms, which can produce 216Vdc of the voltage after the rectifier, the boost function is used to produce the required output voltage of 208Vrms.
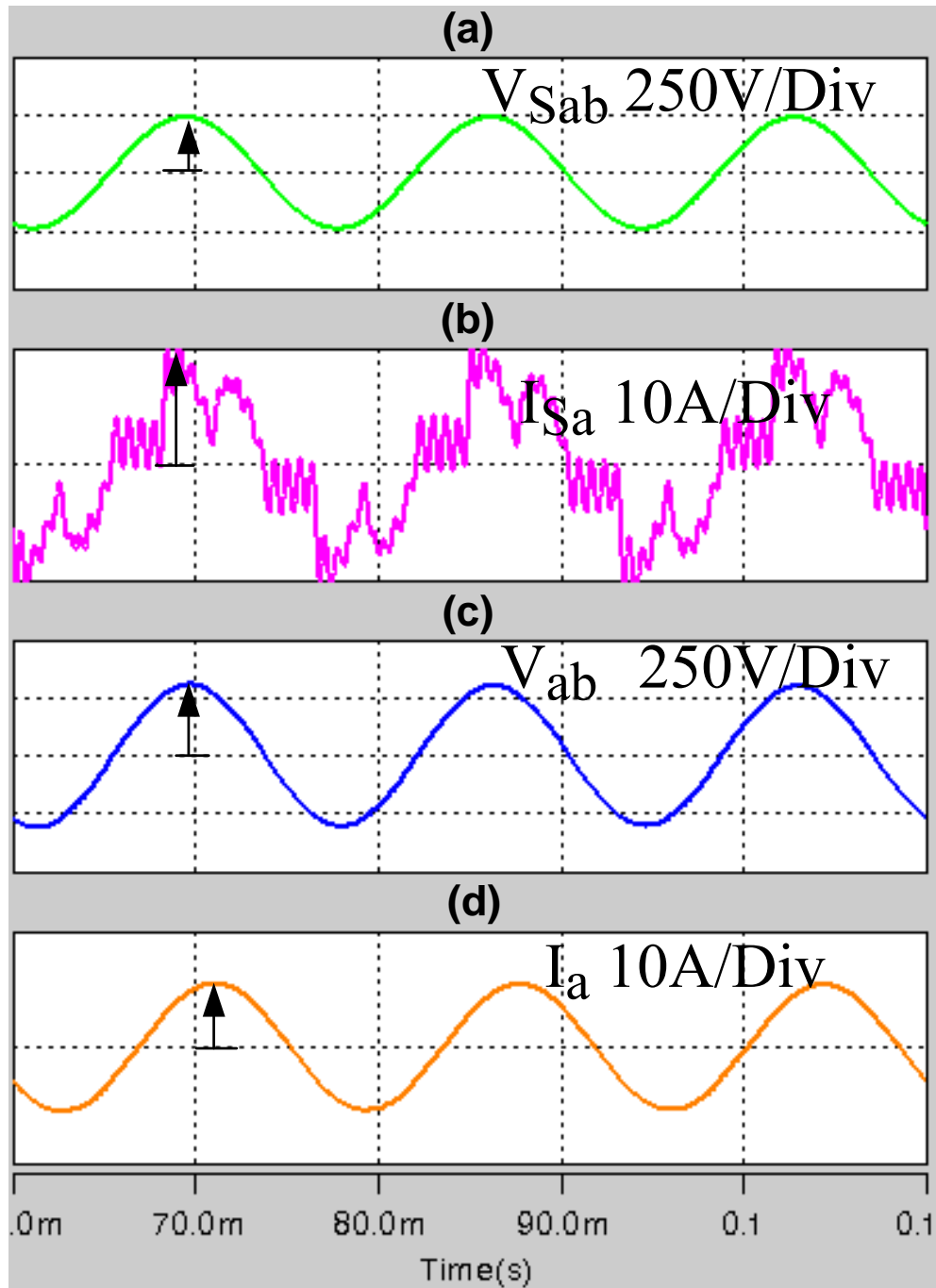
(a) Generator Voltage, $v_{Sab,}$ 160Vrms

(b) Generator Current, i_{sa}

(c) Inverter Voltage after filter, v_{ab}, 208Vrms

(d) Inverter Current, i_{La}

Figure 7-6 Simulation waveforms under the generator voltage of *160Vrms* at *1.5kW* with boost function.

Figure 7-7 Experimental results under the generator voltage of 160Vrms at 1.5kW with the use of the boost control mode; V_{Sab}: generator voltage, i_{sa}: generator current, V_{ab}: inverter output voltage, 208Vrms, i_{La}: inverter output current

To get enough of the required output voltage, the maximum modulation index must be 0.98 as shown in (15) and with this modulation index, the boost factor is 1.61, as in (16). Then *282Vdc* of the capacitor voltage at the Z-source network is created, as in (18), and shown in Figure 7-8 and Figure 7-9 as the results of the simulation and experiment.

(a) Generator Voltage, v_{Sab}, 160Vrms

(b) Z-source Capacitor Voltage, V_{C1} and V_{C2}

(c) Inverter Voltage after filter, v_{ab}, 208Vrms

(d) Inverter Current, i_{La}

Figure 7-8. Simulation waveforms under the generator voltage of 160Vrms at 1.5kW with the use of the boost control mode.

92

Figure 7-9 Experimental results under the generator voltage of 160Vrms at 1.5kW with the use of the boost control mode; V_{Sab}: generator voltage, V_C: voltage across the capacitor of the Z-source network, V_{ab}: inverter output voltage, 208Vrms, i_{La}: inverter output current

In the second condition, the generator voltage of *270Vrms* at *3kW* is applied. With this input voltage level, the voltage after the diode rectifier can be *365Vdc*, which is high enough to generate the required voltage of *208Vrms* without using any boost function. Therefore, the normal operation (no boost, *B=1*) is used and from (5) the modulation index can be determined by

$$M = \frac{\hat{v}_{ac}}{(V_d / 2)} = \frac{\hat{v}_{ac}}{(V_{PN} / 2)} = \frac{170}{(365 / 2)} = 0.93 \qquad\qquad (7\text{-}6)$$

Figure 7-10 and Figure 7-11 show the results of simulation and experiment under this condition.

From these two testing conditions, it is concluded that at different generator voltages, the proposed system can efficiently produce *208Vrms* of output voltage without any additional components or boost circuitry. These simulation and experimental results have verified the principle of the proposed system.

(a) Generator Voltage, v_{Sab}, 270Vrms

(b) Z-source Capacitor Voltage, V_{C1} and V_{C2}

(c) Inverter Voltage after filter, v_{ab}, 208Vrms

(d) Inverter Current, i_{La}

Figure 7-10 Simulation waveforms under the generator voltage of *270Vrms* at *3kW* without using boost control mode.
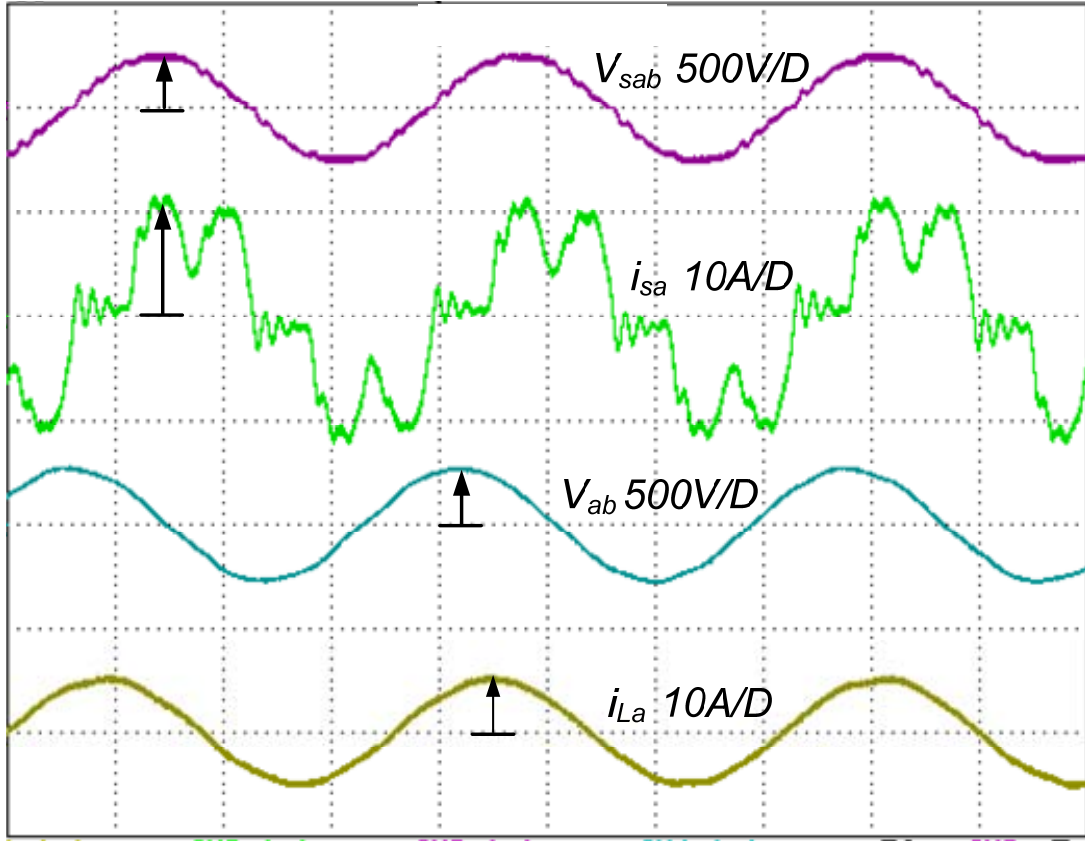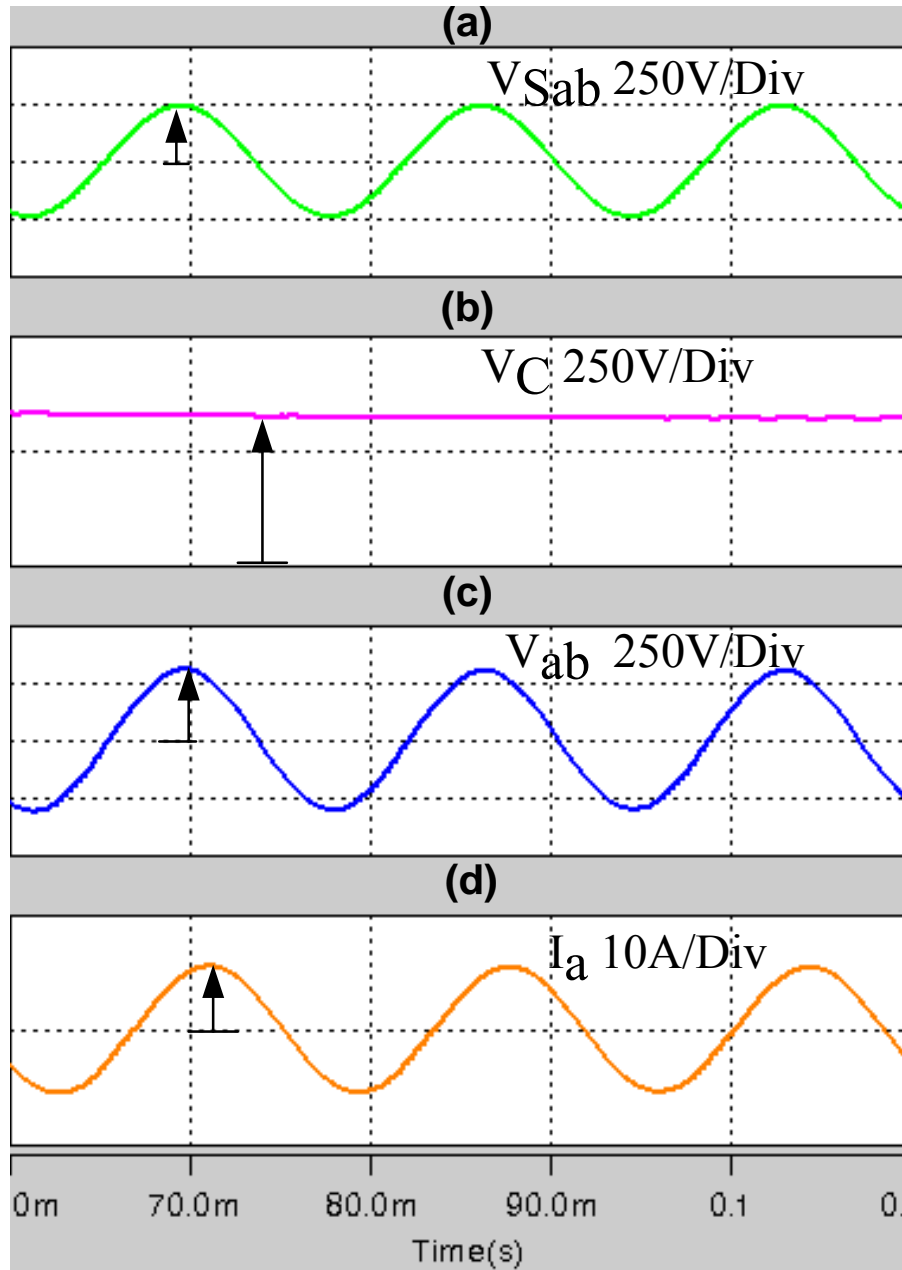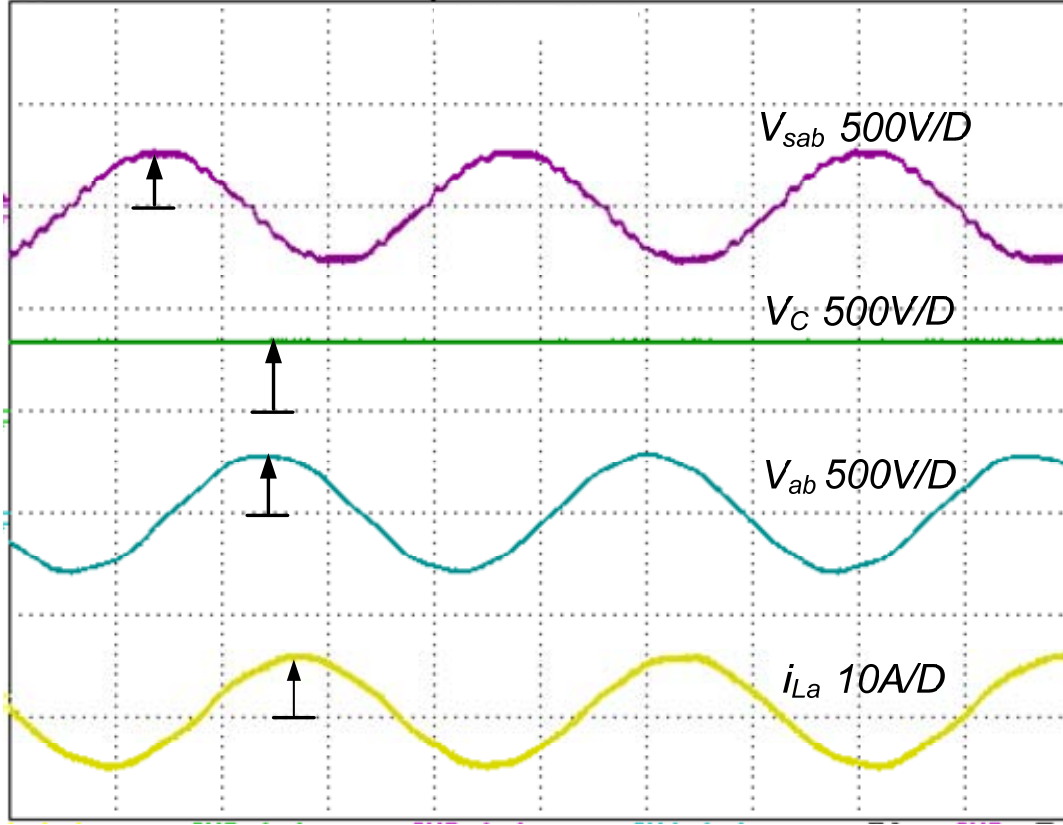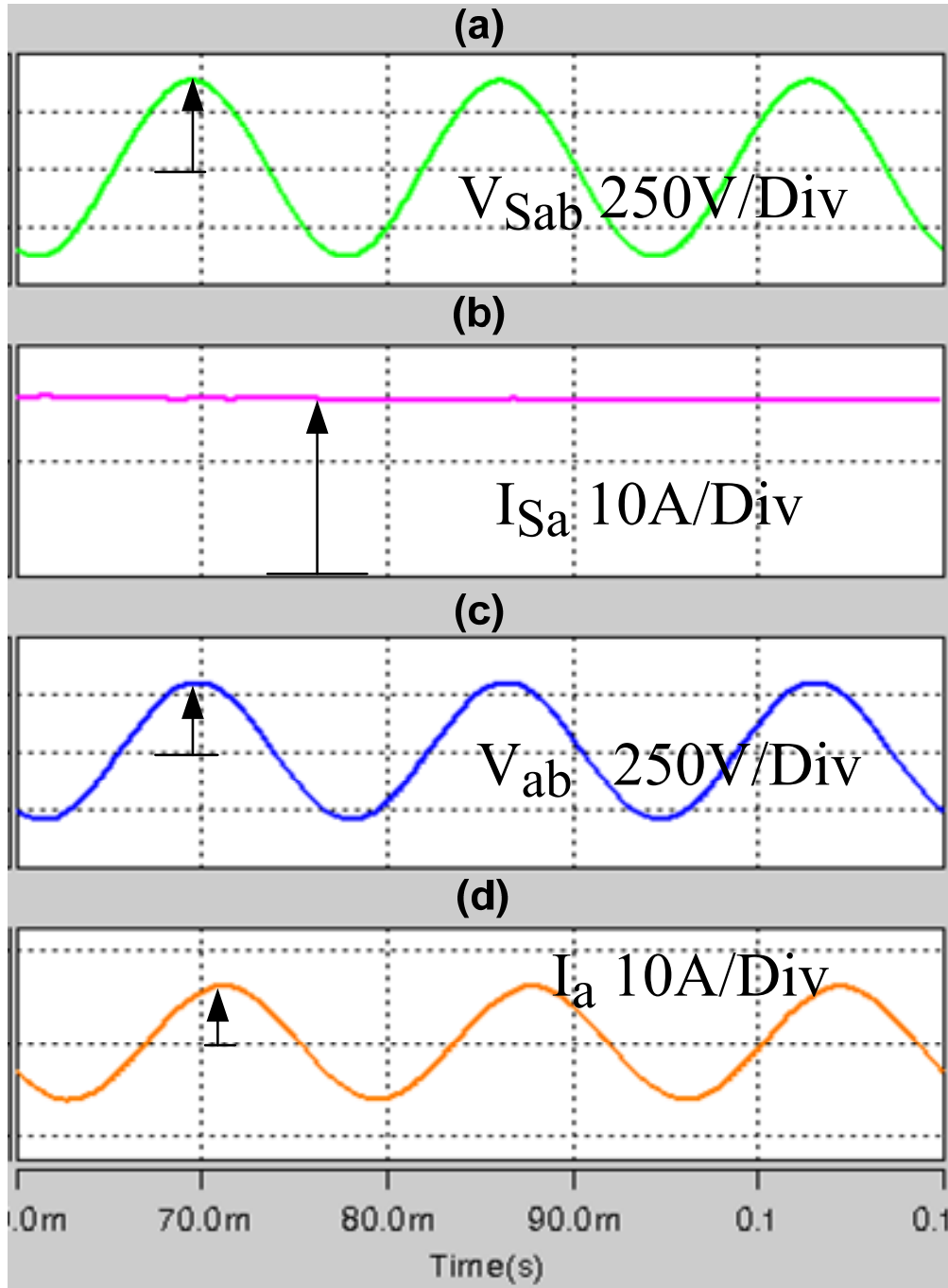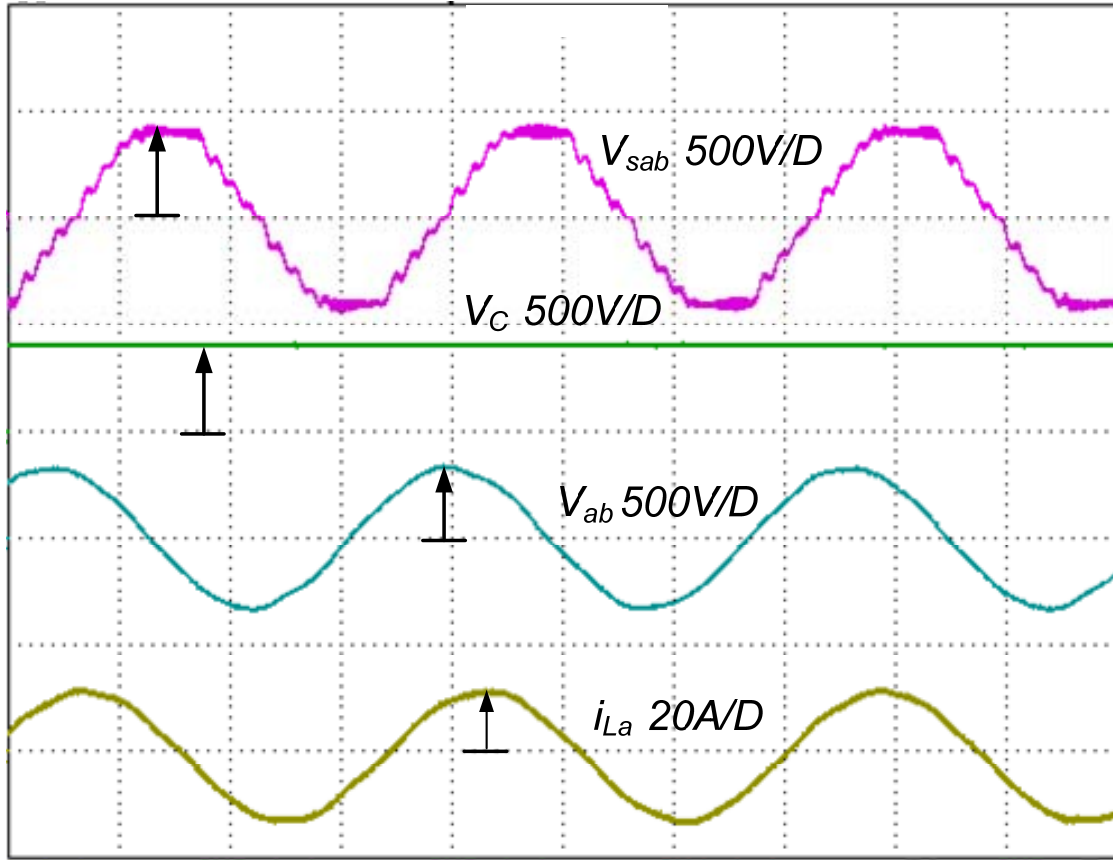
Figure 7-11 Experimental results under the generator voltage of *270Vrms* at *3kW* without using the boost control mode; V_{Sab}: generator voltage, V_C: voltage across the capacitor of the Z-source network, V_{ab}: inverter output voltage, *208Vrms*, i_{La}: inverter output current

Chapter 8. MPPT control and grid interconnection

8.1 Introduction

Power generated by wind turbines is the function of the wind speed. When the wind speed increases, extracted power increases. However, to get optimum extracted power, the Maximum Power Point Tracking (MPPT) control is required. For the proposed system, the MPPT is controlled through the rotational speed. In any wind speed, there is one rotational speed that the wind turbine can extract the maximum power. An alternative way of expression is that to get maximum power, the system is required to keep the power coefficient optimum. So if the power coefficient is kept constant at the optimum point, the system is automatically controlled to have maximum power.

The output voltage and frequency of the generator are also varied as the wind speed change. However, the grid voltage and frequency is kept constant. Wind Energy Conversion Systems (WECSs) are used to convert the variable voltage and frequency to usable constant voltage and constant frequency. WECSs have two important functions: 1) extracting maximum power from the wind and 2) delivering power to the grid with high quality electricity. To achieve these goals, the proposed Z-source inverter needs a MPPT control strategy which will be detailed in this chapter.

8.2 Maximum Power Point Tracking for WECSs

An extracted wind turbine power is usually represented by its power coefficient C_p versus the tip ratio, λ as shown in Figure 8-1. The optimum point occurs when C_p is the maximum point. In

order to have maximum C_p, the wind turbine speed needs to be controlled to get the optimum tip

ratio, λ_{opt}.
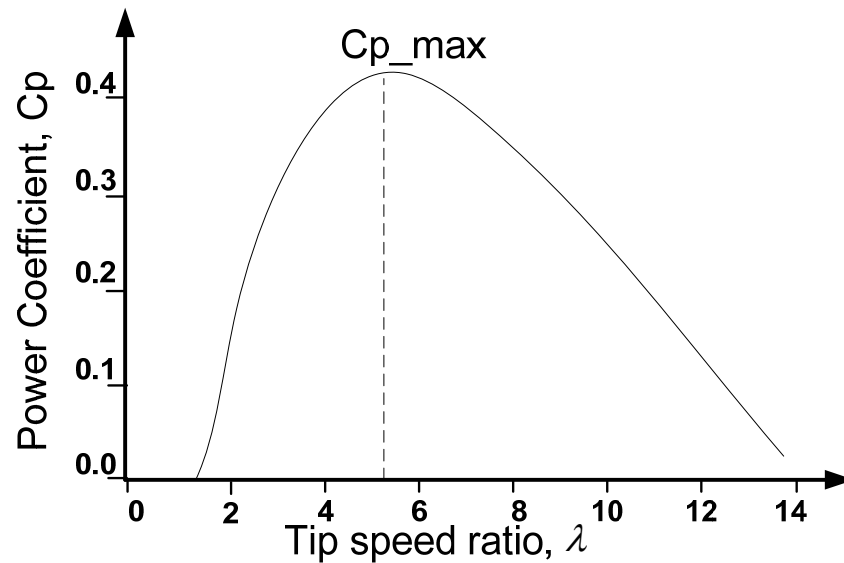
Figure 8-1 Relationship between power coefficient C_p and tip speed ratio λ

The MPPT control can not be applied to the whole wind speed range. It is possible at only a

certain low wind speed. Figure 8-2 shows an example of the relationship of wind speed and

power generated by wind turbine. In this example, the wind turbine start to move when the

wind speed is at around 4 m/s and from this point till the wind rated speed of 15m/s, the optimal

aerodynamic is achievable. From the rated speed (15m/s) to 25 m/s, the power needs to be

limited to avoid overloading of the wind turbine. To protect the wind turbine in case of high

wind speed, the wind turbine will be stopped at the cut out.
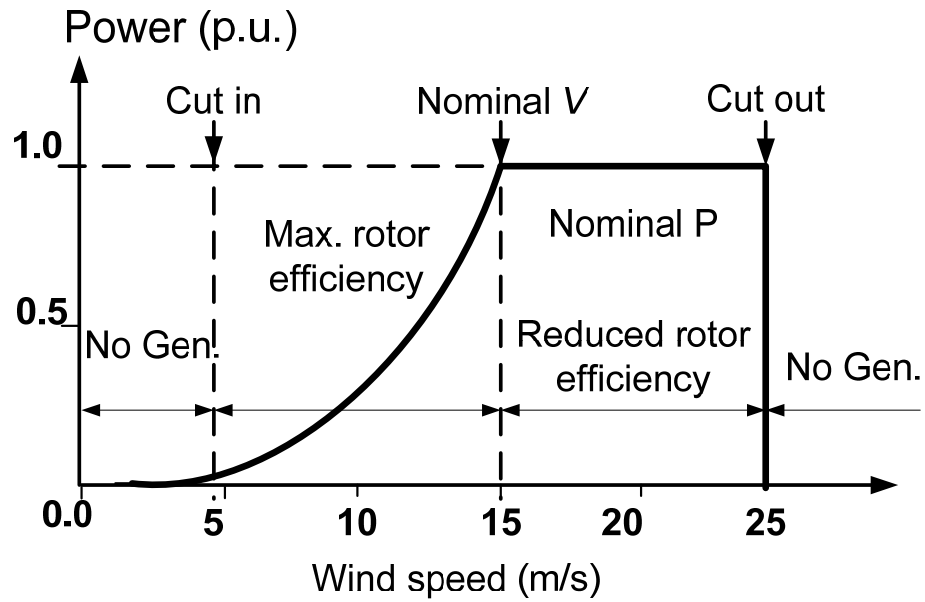
Figure 8-2 Output power of a wind turbine as a function of the wind speed
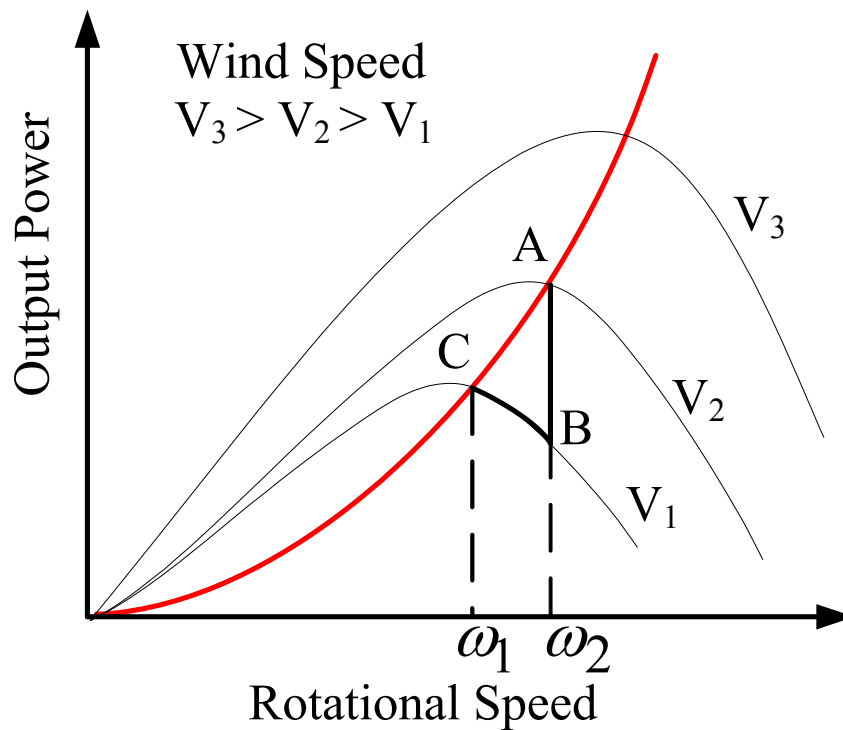
Figure 8-3 Power Output and Rotational Speed of a Wind turbine

During low wind speed, from the start point (for example at 4m/s on the Figure 8-2.) to the maximum rated power of the wind turbine (at 15m/s), the MPPT algorithm is required, so that the maximum power at any wind speed can be extracted. The idea of having the MPPT algorithm is to keep the tip speed ratio constant at the point that the power coefficient is optimum. Therefore, the rotational speed needs to be adjusted to follow the maximum power with respect to wind speed. The Figure 8-3 represents the relationship between the turbine output power and rotational with different wind speeds. At wind speed V_2 the maximum extracted power (A) is achieved at the rotational speed of ω_2. However, when the wind speed decreases to V_1 and with the same rotational speed ω_2, the extracted power is at B which is not at the maximum point. In order to get the maximum point (at C) the rotational speed needs to be changed to ω_1. The rotational speed needs to be dynamically adjusted respecting to the wind speed to obtain the maximum power captured.

By means of a maximum power point tracking (MPPT) algorithm, the power electronic is used to control the wind turbine rotation to get the possible maximum power.

To get the maximum power extraction, the generator speed is adjusted to follow the maximum power point. In general, the MPPT algorithm can be categorized into three methods including TSR control, Power Signal Feedback control, and Hill Calming searching control [40].

8.2.1 TSR Control

Figure 8-4 shows the block diagram of TSR control. In this control the wind speed and turbine speed need to be measured for TSR calculation. Then the optimal TSR is given to the controller. The controller will regulate the wind turbine speed to maintain an optimal TSR. Disadvantages of using TSR control are the need of wind speed measurement and obtaining the optimum value of TSR which is different from one system to another. Moreover, the wind speed may be difficult to obtain.

Tip-Speed Ratio Reference

+
−

Controller

Inverter Output Power Demand

Wind Power System

$$\lambda = \frac{V_{tip}}{V_{wind}} = \frac{R\omega_m}{v}$$

Turbine Speed

Wind Speed
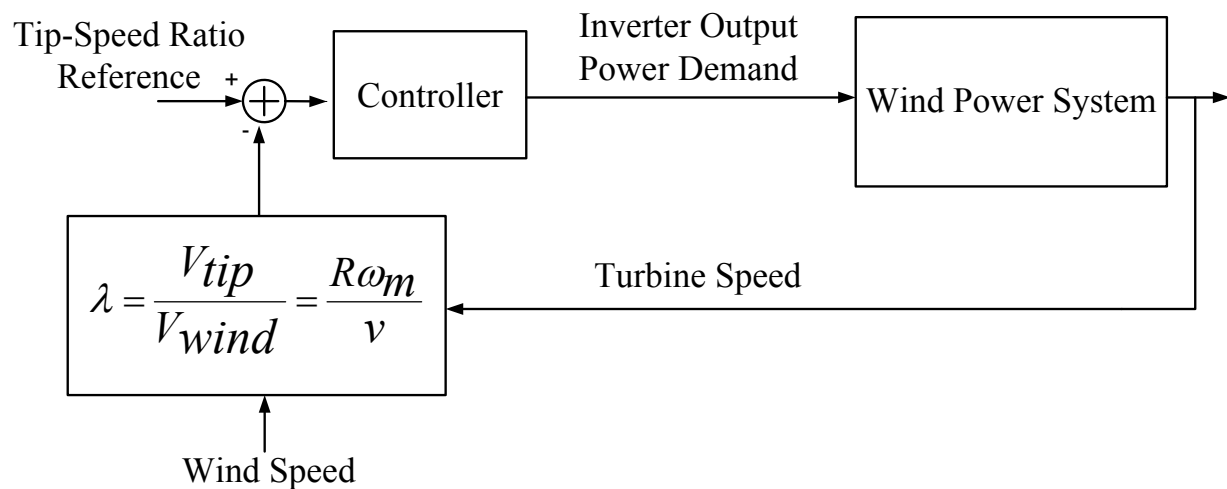
Figure 8-4 TSR Control [40]

8.2.2 Power Signal Feedback (PSF) Control

The block diagram of the PSF control is shown in Figure 8-5. This control requires the knowledge of the wind turbine maximum power curve. The limitation of this control is that the

maximum power curve needs to be obtained via simulations or test for each wind turbines. This makes the PSF control difficult and expensive to implement in practice.
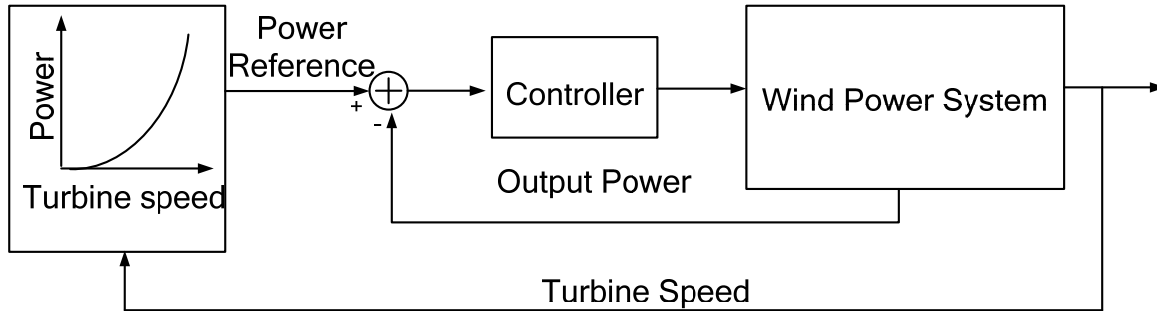
Figure 8-5 Power Signal Feedback (PSF) Control

8.2.3 Hill-Claim Searching (HCS) control

To overcome the drawbacks of two methods mentioned earlier, the HCS method has been proposed to continuously search for the peak output power of the wind turbine as shown in Figure 8-6. When the wind-turbine speed increases, the output power should fundamentally increase. Inversely, when the turbine speed decrease, the speed should decrease as well. This method works well only when the wind turbine inertia is small so that the turbine speed reacts to the wind speed almost instantaneously. However, this method could not be effective for the large wind turbine because the large turbine is difficult to adjust the speed fast.

$$\frac{dP}{d\omega} = 0$$

$$\frac{dP}{d\omega} > 0 \qquad \frac{dP}{d\omega} < 0$$
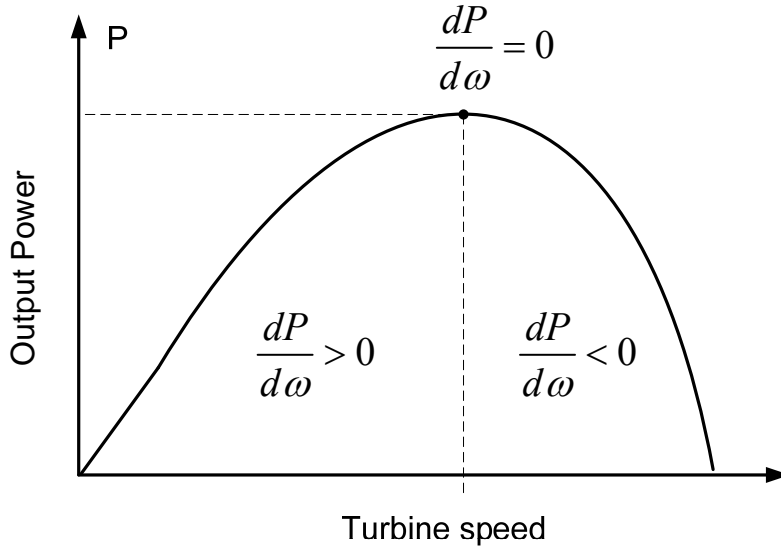
Figure 8-6 Hill-Claim Searching HCS Control

8.3 Proposed power control and grid interconnection

8.3.1 Wind Turbine

The mechanical power that the wind turbine can extract from the wind is expressed as

$$P_m = \frac{1}{2}\rho A C_p v^3 \qquad (8\text{-}1)$$

More details on the wind turbine characteristics have been discussed in the chapter 1.

8.3.2 PMSG

In this system, a PMSG is used as a wind turbine generator. The mechanical torque of the PMSG, T_m and electrical torque, T_e are defined as

103

$$T_m = \frac{P_m}{\omega_m} \tag{8-2}$$

$$T_e = \frac{P_e}{\omega_e} = \frac{2}{P}\frac{P_e}{\omega_m} \tag{8-3}$$

where ω_m is mechanical angular frequency, ω_e is electrical angular frequency, P_e is the electrical power generated by the PMSG and P is number of poles. The motion equation of the PMSG can be expressed in (8-4) and (8-5) [41].

$$J\frac{d\omega_m}{dt} = T_m - T_e - B\omega_m \tag{8-4}$$

$$\dot{\omega}_m = \frac{T_m - T_e - B\omega_m}{J} \tag{8-5}$$

where J is the total moment of inertia and B is the friction coefficient of the PMSG.

The difference between mechanical and electrical torque causes the variation of the generator speed, increasing or decreasing speed. The controllable electrical torque can be regulated to reach an optimal power coefficient by direct the rotational speed. This rotational speed can be indirectly controlled by adjusting the output current command.

8.3.3 Diode Rectifier

In the proposed WECS, controlling of the rotational speed is achieved by varying the generator terminal voltage[42]. The maximum power occurs at different generator speeds for different

wind speeds. For a PMSG, the induced torque can be expressed as

$$T = K_t I_a \qquad\qquad (8\text{-}6)$$

where I_a is stator current and K_t is the torque coefficient of the PMSG. The magnitude of output voltage (V) depends on the back EMF, which is the function of the rotor speed. The back EMF can be expressed as

$$E = K_e \omega_m \qquad\qquad (8\text{-}7)$$

where K_e is the back EMF coefficient of the PMSG.
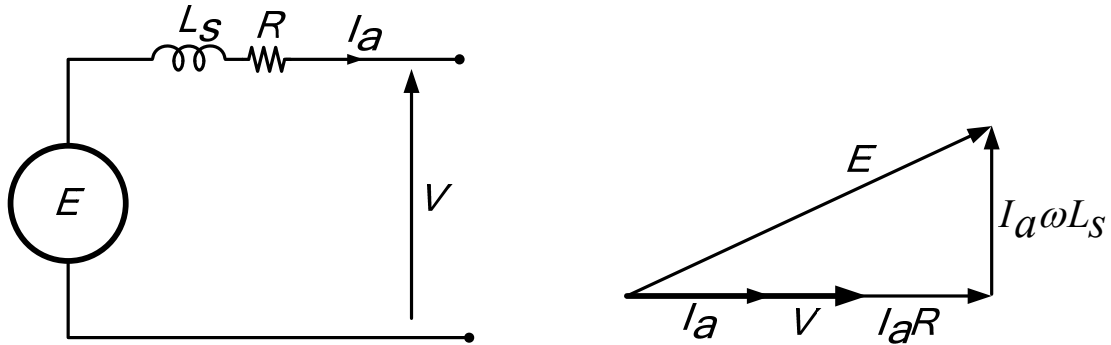
Figure 8-7 Equivalent circuit of PMSG and phasor diagram under unity power factor

Assume that the extracted power is close to unity power factor as shown in Figure 8-7 [41, 42], the *rms* phase voltage, V, of the PMSG 's terminal can be represented as

$$V = E + I_a(R + j\omega L_S) \qquad\qquad (8\text{-}8)$$

With unity power factor, the phase voltage is

$$V = \sqrt{E^2 - (I_a \omega L_s)^2} - I_a R_a \qquad (8\text{-}9)$$

where I_a, L_s and R_a are the RMS-phase current, the inductance and the resistor of PMSG, respectively. After the three-phase voltage converting to a DC voltage through the diode rectifier, the voltage at the rectifier can be written as (8-10)[43, 44].

$$V_d = \frac{3\sqrt{6}}{\pi}V - 2V_{diode} - \frac{3}{\sqrt{6}}\omega L_s I_a \qquad (8\text{-}10)$$

Assume that there is no energy losses, the electrical power can be ideally expressed as

$$P_e = 3VI_a = V_d I_d. \qquad (8\text{-}11)$$

where I_d is the output current of diode rectifier bridge. The current relationship between the ac and dc side of the diode rectifier is shown in (8-12).

$$I_d = \frac{\pi}{\sqrt{6}}I_a \qquad (8\text{-}12)$$

From (8-10), by neglecting the PMSG's wire resistant and small voltage drop at diodes, the voltage at the rectifier can be written as

$$V_d = \frac{3\sqrt{6}}{\pi}\omega_m \sqrt{K_e^2 - \left(\frac{T\omega L_s}{\omega_m K_t}\right)^2}. \qquad (8\text{-}13)$$

The mechanical power from wind turbine mainly depends on wind speed and the power

coefficient as shown in (8-1). The extracted power is the function of rotor speed which is governed by mean of MPPT control methods. This MPPT control methods will be discussed in the next topic. In (8-11) to (8-13), it is promising to get the dc voltage as a function of the generator speed. Therefore, in this proposed WECS, the generator speed can be easily controlled by regulating the dc voltage. As the result, the maximum extracted power can be controlled through the Vd. The beautiful of using the PMSG with diode rectifier is that the MPPT control can be achieved by controlling the dc voltage.

8.3.4 MPPT control for Z-source inverter for WECS

For the proposed Z-source inverter for WECS shown in Figure 8-8, there are three possible MPPT control structures for the proposed system. These control structures include MPPT based power control, MPPT base dc capacitor voltage control and MPPT based inverter bridge voltage control, shown in Figure 8-9, Figure 8-10, and Figure 8-11, respectively.
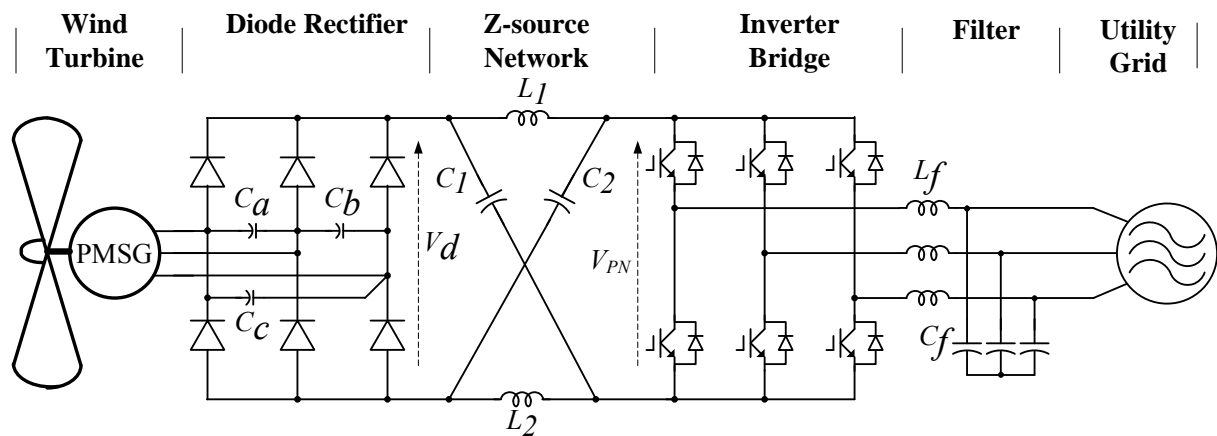
Figure 8-8 Proposed Z- source inverter for wind power generation

8.3.4.1　MPPT based power control

The MPPT with power control method is shown in Figure 8-9. This control structure comprises of two control loops, a power loop and a dc capacitor voltage loop. In the power loop, the power reference is determined by characteristic of wind turbine and the rotational speed. In this case, the measurement of the rotational speed is required. In the dc capacitor voltage loop, the capacitor voltage of the Z-source network is regulated to guarantee the power delivery to the grid. The shoot-through duty ratio is determined in this control loop as shown in Figure 8-9.
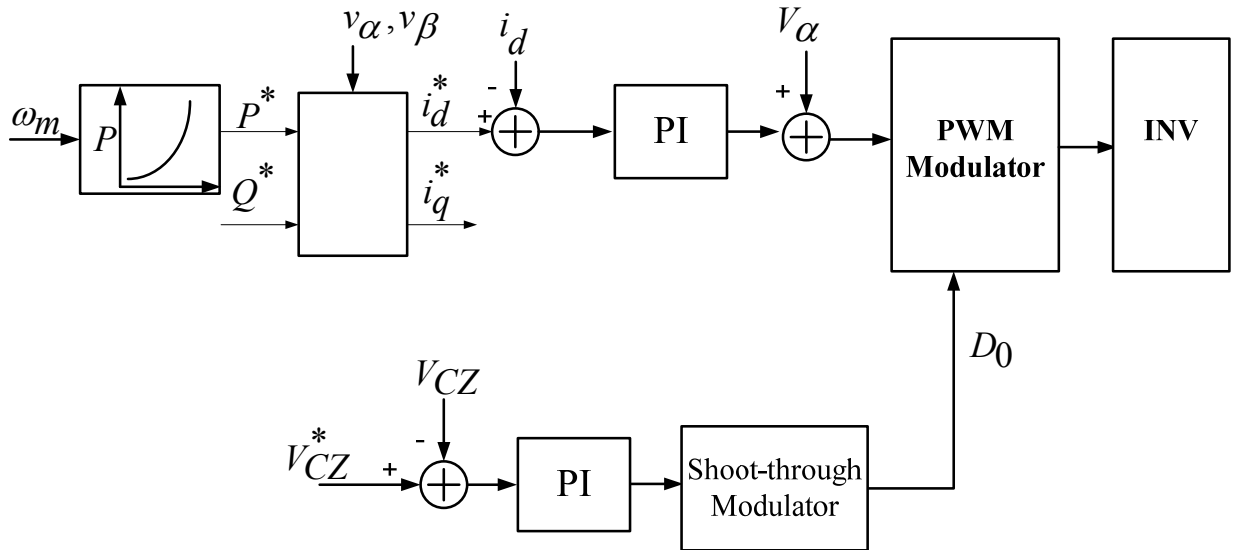
Figure 8-9 Control configuration; MPPT with power control method

8.3.4.2　MPPT control based dc capacitor voltage

Figure 8-10 shows the control configuration through the dc capacitor voltage. Reference voltage

of the dc capacitor was selected regarding to appropriate voltage of the utility grid. There are

two-control loops, current loop and voltage loop. In the current loop, the dc capacitor is regulated

through the output current, i_d. For example, if the dc voltage increases because of increasing of

input power and wind speed, the system will deliver more power to bring down the dc capacitor

voltage. As the result, the system will push more power to the utility grid.

To obtain maximum power control, the rotor speeds need to be varied with changing of wind

speed. The shoot-through state duty ratio is determined by the dc capacitor voltage, Vc, and the

dc voltage of the diode bridge rectifier, V_d. This V_d is determined by the wind characteristic and

the rotational speed.
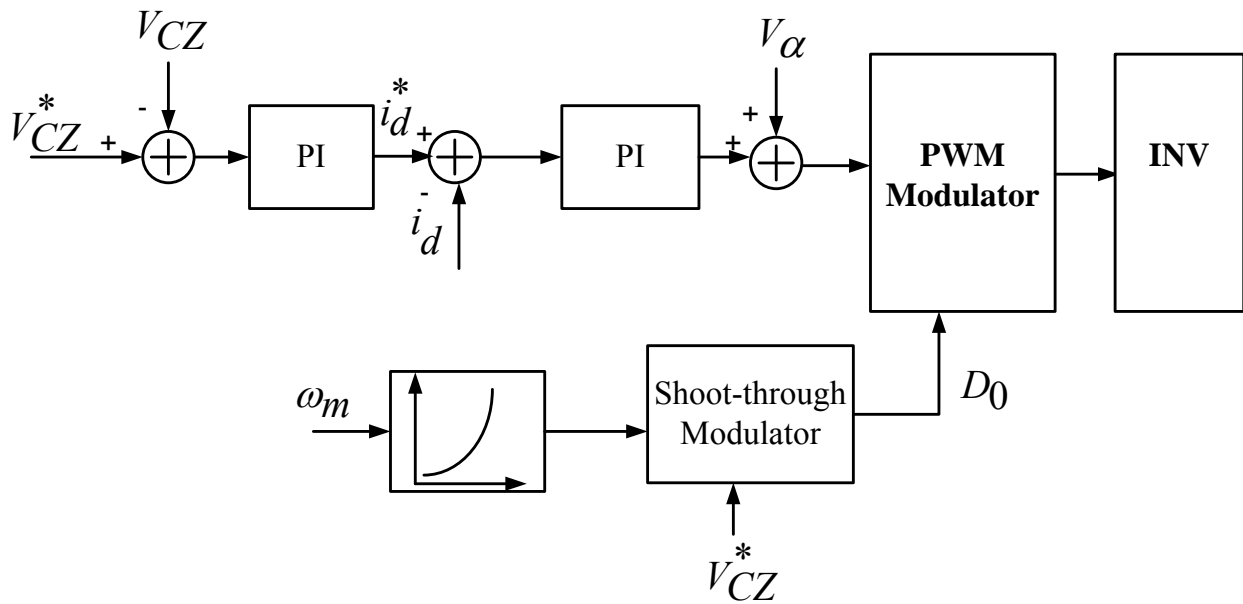
Figure 8-10 Control configuration; MPPT with capacitor voltage (V_C) control method

8.3.4.3   MPPT based inverter bridge voltage

In the MPPT based inverter bridge voltage control strategy, the reference voltage for dc link (inverter bridge voltage) is set to be appropriate voltage for producing the desired inverter output voltage. The configuration is shown in Figure 8-11. This structure is similar to the MPPT based capacitor voltage. The difference is that in the MPPT based inverter bridge voltage, the capacitor voltage reference signal is determined by the inverter bridge voltage V_{PN} and the diode rectifier voltage, V_d. This control strategy requires the measurement of the diode rectifier voltage and this measuring would be difficult, since it experience with the shoot-through state.
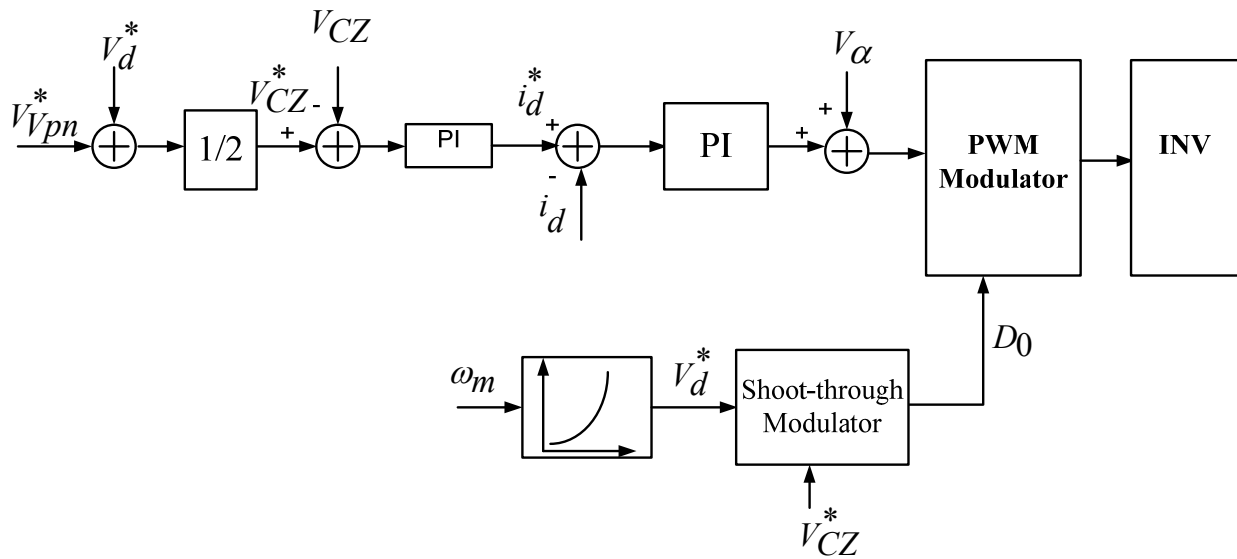
Figure 8-11 Control configuration; MPPT with inverter bridge voltage (V_{PN}) control method

In comparison to these three MPPT control structures, the MPPT control based controlling capacitor voltage is more practical since the capacitor voltage is easier to control and measure whereas the inverter bridge voltage become zero when shoot-through state happen. This condition may cause the difficulty to measure the voltage. Even though the MPPT control based

power control is also practical, this control strategy requires the rotational speed sensor.

8.4 Control of grid interconnection with power control

In this section, the control structure shown in Figure 8-10 will be discussed. The completed control configuration of the system is shown in Figure 8-12. Two main control loops are used in order to govern two independent variables, the modulation index M and the shoot through duty ratio D_0. The control of the modulation index used for controlling the output power is detailed in this section, whereas the control of the shoot-through duty ratio employed for regulating the voltage of the Z-source's capacitor will be discussed in the next section. To control the power, the control method uses the current reference in current controlled PWM to get the desired output current of the inverter.

The current injected into the utility network needs to be synchronized with the utility grid voltage. The *dq PLL* synchronization method is state-of-the-art and is more efficient. Therefore, in this system the three-phase *dq PLL* method is used for grid synchronization.

The control signal is obtained from the following procedures. The three phase utility voltages can be described as in (8-14),

$$V_{abc} = V_m \cdot \begin{bmatrix} Cos\theta \\ Cos\left(\theta - \dfrac{2\pi}{3}\right) \\ Cos\left(\theta + \dfrac{2\pi}{3}\right) \end{bmatrix} \qquad (8\text{-}14)$$

where $V_{abc} = [V_a\ V_b\ V_c]^T$.
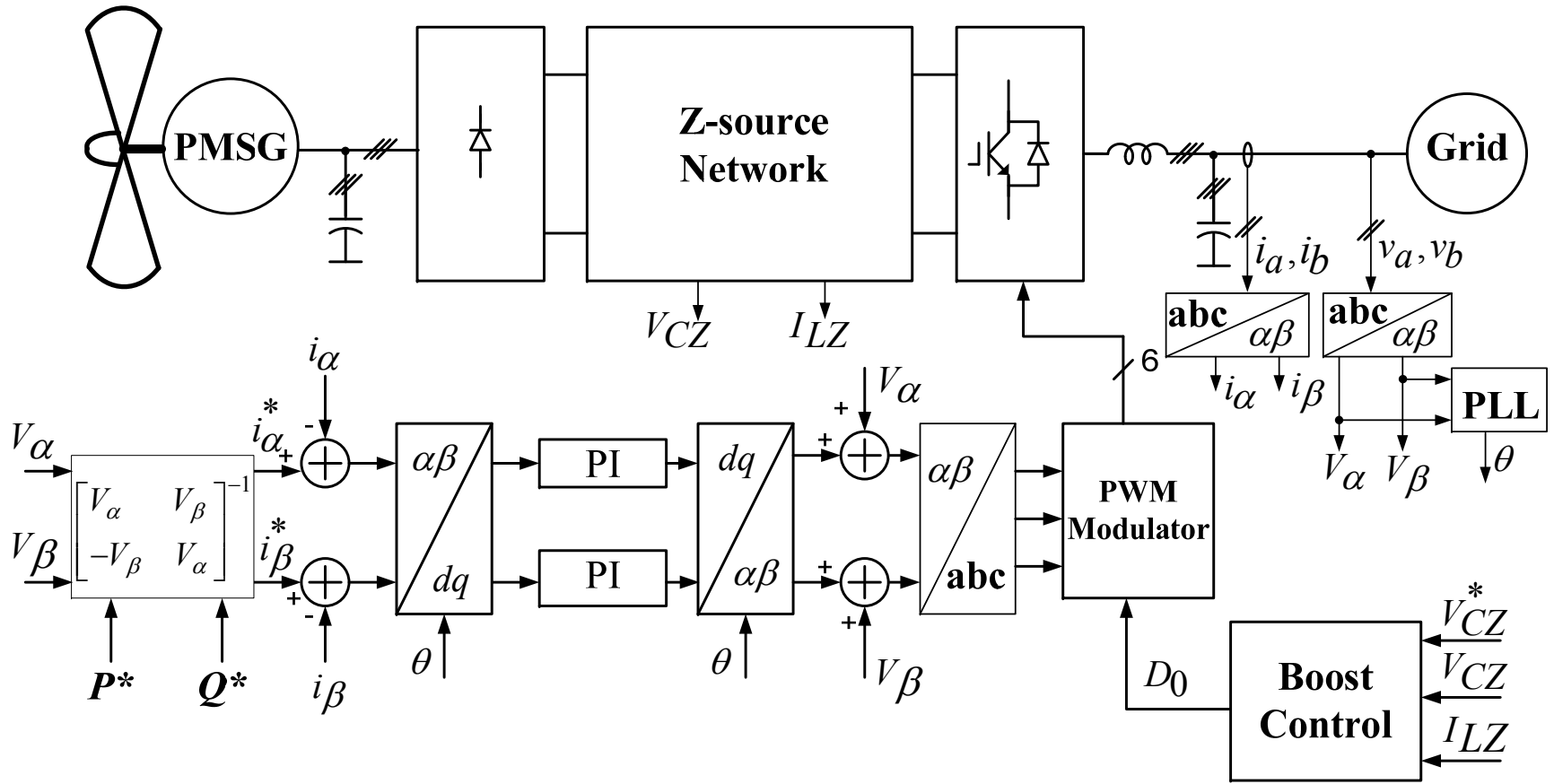
Figure 8-12 Proposed system with control configuration based power control method

$$\begin{bmatrix} V_\alpha \\ V_\beta \end{bmatrix} = \frac{2}{3} \begin{bmatrix} 1 & -\dfrac{1}{2} & -\dfrac{1}{2} \\ 0 & -\dfrac{\sqrt{3}}{2} & \dfrac{\sqrt{3}}{2} \end{bmatrix} \begin{bmatrix} V_a \\ V_b \\ V_c \end{bmatrix} \tag{8-15}$$

For balanced utility voltages, equation (8-14) can be expressed in the stationary reference frame as shown in (8-15). This utility voltage can be written in the synchronous reference frame using the *PLL* output angle as in (8-16).

$$\begin{bmatrix} V_d \\ V_q \end{bmatrix} = \begin{bmatrix} Cos\theta & -Sin\theta \\ Sin\theta & Cos\theta \end{bmatrix} \begin{bmatrix} V_\alpha \\ V_\beta \end{bmatrix} \tag{8-16}$$

The real and active powers can be derived as (8-17) and (8-18), respectively.

$$P = V_\alpha I_\alpha + V_\beta I_\beta \tag{8-17}$$

$$Q = V_\beta I_\alpha - V_\alpha I_\beta \tag{8-18}$$

P^* and Q^* can be obtained by using the maximum power tracking system [45, 46]. The reference of real and active power can be expressed as

$$\begin{bmatrix} P^* \\ Q^* \end{bmatrix} = \begin{bmatrix} V_\alpha^* & V_\beta^* \\ -V_\beta^* & V_\alpha^* \end{bmatrix} \begin{bmatrix} i_\alpha^* \\ i_\beta^* \end{bmatrix} \tag{8-19}$$

$$\begin{bmatrix} i_\alpha^* \\ i_\beta^* \end{bmatrix} = \frac{1}{V_\alpha^2 + V_\beta^2} \begin{bmatrix} V_\alpha^* & -V_\beta^* \\ V_\beta^* & V_\alpha^* \end{bmatrix} \begin{bmatrix} P^* \\ Q^* \end{bmatrix} \tag{8-20}$$

where $\begin{bmatrix} i_\alpha^* & i_\beta^* \end{bmatrix}^T$ is the current reference. The error signal is obtained by subtracting the current reference signal from the inverter current signal. These error signals are converted to the *dq* rotational reference frame using (8-21). The error signal is directly injected to the PI controller to generate the control outputs, u_d and u_q. These control signals are converted to the stationary reference frame by (8-22). Ultimately, the stationary voltage reference signal can be described in (8-23) and (8-24), where V_α and V_β are added in order to decrease the gain of the PI controller.

$$\begin{bmatrix} \square i_d \\ \square i_q \end{bmatrix} = \begin{bmatrix} Cos\theta & -Sin\theta \\ Sin\theta & Cos\theta \end{bmatrix} \begin{bmatrix} \square i_\alpha \\ \square i_\beta \end{bmatrix} \tag{8-21}$$

$$\begin{bmatrix} u_\alpha \\ u_\beta \end{bmatrix} = \begin{bmatrix} Cos\theta & -Sin\theta \\ Sin\theta & Cos\theta \end{bmatrix}^{-1} \begin{bmatrix} u_d \\ u_q \end{bmatrix} \tag{8-22}$$

$$v_{r\alpha}^* = u_\alpha + V_\alpha \tag{8-23}$$

$$v_{r\beta}^* = u_\beta + V_\beta \tag{8-24}$$

8.5 Simulation results

It is assumed that the wind speed changes dramatically, so the power and voltage generated by the wind turbine system are varied substantially. It is noticed that in reality, when the wind speed changes, the power and the voltage of the wind turbine are changed in the same direction. As the

wind speed increases, the output power and output voltage are increased.

The following simulation is assumed in the worst case where the power input is greatly changed. The control structure is based on the MPPT power control method as shown in Figure 8-13. Figure 8-16 shows the simulation waveforms when the power changes from 5kW to 10kW and Figure 8-15 shows the power step change from 10kW to 5kW. In Figure 8-16, the system provides more power, resulting in the input voltage and the voltage across the capacitor dropping. The boost control loop will keep the voltage across the capacitor constant and bring it back to the setting level given by reference signal.
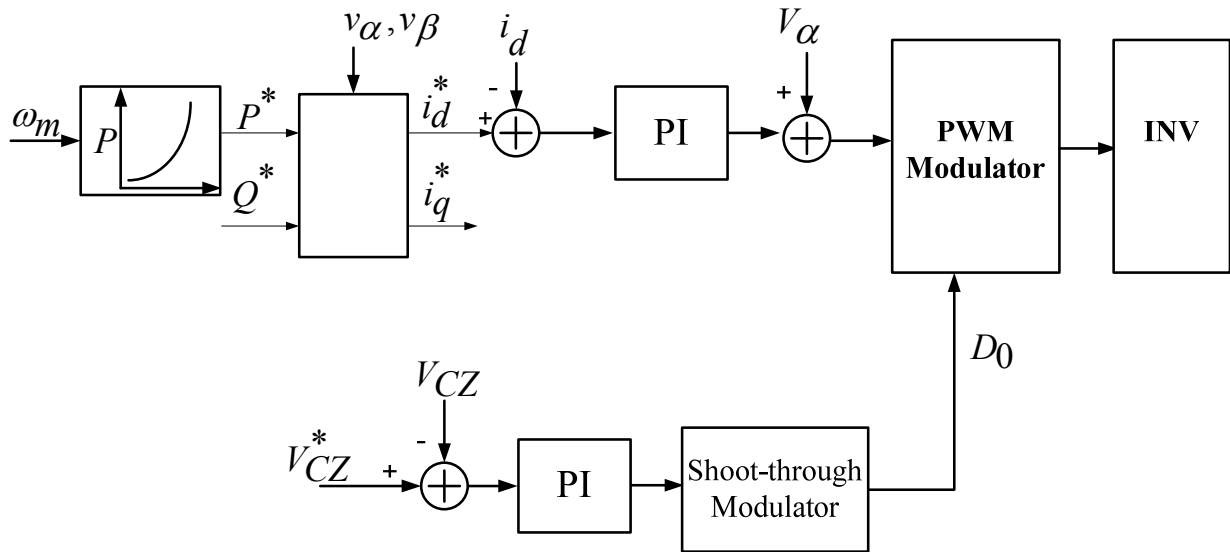
Figure 8-13 Control configuration; MPPT with power control method
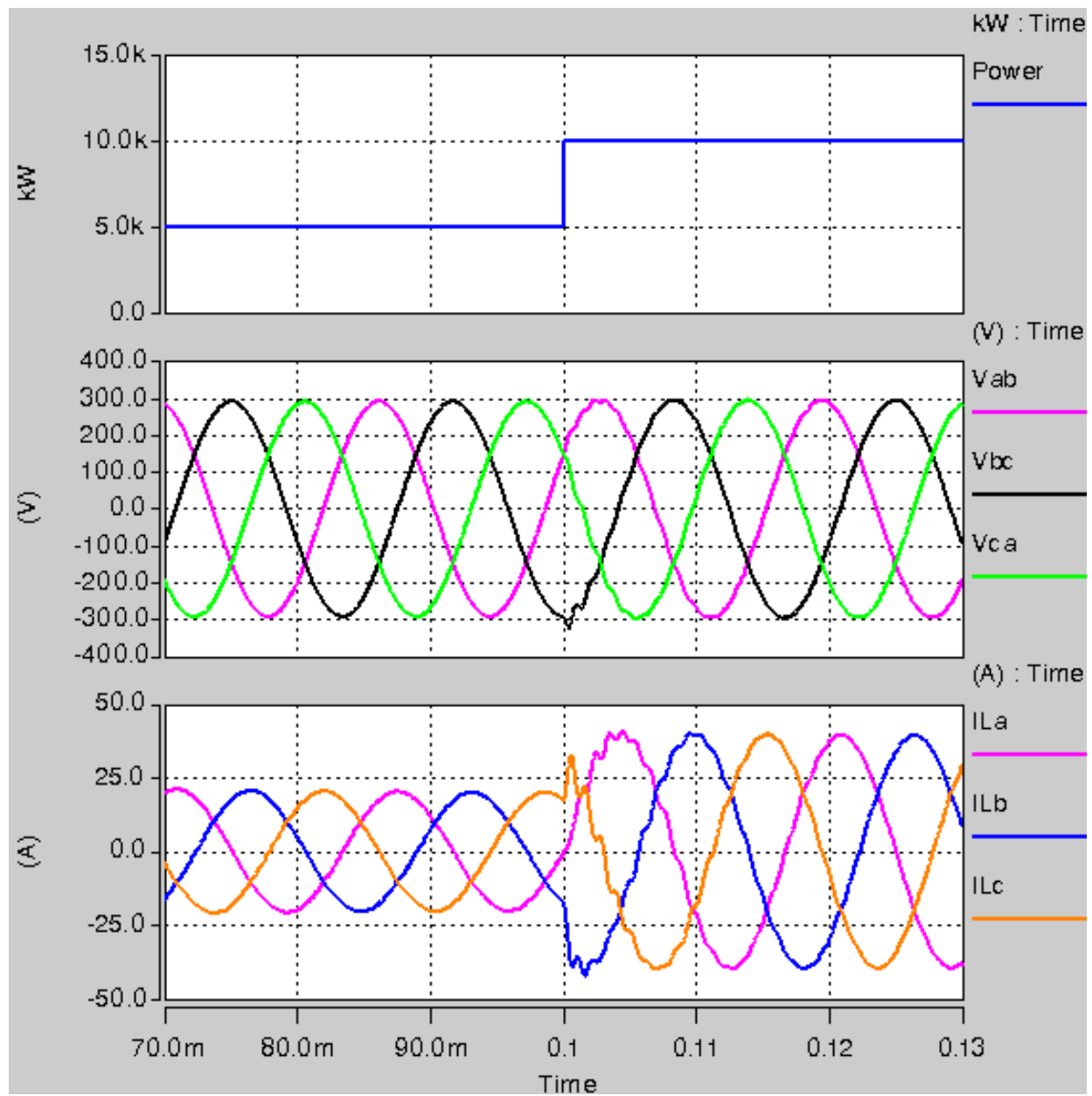
Figure 8-14 Simulation waveforms when power step change from 5 kW to 10 kW
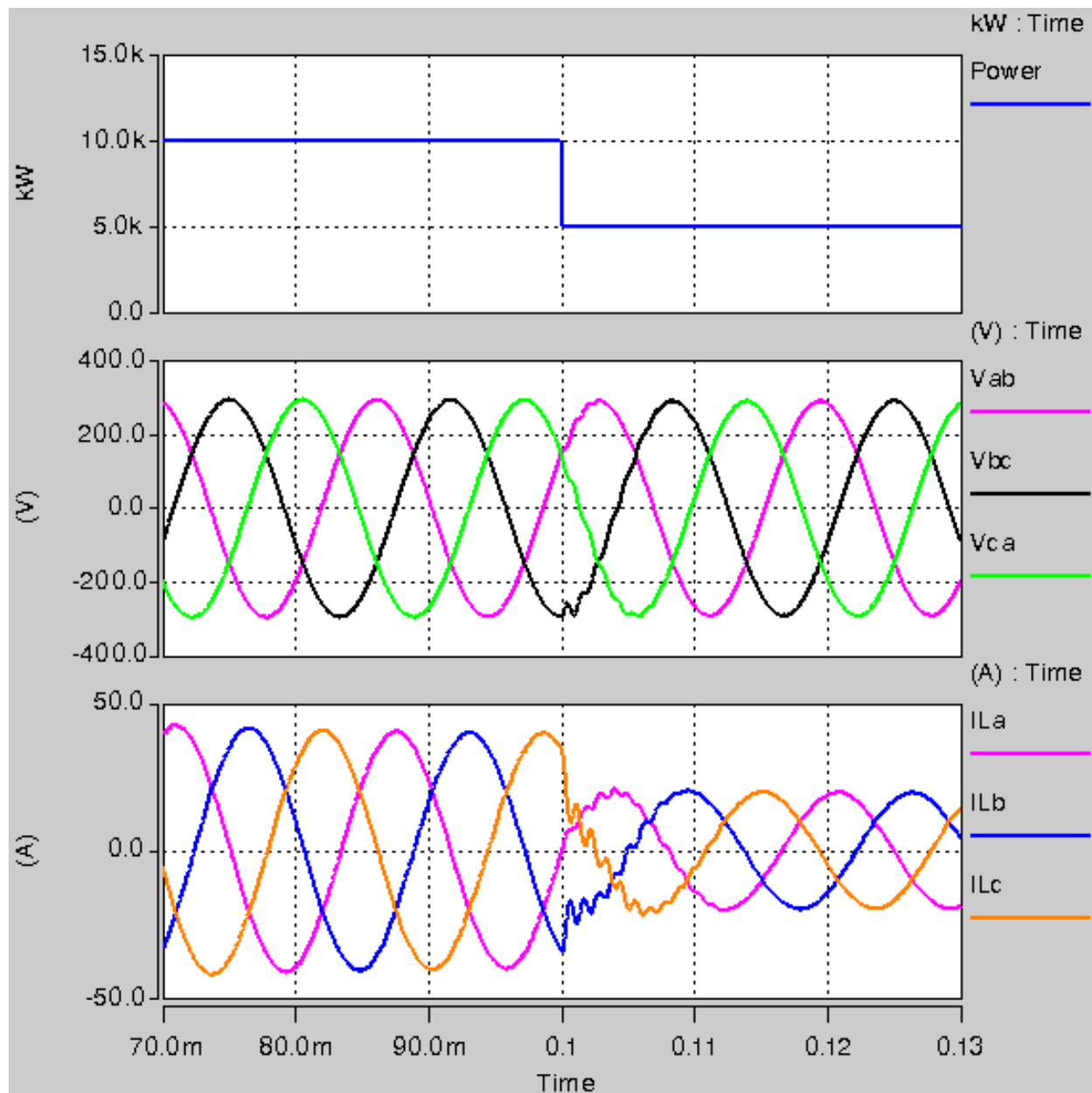
Figure 8-15 Simulation results when power step change from 10kW to 5 kW

Figure 8-17 shows the step-down power change from 10kW to 5kW. The capacitor voltage increases, so that the boost control mode provides a higher shoot-through state reference in order to reduce the shoot-through duty ratio. As a result, the voltage across the capacitor voltage is reduced.
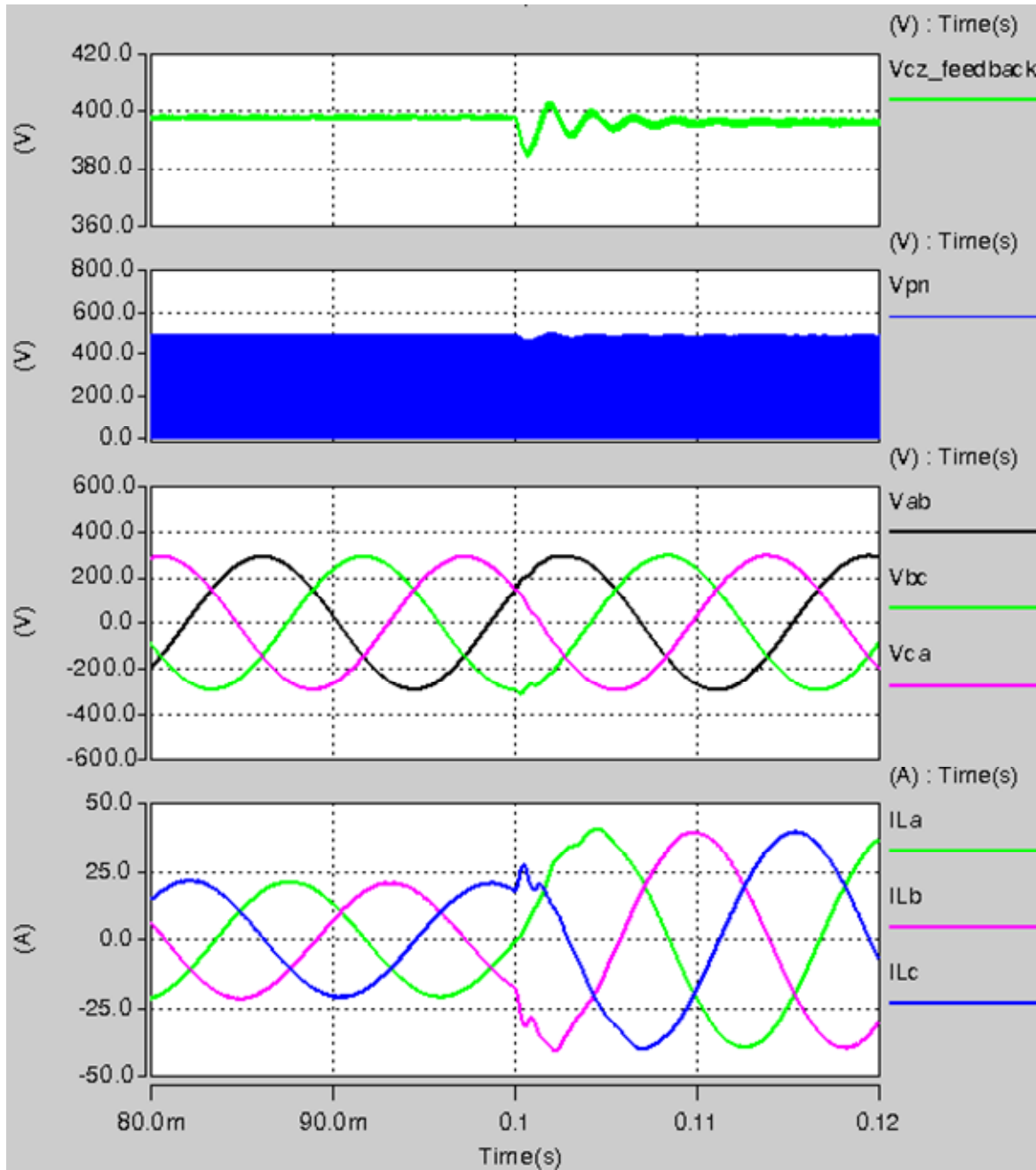
Figure 8-16 Simulation results when the power changes from 5kW to 10kW, from top: the voltage across the capacitor of the Z-source network, the voltage across the inverter bridge, the output voltage and the inverter current
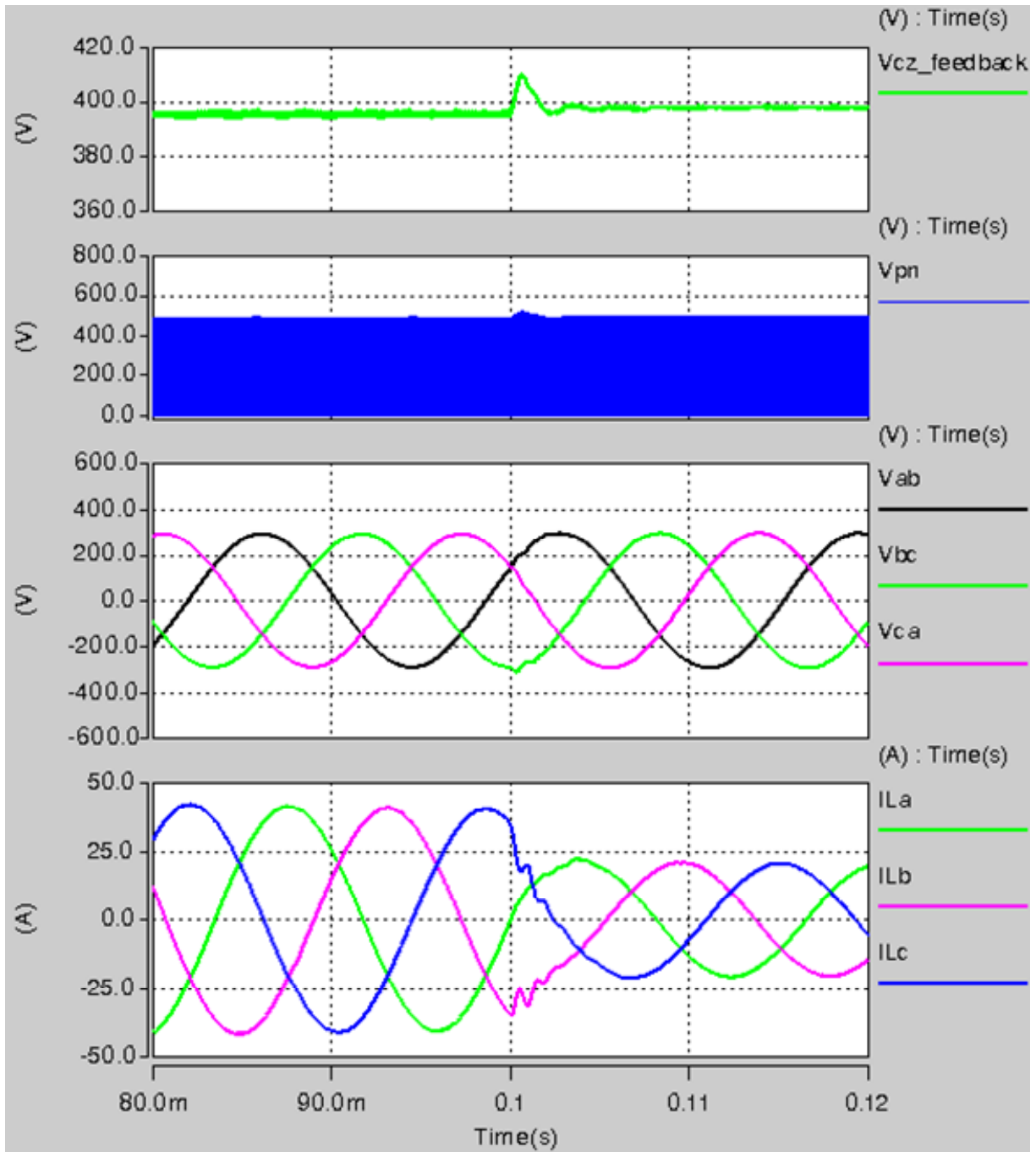
Figure 8-17 Simulation results when the power changes from 10kW to 5kW, from top: the voltage across the capacitor of the Z-source network, the voltage across the inverter bridge, the output voltage and the inverter current
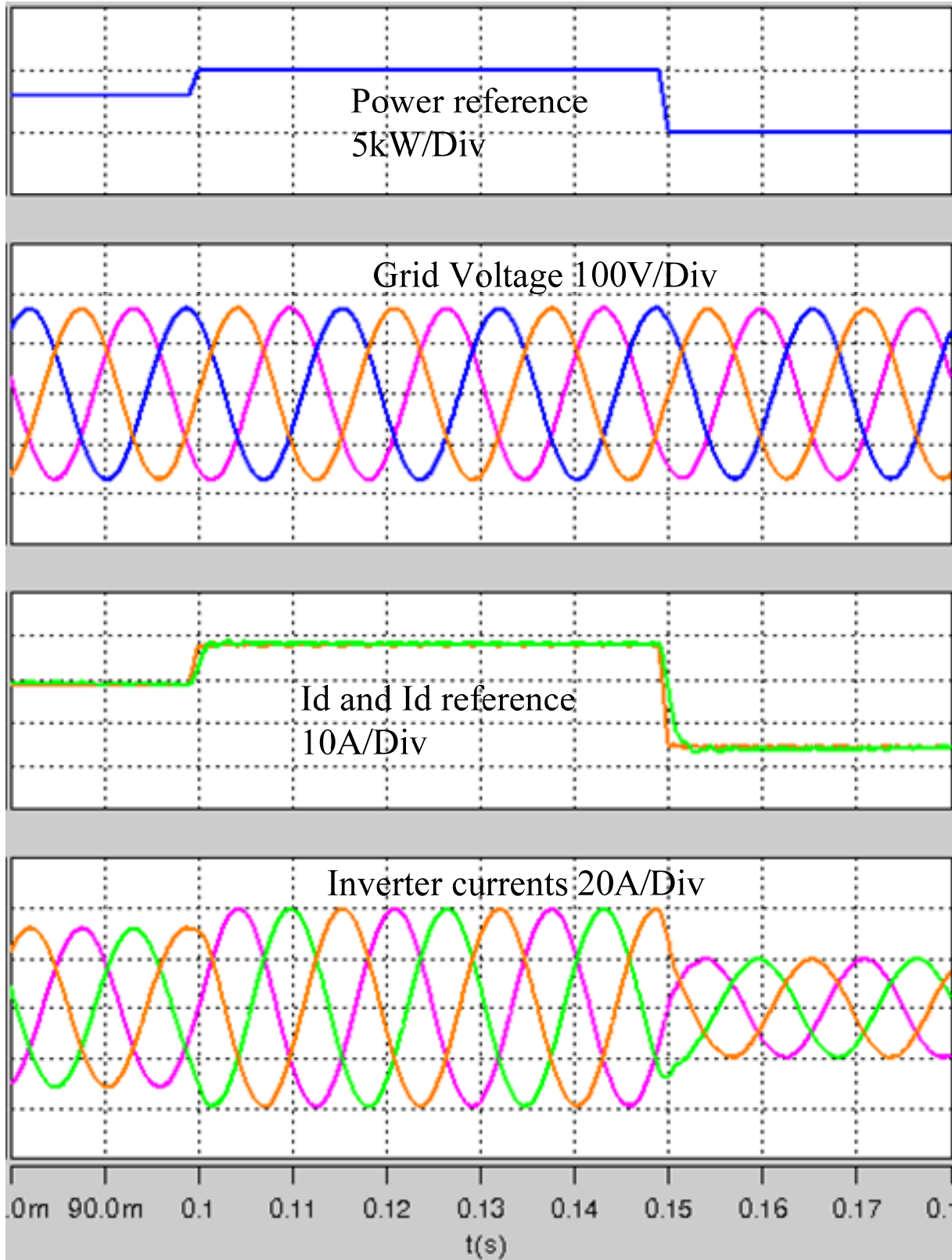
Figure 8-18 Simulation results of grid interconnection under variation of input power

Figure 8-18 shows simulation results of the grid interconnection under the power variation. The input power is varying, so with the control algorithm proposed. The *id* reference and *id* feedback is changed to regulate power and following power reference. The grid voltage is still constant but the output current varies according to the power reference. In this control structure, the power reference is determined from the wind turbine characteristic and rotor speed.

8.6 Experimental results
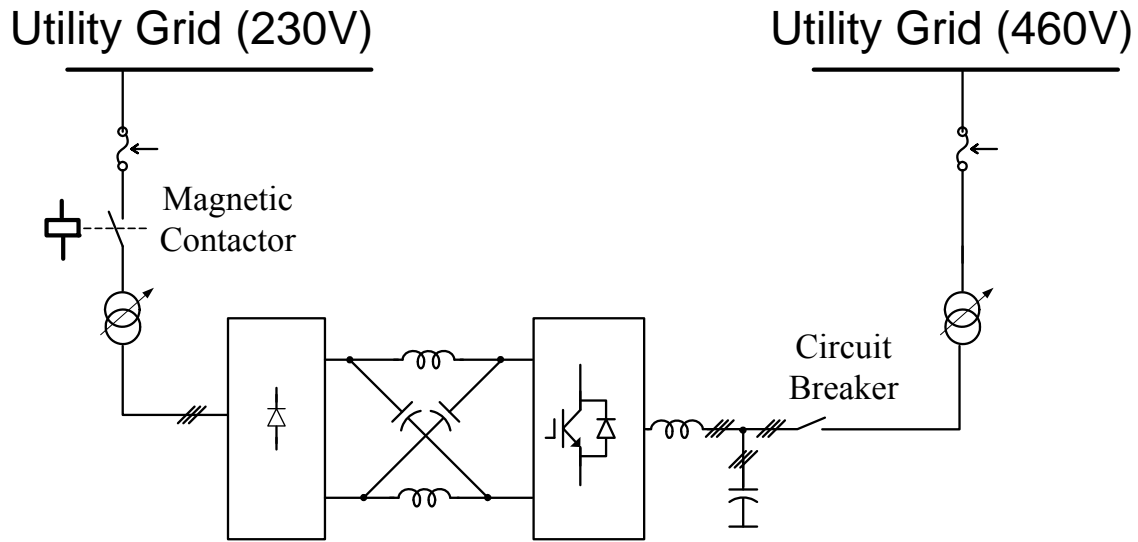
Figure 8-19 Experimental set up block diagram

The experimental set up is shown in Figure 8-19 where the input of inverter comes from the 230V-utility grid through the auto-transformer. The input protection includes the fuse and magnetic contactor. At the output side, the system is connected to the 460V-utility grid through another auto-transformer (use only for stepping up the voltage). The picture of this set up is shown in Figure 8-20 where Z_inductor and Z_capacitor stand for the inductor and capacitor of the inverter's impedance network.
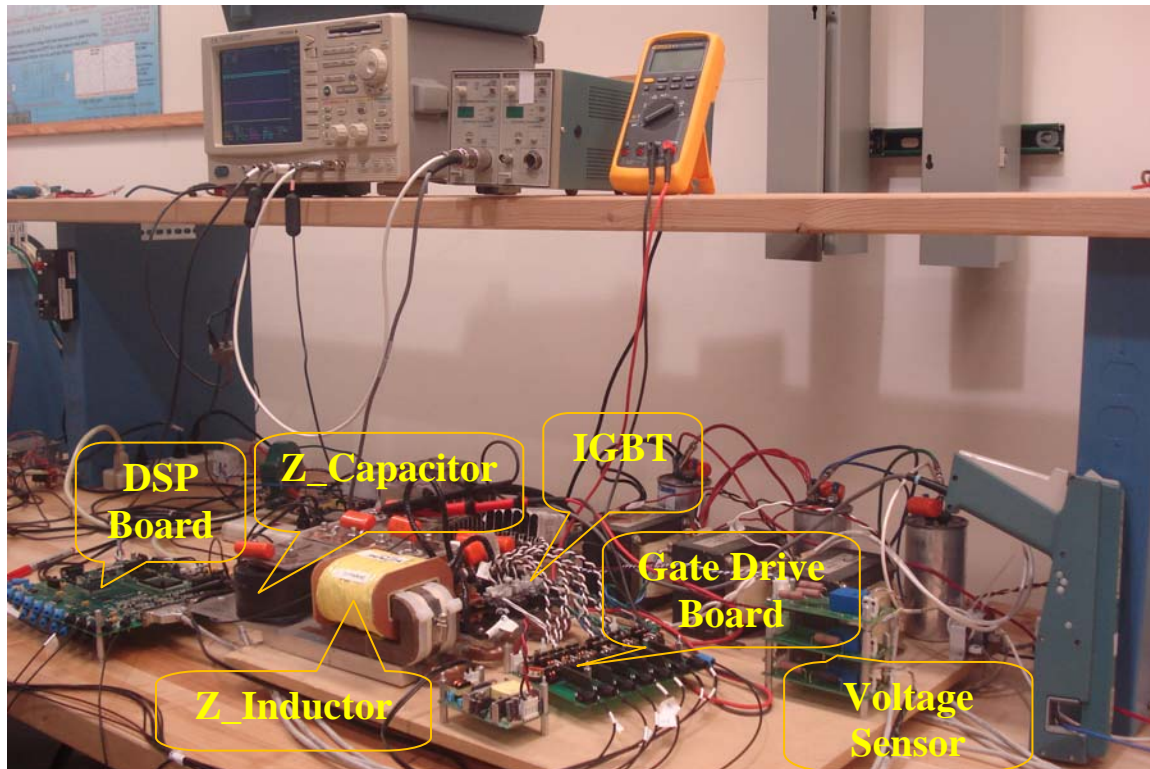
Figure 8-20 Experimental set up

Figure 8-21 shows the experimental results conducted by the set up mentioned above and shown in Figure 8-19 and Figure 8-20. The first waveform (top one) is the phase voltage of the utility grid, the second waveform (middle) is the inverter output voltage, and the third one (bottom) is the inductor current injected to the utility grid. The inverter current is injected to the utility grid as commanded where the output voltage of the inverter represents the synchronization ability of the inverter to the utility grid. The experimental result shows that the system and control work properly on grid interconnection.
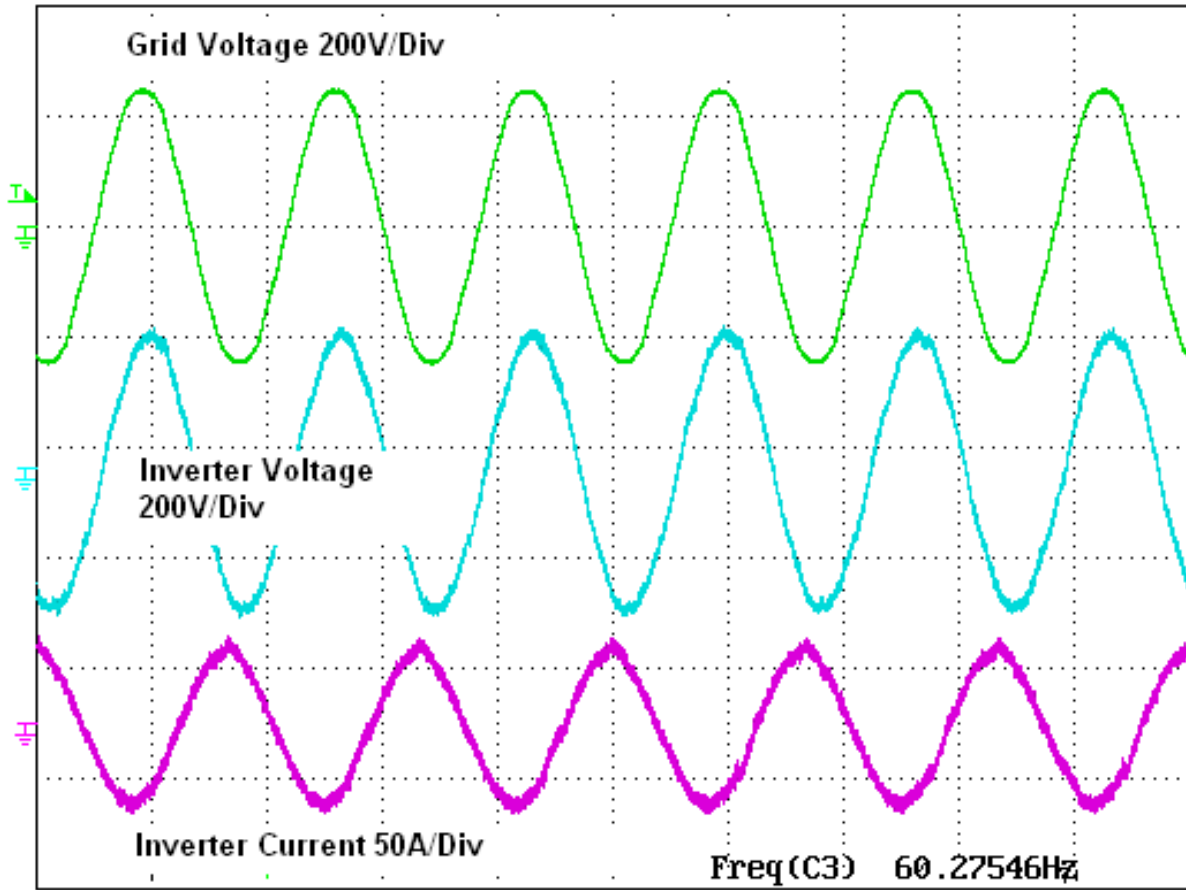
Figure 8-21 Experimental results Grid voltage, inverter voltage and inverter current

Chapter 9. Contributions and future work

9.1 Conclusions

The first part of this dissertation has reviewed converter topologies which have been utilized in wind energy conversion systems. From this review, full-power converter concepts are widely used on the small to medium size WECS, since they provide more efficient power. The full-power converter concept has benefits of control flexibility and high efficiency of the generator. For the large WECSs, the DFIG is one of competitive candidates whose feature is outstanding on small size inverter required. With this smaller inverter, it results in reducing of power electronic losses and cost.

The proposed Z-source inverter/converter for WECS has been theoretically and experimentally explained in details. The Z-source inverter employs the maximum boost control method as its control strategy. The 10 kW Z-source inverter system has been implemented to verified the proposed principle and control strategy. For the given operational conditions of low wind speed and the resulting low input voltage, the Z-source inverter can boost the output voltage efficiently without any additional components or boost circuitry. Equations, simulations and experimental results were shown to demonstrate this concept. Also, when wind speed is high, providing higher input voltage, the Z-source inverter can also work like the traditional inverter without the boost function. In summary, this novel circuit can provide a constant 208Vrms output voltage while the input voltage varies above and below this level. Without the need for additional boost circuitry as is required by the traditional voltage source inverter, the Z-source inverter provides high performance, a minimized component count, increased efficiency and reduced cost. Simulation and experimental results of the proposed system verified its ability

to receive input voltage above and below its constant output voltage. This outstanding performance makes the proposed system suitable for wind turbine distributed generation systems.

9.2 Main contributions

- Proposed the Z-source inverter/converter for wind energy conversion systems

- Designed and built a 10kW Z-source inverter for testing the functionality of the proposed system

- Proposed the MPPT control method for the proposed Z-source inverter and this proposed method has been verified by simulation results

9.3 Recommendations for future work

- Test the proposed MPPT control method and the Z-source inverter with wind turbine simulator as shown in Figure 9-1 and Figure 9-1

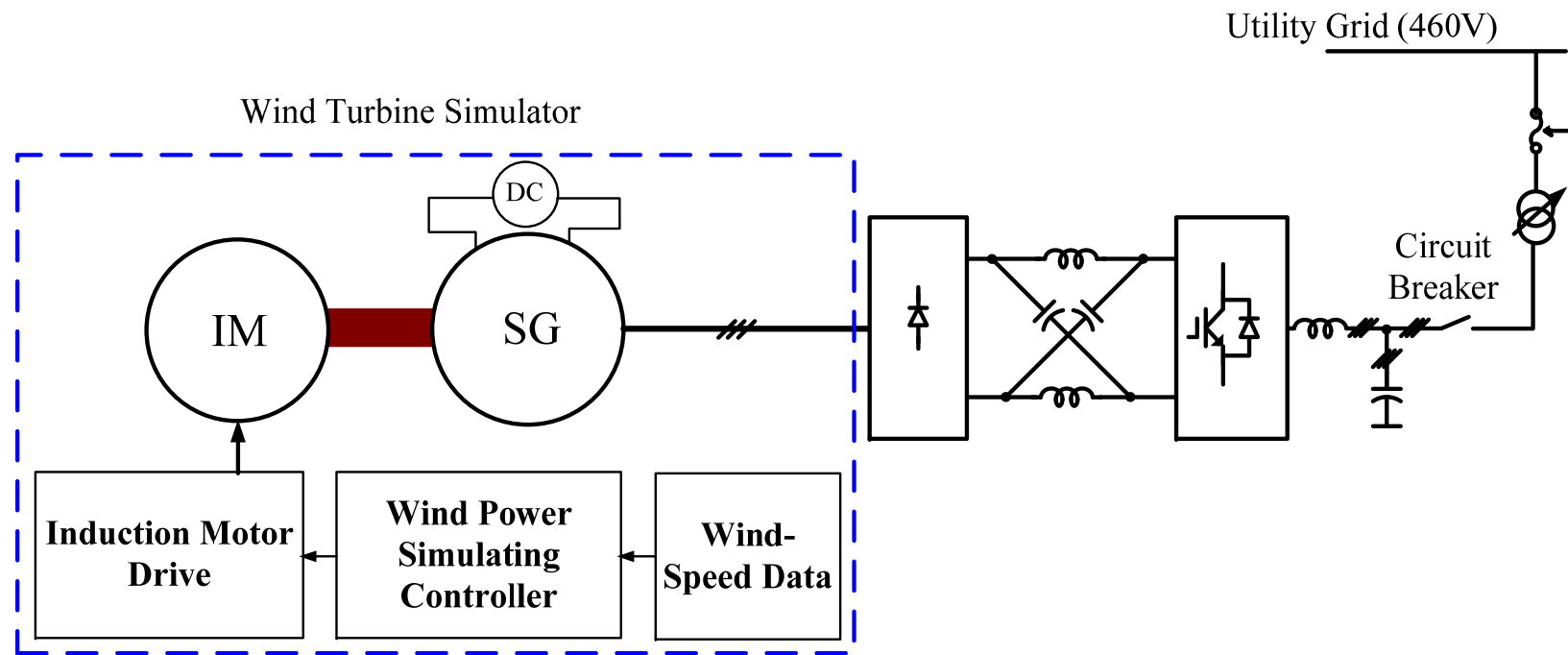- Combine the system with micro grid systems

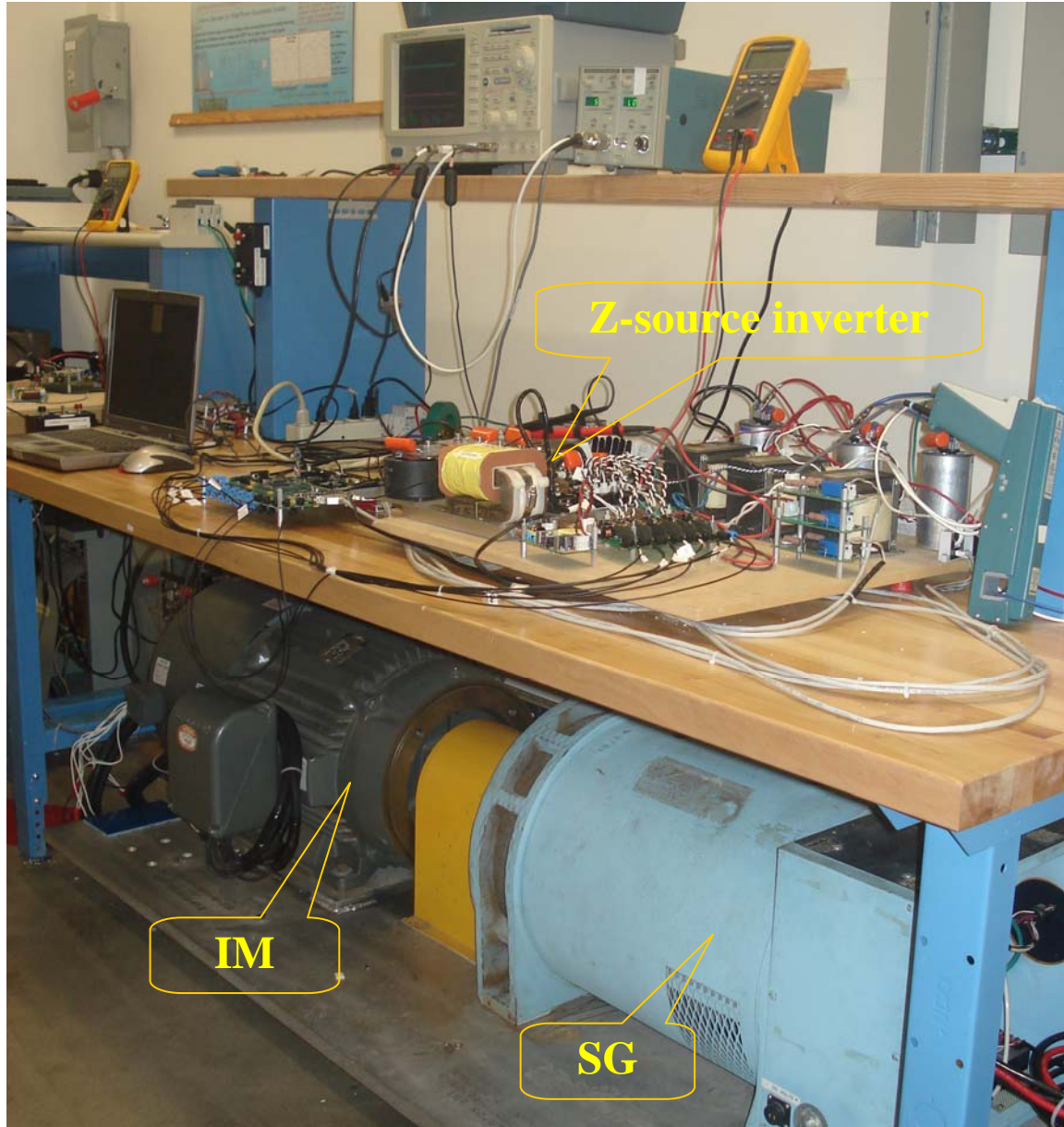Figure 9-1 The Z-source inverter/converter system with wind turbine simulator diagram

Figure 9-2 The Z-source inverter/converter system with wind turbine simulator set up

BIBLIOGRAPHY

BIBLIOGRAPHY

[1]   F.Z. Peng, "Z-Source Inverter," *IEEE Transaction on Industry Applications,* vol. 39, pp. 504-510, March/April 2003

[2]   AWEA, "American Wind Energy Association Annual Wind Industry Report," 2008.

[3]   R. Wiser and M. Bolinger, "2008 Wind Technologies Market Report," U. S. Department of Energy, Washington, DC: pp. 9-10, 2009.

[4]   S. N. Bhadra, S. Banerjee and D. Kastha, *Wind Electrical System*. New Delhi: Oxford University Press, 2005.

[5]   http://en.wikipedia.org/wiki/Windmill.

[6]   http://www.boeing.com/companyoffices/aboutus/wonder_of_flight/airfoil.html.

[7]   http://www.free-online-private-pilot-ground-school.com/aerodynamics.html.

[8]   http://science.howstuffworks.com/environmental/green-science/wind-power3.htm.

[9]   http://www.statemaster.com/encyclopedia/Darrieus-wind-turbine.

[10]   http://buckville.com/drupal/misc/turbine_efficiency.jpg.

[11]   M. R. Patel, *Wind and Solar Power Systems*. New York: CRC Press, 1999.

[12]   W. Kramer, S. Chakraborty, B.Kroposki and H. Thomas, "Advanced Power Electronic Interfaces for Distributed Energy Systems Part1: Systems and Topologies," National Renewable Energy Laboratory, the U.S. Department of Energy, 2008.

[13]   F. Blaabjerg, Z. Chen, R. Teodorescu, and F. Iov, "Power Electronics in Wind Turbine Systems," in *Power Electronics and Motion Control Conference, 2006. IPEMC 2006. CES/IEEE 5th International*, pp. 1-11, 2006.

[14]   D. Yao and R. G. Harley, "Present and future trends in wind turbine generator designs," in *IEEE Power Electronics and Machines in Wind Applications, PEMWA 2009*, pp. 1-6, 2009,

[15]   F. Blaabjerg, C. Zhe, and S. B. Kjaer, "Power electronics as efficient interface in dispersed power generation systems," *IEEE Transactions on Power Electronics,* vol. 19, pp. 1184-1194, 2004.

[16]   R. Pena, J. C. Clare, and G. M. Asher, "Doubly fed induction generator using back-to-back PWM converters and its application to variable-speed wind-energy generation," *IEE Proceedings Electric Power Applications,* vol. 143, pp. 231-241, 1996.

[17]   L. Rajaji and C. Kumar, "Neuro fuzzy soft starter for grid integration with pitch regulated wind turbine system," in *International Conference on Electrical and Computer Engineering, ICECE 2008*, pp. 349-354, 2008.

[18]   *G. W. Walter J Lukitsch PE, Jeff Theisen, and John Streicher*, "AC Drives and Soft Starter Application Guide," in http://www.netaworld.org/, 2009.

[19]   L.H. Hansen, L. Helle F. Blaabjerg, E. Ritchie, S. Munk-Nielsen, P. Sorensen, H.Bindner, and B.Bak-Jensen., "Conceptual survey of generators and power electronics for wind turbines
" Technical Report, Risø National Laboratory, Roskild, Denmark 2001.

[20]   Z. Chen and E. Spooner, "Current source thyristor inverter and its active compensation system," *IEE Proceedings-Generation, Transmission and Distribution,* vol. 150, pp. 447-454, 2003.

[21]   Z. Chen and E. Spooner, "Grid power quality with variable speed wind turbines," *IEEE Transactions on Energy conversion,* vol. 16, pp. 148-154, 2001.

[22]   I. Schiemenz and M. Stiebler, "Control of a permanent magnet synchronous generator used in a variable speed wind energy system," in *IEEE International Electric Machines and Drives Conference, IEMDC*, pp. 872-877, 2001.

[23]   M. G. Simoes, B. K. Bose, and R. J. Spiegel, "Fuzzy logic based intelligent control of a variable speed cage machine wind generation system," *IEEE Transactions on Power Electronics,* vol. 12, pp. 87-95, 1997.

[24]   S. Muller, M. Deicke, and R. W. De Doncker, "Doubly fed induction generator systems for wind turbines," *IEEE Industry Applications Magazine,* vol. 8, pp. 26-33, 2002.

[25]   J.M. Carrasco, J.T. Bialasiewicz, L. G. Franquelo. E.Galvan, R.C.Portillo Guisado, M. A. Martin Prats, J.I. Leon, and N. Moreno-Alfonso, "Power-Electronics Systems for the Grid Integration of Renewable Energy Sources: A Survey," *IEEE Transaction on Industry Electronics,* vol. 53, pp. 1002-1016, August 2006.

[26]   L. M. Tolbert, F. Z. Peng, and T. G. Habetler, "A multilevel converter-based universal power conditioner," in *IEEE Power Electronics Specialists Conference, PESC 99*, pp. 393-399 , 1999.

[27] F.Z .Peng, J.S. Lai, J. McKeever, and J. VanCoevering, "A multilevel voltage-source converter system with balanced DC voltages," in *IEEE Power Electronics Specialists Conference, PESC '95*, pp. 1144-1150, 1995

[28] F. Blaabjerg, R. Teodorescu, M. Liserre, and A. V. Timbus, "Overview of Control and Grid Synchronization for Distributed Power Generation Systems," *IEEE Transactions on Industrial Electronics,* vol. 53, pp. 1398-1409, 2006.

[29] J. Svensson, "Synchronisation methods for grid-connected voltage source converters," *IEE Proceedings- Generation, Transmission and Distribution,* vol. 148, pp. 229-235, 2001.

[30] A. Timbus, R. Teodorescu, F. Blaabjerg, and M. Liserre, "Synchronization Methods for Three Phase Distributed Power Generation Systems. An Overview and Evaluation," in *IEEE Power Electronics Specialists Conference, PESC '05*, pp. 2474-2481,2005.

[31] G. Saccomando and J. Svensson, "Transient operation of grid-connected voltage source converter under unbalanced voltage conditions," in *IEEE Industry Applications Conference*, pp. 2419-2424 , 2001.

[32] V. Kaura and V. Blasko, "Operation of a phase locked loop system under distorted utility conditions," *IEEE Transactions on Industry Applications,* vol. 33, pp. 58-63, 1997.

[33] L. N. Arruda, S. M. Silva, and B. J. Cardoso Filho, "PLL structures for utility connected systems," in *IEEE Industry Applications Conference*, 2001, pp. 2655-2660

[34] K. Holland, M. Shen, and F. Z. Peng, "Z-source inverter control for traction drive of fuel cell - battery hybrid vehicles," in *Industry Applications Conference, Fourtieth IAS Annual Meeting.* Conference Record of the 2005, pp. 1651-1656 Vol. 3, 2005.

[35] M. Shen, J. Wang, A. Joseph, F.Z. Peng, L.M. Tolbert, and D.J. Adams, "Constant Boost Control of the Z-Source Inverter to Minimize Current Ripple and Voltage Stress," *IEEE Transaction on Industry Applications,* vol. 42, pp. 770-778, May/June 2006.

[36] F.Z. Peng, M. Shen, and Z. Qian, "Maximum Boost Control of Z-Source Inverter," *IEEE Transaction on Power Electronics,* vol. 20, pp. 833-838, July 2005.

[37] S. Seung-Ho, K. Shin-il, and H. Nyeon-kun, "Implementation and control of grid connected AC-DC-AC power converter for variable speed wind energy conversion system," in *IEEE Applied Power Electronics Conference and Exposition 2003, (APEC '03)*, pp. 154-158, 2003

[38] F.Z.Peng, A. Joseph ,J. Wang, M. Shen, L. Chen, Z. Pan, E. Ortiz-Rivera and Y. Huang, "Z-source inverter for motor drives," *IEEE Transactions on Power Electronics,* vol. 20, pp. 857-863, 2005.

[39]   D. Xu and Z. Luo, " A Novel AC-DC Converter for PMSG Variable Speed Wind Energy Conversion Systems," in *IEEE 6ᵗʰ International Power Electronics and Motion Control Conference, IPEMC'09,* pp.117-1122, 2009.

[40]   W. Quincy and C. Liuchen, "An intelligent maximum power extraction algorithm for inverter-based variable speed wind turbine systems," *IEEE Transactions on Power Electronics,* vol. 19, pp. 1242-1249, 2004.

[41]   R. J. Wai, C. Y. Lin, and Y. R. Chang, "Novel maximum-power-extraction algorithm for PMSG wind generation system," *in IET on Electric Power Applications,* vol. 1, pp. 275-283, 2007.

[42]   A. M. Knight and G. E. Peters, "Simple wind energy controller for an expanded operating range," *in IEEE Transaction on Energy Conversion,* vol. 20, pp. 459-466, 2005.

[43]   N. Mohan, W. P. Robbins, and T. Underland, *Power Electronics, Converters, Applications and Design*, 3rd ed., New York: Wiley, 2003.

[44]   K. Amei, Y. Takayasu, T. Ohji, and M. Sakui, "A maximum power control of wind generator system using a permanent magnet synchronous generator and a boost chopper circuit," in *Proceedings of the Power Conversion Conference, 2002. PCC Osaka 2002.* pp. 1447-1452 vol.3, 2002.

[45]   E. Koutroulis and K. Kalaitzakis, "Design of a maximum power tracking system for wind-energy-conversion applications," *IEEE Transactions on Industrial Electronics,* vol. 53, pp. 486-494, 2006.

[46]   M. G. Simoes, B. K. Bose, and R. J. Spiegel, "Design and performance evaluation of a fuzzy-logic-based variable-speed wind generation system," *IEEE Transactions on Industry Applications,* vol. 33, pp. 956-965, 1997.

[47]   K. Yukita, S. Washizu, K. Taniguchi, M. Oshima, N. Hayashi, K. Ichiyanagi, and Y. Goto , "A Pole Change Generator for Micro Windmill with Maximum Power Point Tracking System," *IEEE 22nd International Symposium on Intelligent Control, 2007. ISIC 2007*, pp.640-645, 1-3 Oct. 2007.

[48]   M.E. Haque, K.M. Muttaqi, and M. Negnevitsky, "Control of a stand alone variable speed wind turbine with a permanent magnet synchronous generator," *IEEE Power and Energy Society General Meeting - Conversion and Delivery of Electrical Energy in the 21st Century*, pp.1-9, 20-24 July 2008.

[49]   T. Tafticht, K. Agbossou, and A. Cheriti,; , "DC bus control of variable speed wind turbine using a buck-boost converter," *IEEE Power Engineering Society General Meeting,* pp.1-5, 2006